Graduate School ETD Form 9
(Revised 12/07)

PURDUE UNIVERSITY
GRADUATE SCHOOL
Thesis/Dissertation Acceptance

This is to certify that the thesis/dissertation prepared

By Ayana T. Pusha

Entitled
MULTIPLE TURBINE WIND POWER TRANSFER SYSTEM LOSS AND EFFICIENCY ANALYSIS

For the degree of Master of Science in Mechanical Engineering

Is approved by the final examining committee:

Afshin Izadian
Co-Chair

Sohel Anwar
Co-Chair

Tamer Wasfy

To the best of my knowledge and as understood by the student in the *Research Integrity and Copyright Disclaimer (Graduate School Form 20)*, this thesis/dissertation adheres to the provisions of Purdue University's "Policy on Integrity in Research" and the use of copyrighted material.

Approved by Major Professor(s): Afshin Izadian

Approved by: Sohel Anwar 08/31/2012
Head of the Graduate Program Date

Graduate School Form 20
(Revised 9/10)

PURDUE UNIVERSITY
GRADUATE SCHOOL

Research Integrity and Copyright Disclaimer

Title of Thesis/Dissertation:

MULTIPLE TURBINE WIND POWER TRANSFER SYSTEM LOSS AND EFFICIENCY ANALYSIS

For the degree of Master of Science in Mechanical Engineering

I certify that in the preparation of this thesis, I have observed the provisions of *Purdue University Executive Memorandum No. C-22,* September 6, 1991, *Policy on Integrity in Research.**

Further, I certify that this work is free of plagiarism and all materials appearing in this thesis/dissertation have been properly quoted and attributed.

I certify that all copyrighted material incorporated into this thesis/dissertation is in compliance with the United States' copyright law and that I have received written permission from the copyright owners for my use of their work, which is beyond the scope of the law. I agree to indemnify and save harmless Purdue University from any and all claims that may be asserted or that may arise from any copyright violation.

Ayana T. Pusha
_____
Printed Name and Signature of Candidate

01/23/2013
_____
Date (month/day/year)

*Located at http://www.purdue.edu/policies/pages/teach_res_outreach/c_22.html

MULTIPLE TURBINE WIND POWER TRANSFER SYSTEM LOSS AND EFFICIENCY ANALYSIS

A Thesis

Submitted to the Faculty

of

Purdue University

by

Ayana T. Pusha

In Partial Fulfillment of the

Requirements for the Degree

of

Master of Science in Mechanical Engineering

May 2013

Purdue University

Indianapolis, Indiana

ACKNOWLEDGEMENTS

I would like to thank my research advisors Dr. Afshin Izadian for giving me the opportunity to participate in this research. Thank you for your patience and guidance. I am truly grateful for the chance to be a witness to your love for and commitment to research. The knowledge that I acquired through this journey has made me understand and respect the planning and efforts that are involved in successful research. I have much appreciation for you always finding the time in your busy schedule to answer questions and to point me in the right direction as well as encourage and support me. I have become a better researcher because of all of these things.

I am grateful for Dr. Sohel Anwar for his expertise and encouragement and Dr. Tamer Wasfy who made time to be a member of my advisory committee.

I am also thankful for the individuals that I shared lab space with and the relationships that were developed as a result. Thank you for sharing your struggles in research, always having a listening ear, and for the laughter. Thank you Likhita Gavini, Nate Girrens, Hadi Hafizi, Hang Yeng and Sina Hamzehlouia.

Finally, I would like to thank my family for being a source of encouragement and believing in and continually nurturing my potential.

TABLE OF CONTENTS

Page

Page

Page

LIST OF TABLES

LIST OF FIGURES

Figure Page

Figure Page

Figure Page

Appendix Figure

ABSTRACT

Pusha, Ayana T. M.S.M.E., Purdue University, May 2013. Multiple Turbine Wind Power Transfer System Loss and Efficiency Analysis. Major Professor: Afshin Izadian.

A gearless hydraulic wind energy transfer system utilizes the hydraulic power transmission principles to integrate the energy of multiple wind turbines in a central power generation location. The gearless wind power transfer technology may replace the current energy harvesting system to reduce the cost of operation and increase the reliability of wind power generation. It also allows for the integration of multiple wind turbines to one central generation unit, unlike the traditional wind power generation with dedicated generator and gearbox. A Hydraulic Transmission (HT) can transmit high power and can operate over a wide range of torque-to-speed ratios, allowing efficient transmission of intermittent wind power. The torque to speed ratios illustrates the relationship between the torque and speed of a motor (or pump) from the moment of start to when full-load torque is reached at the manufacturer recommended rated speed.

In this thesis, a gearless hydraulic wind energy harvesting and transfer system is mathematically modeled and verified by experimental results. The mathematical model is therefore required to consider the system dynamics and be used in control system development. Mathematical modeling also provided a method to determine the losses of the system as well as overall efficiency. The energy is harvested by a low speed-high torque wind turbine connected to a high fixed-displacement hydraulic pump, which is connected to hydraulic motors. Through mathematical modeling of the system, an enhanced understanding of the HTS through analysis was gained that lead to a highly

efficient hydraulic energy transmission system. It was determined which factors significantly influenced the system operation and its efficiency more. It was also established how the overall system operated in a multiple wind turbine configuration.

The quality of transferred power from the wind turbine to the generator is important to maintaining the systems power balance, frequency droop control in grid-connected applications, and to ensure that the maximum output power is obtained. A hydraulic transmission system can transfer large amounts of power and has more flexibility than a mechanical and electrical system. However high-pressure hydraulic systems have shown low efficiency in wind power transfer when interfaced with a single turbine to a ground-level generator. HT's generally have acceptable efficiency at full load and drop efficiency as the loading changes, typically having a peak around 60%. The efficiency of a HT is dependent on several parameters including volumetric flow rate, rotational speed and torque at the pump shaft, and the pressure difference across the inlet and outlet of the hydraulic pump and motor.

It has been demonstrated that using a central generation unit for a group of wind turbines and transferring the power of each turbine through hydraulic system increases the efficiency of the overall system versus one turbine to one central generation unit. The efficiency enhancement depends on the rotational speed of the hydraulic pumps. Therefore, it is proven that the multiple-turbine hydraulic power transfer system reaches higher efficiencies at lower rotational speeds. This suggests that the gearbox can be eliminated from the wind powertrains if multiple turbines are connected to the central generation unit. Computer simulations and experimental results are provided to quantify the efficiency enhancements obtained by adding the second wind turbine hydraulic pump to the system.

1. INTRODUCTION TO WIND ENERGY

Harnessing the energy of wind has been one of man's earliest achievements, which has led to wind-generated electricity. To date, most wind power generation systems consist of a wind turbine, a gearbox, and a generator to harvest the wind energy and produce electric power. A gearbox is required to speed up the wind turbine's shaft before it is connected to electric generators. However, gearboxes are expensive, bulky, and require regular maintenance, which makes wind energy production expensive.

1.1 Background and Motivation

Wind is the fastest growing and most widely used form of the emerging renewable energy technologies in the generation of electricity. Due to the many advances in wind generation technology, the potential for wind as a power source is immense. Wind energy is the kinetic energy of air in motion and when converted into useful forms of energy becomes wind power which can be used to generate electricity or mechanical power. Wind turbines use the kinetic energy found in wind to rotate a propeller with two to three blades. This propeller is connected to a rotor hub that spins a central shaft through a gear box that dramatically increases the rotational speed of the shaft. The shaft is then used to power an electric generator to make electricity. The generator produces electricity through electromagnetic induction which is the result of a conductor moving through a magnetic field. Electricity can then be sent out to the power grid or stored for later use. Wind turbines should be mounted as tall as necessary to capture wind speeds above 5 miles per hour (2.24 m/s) to start generating power and to be as effective and efficient as possible.

Shown in Figure 1.1, the subsystems of a traditional wind turbine include the following components [1]:

- The rotor which comprises of the blades (two to three) and the hub. The hub connects the blades to the motor through the use of a gear.

- The drivetrain, contains the rotating parts, includes a low speed shaft on the rotor side, a gearbox, and a high speed shaft on the generator side. The other drivetrain components are a mechanical break, support bearings, one or more couplings, and the rotating parts of the generator.

- The nacelle, acting as protection from the elements, is the wind turbine housing for and the mainframe and the yaw system. The mainframe provides for the mounting and proper alignment of the drive train components. The yaw system keeps the rotor shaft properly aligned with the wind.

- The tower structure and supporting foundation.

- The control system includes sensors (speed, position, flow, current, and voltage), actuators (motors, pistons, magnets, and solenoids), controllers, and power amplifiers.

- Electrical components such as transformers, cables, power electronic converters, switchgears, power factor correction capacitors, yaw and pitch motors.

For a traditional wind power generation system to harvest wind energy and produce electric power, the subsystems mentioned above are required. These components, the gearbox specifically, are costly and massive in size. Regular maintenance is required which can considerably increase operation costs. The gearless power transfer system will transfer power of a high torque/low speed wind turbine to a high speed generator

increasing the efficiency. This alternative to the traditional design of the wind turbine power train may replace the current energy harvesting technologies to reduce the cost and increase the reliability of wind power generation.

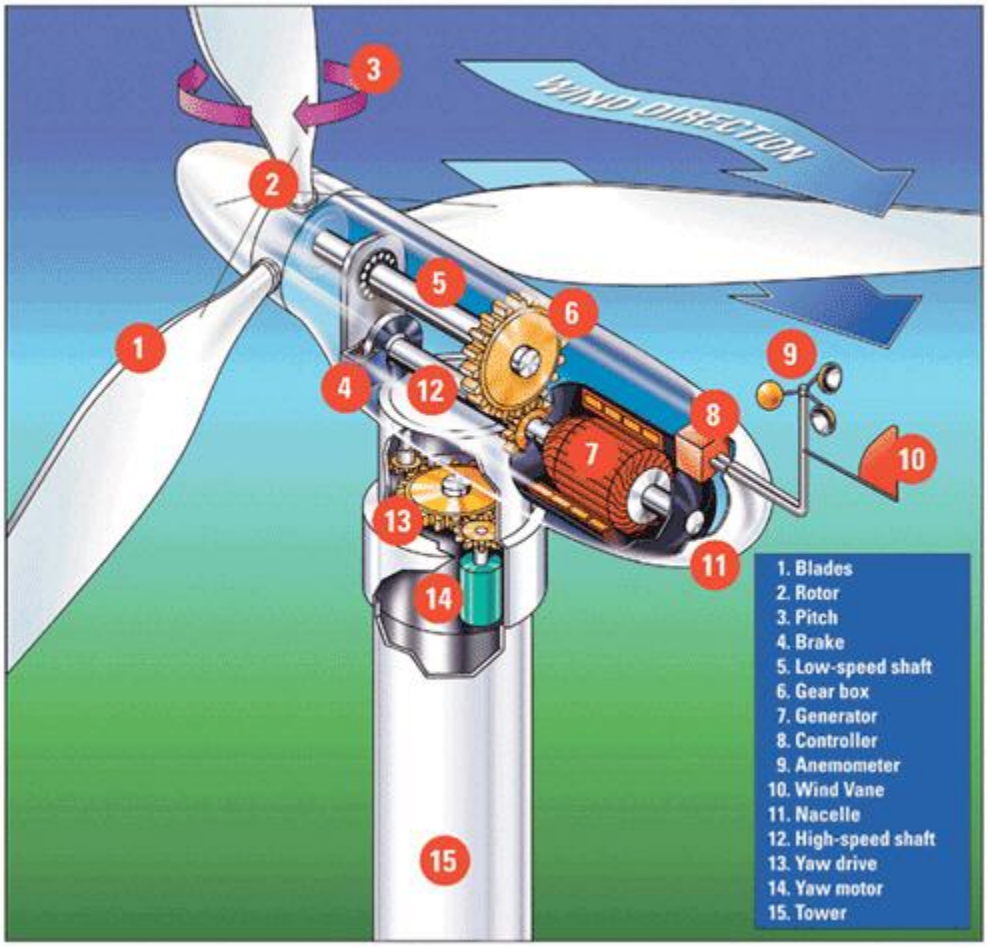

Figure 1.1 Wind Turbine Components [41]

1.2 Statement of the Problem/Purpose of Project

Of the emerging renewable energy technologies, wind being the fastest growing and most widely used in the production of electricity, has the potential to be an immense power source. For a traditional wind power generation system to harvest wind energy and produce electric power, the required components include a wind turbine, gearbox, transformer, and a generator. These components, the gearbox specifically, are

expensive, and require regular maintenance, which makes the wind energy production expensive. They also cause the towers that house them to be massive in size. Each wind turbine requires its own generator and power converter causing synchronization throughout the power plant of the harvested power difficult to control. Furthermore there is a tremendous amount of noise generated from the wind turbine blades.

The aim of this project is to design and simulate a high-pressure hydraulic system to couple and transfer energy harvested from multiple-wind turbines to a central power generation unit. The gearbox of a traditional wind turbine will be removed and replaced with a hydraulic pump in the nacelle that is connected to a hydraulic motor and generator by way of high pressure hydraulic piping on ground level. By eliminating the gearbox, there will be an increase in the power transfer efficiency. Operation and capital costs of the wind power plant could be reduced considerably. A control unit consisting of a directional valve coupled to a PI controller will control the speed rotation through the use of a bypass auxiliary power unit in a closed loop control system. This new approach integrates electrical and mechanical systems to produce renewable energy. Unlike traditional wind power generation, the hydraulic transmission system also allows for the integration of multiple wind turbines to one central generation unit and utilization of several forms of storage units.

1.3 Research Goals and Approach

Thesis presents an alternative approach to the traditional wind turbine design by proposing a gearless power transfer system. The prototype developed, has removed the standard gearbox and instead uses a hydraulic transmission. A hydraulic transmission contains a hydraulic pump that provides a hydraulic motor with hydraulic fluid through high-pressure hydraulic pipelines. The speed of rotation of the pump's shaft determines how much fluid is produced and delivered to the motor affecting its shaft velocity.

A gearless power transfer system allows for the removal of the large gearbox to reduce the size of the nacelle and the cost of maintenance but to fully uncover the commercial potential of such a system the following goals must be implemented:

1. To calculate the losses of each component in the gearless power transfer system,

2. To determine the overall efficiency of the system by calculating the power transferred from the hydraulic pump to hydraulic motor, and

3. To establish a method to increase system efficiency.

To achieve these goals three steps were taken. A model of each component of the system was developed to discover the dynamics of the system. A loss model was also developed to determine the loss of each component as well. These models were validated with simulation software in Matlab. Next a gearless power transfer system prototype was assembled to obtain experimental results. These results include the power transfer through the system and the overall system efficiency. Thirdly, the simulation results obtained were then validated by experimental results.

1.4 Thesis Outline

Comprised of eight chapters, this thesis begins with Chapter 1 which begins with the Background and Motivation, Statement of the Problem and Purpose, and includes Research Goals and the Approach taken to complete this research. Chapter 2 discusses the history of the traditional wind turbine, siting specifications, and wind characteristics. Most importantly there will be a comparison of the traditional wind turbine to the hydraulic system proposed in this research. Chapter 3 provides mathematical modeling of the system components to evaluate system dynamics and control development. Chapter 4 assists in the understanding of system losses and how these losses affect the overall system efficiency. Validation of the mathematical model and loss model using a Matlab

simulation toolbox is attained in Chapter 5. Chapter 6 discusses in detail the design and fabrication of a gearless power transfer system as an experimental setup. Experimental results are examined in Chapter 7. Chapter 8 ends the thesis with the conclusion of the research, recommendations, and future work.

2. HISTORY OF WIND ENERGY

2.1 Traditional Wind Turbines

A wind turbine is a machine that converts the power in wind into electricity. In modern wind turbines, the actual conversion process uses aerodynamic force of lift to produce a net positive torque on a rotating shaft, resulting in the production of mechanical power and then in its transformation to electricity in a generator. Wind turbines can only produce energy in response to the wind that is immediately available unlike almost all other generators [1]. The design of modern large scale wind turbines have led to two configurations, horizontal axis wind turbine (HAWT) and vertical axis wind turbine (VAWT), with HAWT's being the most common. HAWT's are designed with the rotor and electric generator located at the top of the tower to have their axis of rotation parallel to the ground and must be pointed into the wind. VAWT's are designed with the axis of rotation vertically and does not need to be pointed into the wind to be operational. The generator and gear box can be placed near the ground, making it easier to maintain. In this research only HAWT's will be discussed in detail.

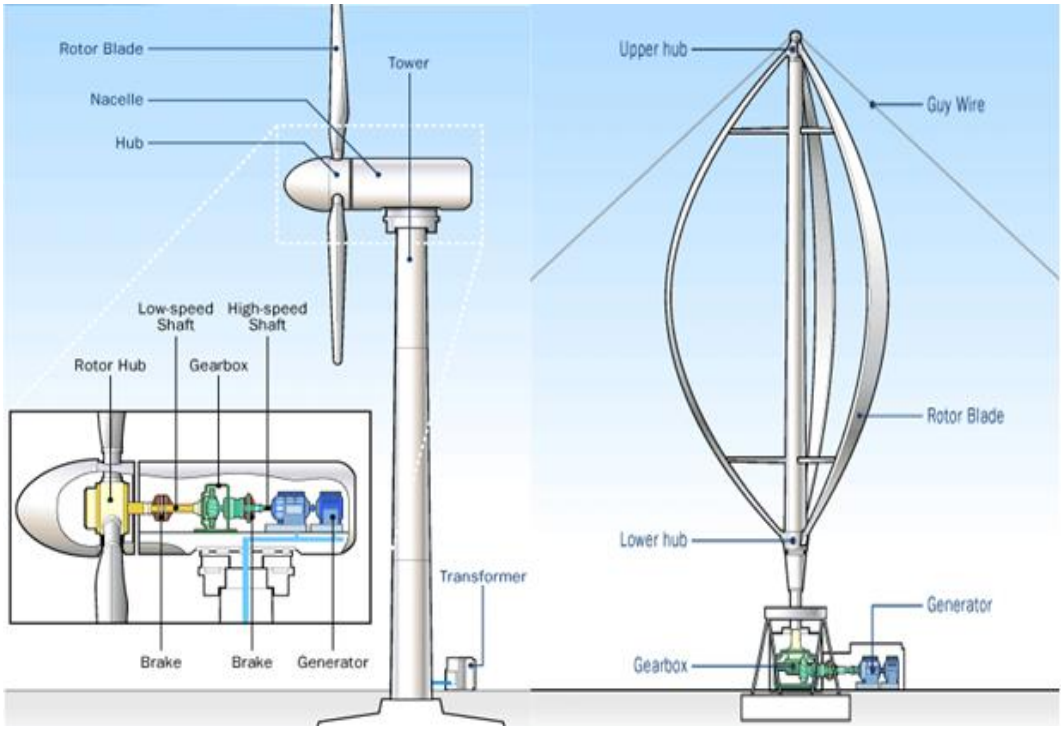

Figure 2.1 HAWT/VAWT configuration

To effectively construct a horizontal axis wind turbine the necessary components (See Figure 2.1) include a rotor subsystem, drivetrain subsystem, nacelle subsystem, tower subsystem, and ground equipment. The rotor subsystem comprises of the hub and blades of the wind turbine and is considered to be the most important components from a performance and overall cost standpoint. Two or three blades are connected to a central hub and act as a propeller. As the rotor turns, the blades generate an imaginary surface whose projection on a vertical plane is called a swept area. The rotor orientation denotes the location of the rotor with respect to the tower and can be either downwind or upwind. A downwind rotor faces the same direction in which the wind is blowing while an upwind rotor is facing into or against the wind. For large scale wind turbines, the rotor subsystem usually includes a mechanism for adjusting blade pitch. Blade pitch is the angle between the blade chord line and the plane of rotation. The pitch change mechanism provides a means to controlling starting and stopping torque, and peak power controlling either the angle of the outboard section of each blade or the entire blade.

Materials used to construct rotor blades are glass fiber composites, steel spars with non-structural composite fairings, and welded steel airfoils. These materials are chosen by system engineering and established based on the size, weight, maintenance and cost of wind turbine [1, 3].

The drivetrain of a wind turbine involves a combination of mechanical and electrical components required to convert the mechanical power received from the rotor hub to electrical power. There is a low speed shaft located on the rotor side, a gearbox that increases the rate of rotation of the rotor from a low value to a speed that can drive a generator, a high speed shaft on the generator side, a rotor brake and an electric generator. The low speed shaft is the most critical component of an HAWT because of its dual structural/mechanical function. Rotor weight, thrust, torque, and lateral forces cause fatigue loading on this component whose design lifetime usually equals or exceeds that of the total system. The gearbox has a step up ratio that is equal to the generator shaft speed divided by the turbine shaft speed that is as high as 100. The electric generators used for larger wind turbines are AC induction or synchronous generators. They provide a constant or near constant rotational speed of the generator when the generator is directly connected to a utility network. Induction generators are used on the majority of wind turbines that are installed in grid connected applications due to the torsional damping provided by their inherent slip. High slip can provide a modest amount of softness to the drivetrain although efficiency is reduced in the process. These generators operate within a narrow range of speeds slightly higher than its synchronous speed and are rugged, inexpensive, and easy to connect to an electrical network. Synchronous generators are more beneficial than induction generators in that they provide higher power quality and higher efficiency but require external voltage regulators and are unable to provide significant softness or damping to the drivetrain [1, 3].

The nacelle is the structure that houses and protects the machine bedplate or main frame and the yaw orientation system. It is the primary load path from the turbine shaft to the tower and is a combination of welded and bolted steel sections which form trusses

or box beams. The bedplate is used to mount the shaft bearings, drivetrain components, and the yaw orientation system. The yaw orientation system is employed to keep the rotor shaft properly aligned with the wind. The primary component of the yaw system is an active yaw drive with a large bearing that connects the bedplate to the tower. There are also one or more motors that drive a pinion gear against a bull gear attached to the yaw bearing. Yaw breaks hold the nacelle in position while a yaw slip ring transfers electrical power, control signals, and data from the moving nacelle to stationary cables in the tower [3].

The tower of a wind turbine raises the rotor and drivetrain to an elevation of 1 to 1.5 times the rotor diameter or a minimum of 20 meters. The height of the tower is calculated based on the marginal increase in energy capture and the marginal increase in system cost (construction and maintenance cost). In modern wind turbines, towers are primarily free standing and made of steel tubing, lattice, or concrete. Towers are supported on large foundations or smaller foundations with tie downs consisting of rock anchors. Anchor bolts securing the tower to the foundation usually extend down to the bottom of the concrete. A ladder and power lift is added for maintenance as well as cables for carrying power, control signals, and operational data between the nacelle yaw slip ring and the ground [1, 3].

Ground equipment includes any components that interface the wind turbine with the electric utility or distribution system. These components include a ground control unit, data recording devices, transformers, circuit breakers, and electronics [3].

2.2 Siting

Wind turbines operate as a part of a larger power producing and consuming system such as large electrical networks, isolated diesel powered grid systems, or as stand-alone power for a specific load. To integrate wind power into these systems, its needs to be considered the ideal location to place wind turbines, turbine installation, turbine operation

and grid connection. Turbines may be installed as a single unit or as a wind farm, or array. The installation of an individual wind turbine or an array of turbines require a significant amount of planning, coordination, and design work [1].

2.2.1 Choosing a Location

Wind turbine siting can be defined as the method in which a wind turbine or wind farm is placed to maximize the cost of energy while minimizing noise, visual impacts and the unit cost of generating electricity [1 ,4]. A siting study needs to be completed before the installation of wind turbines to determine where to locate them. A siting study ranges from the placement of a single wind turbine or of multiple wind turbines in a wind farm to wind prospecting for suitable turbine sites over a wide geographical area.

There are five stages that the siting of a single turbine or wind farm for utility interconnection can be divided into. The first stage is the identification of geographic areas needing further study. Areas with high average wind speeds within the region of interest are identified using a wind resource atlas and any other available wind data. The characteristics of turbine types or designs under consideration are used to establish the minimum useful wind speed for each type. The selection of candidate sites involves the potential windy sites within the region being identified where the installation of one or more wind turbines appears to be practical from engineering and public acceptance standpoints. If there is significant variation within the candidate site, detailed analysis is required to identify the best areas. To evaluate wind resource, topological considerations, ecological observations, and computer modeling may be used while geologic, social and cultural issues are considered [1].

Preliminary evaluation of the candidate site is stage three of siting. At this point each potential candidate site is ranked according to its economic potential and the most viable sites are examined for any environmental impact, public acceptance, safety, and operational problems that would adversely affect their suitability as a wind turbine site. Once the best candidate sites are selected, a preliminary measurement program may be

required. A more comprehensive measurement may be required to choose a final site which includes wind shear and turbulence in addition to wind speed and prevailing wind directions. Stage five, or micro-siting, allows for the exact location of the turbines and their energy production needs to be determined. This is usually completed with computer programs that can model the wind field and the various aerodynamic interactions between turbines that affect energy capture [1].

Micro-siting is the placement of multiple wind turbines in an existing wind farm. Maximizing production is the main objective to adding wind turbines but wind flow, terrain, equipment access, environmental and land use issues, and visual impact must be taken into consideration. To maximize production, careful attention must be paid to the prevailing wind direction(s), wind obstructions from man-made structures or vegetation, and terrain effects. Another important factor is the impact of wind disturbance caused by one turbine on another turbine. To eliminate reduced wind speeds and increased turbulence due to other turbines in the area, turbines should be placed at least two rotor diameters apart in the plane perpendicular to the prevailing wind direction and at least ten rotor diameters apart in the plane parallel to the prevailing wind direction. Due to the turbulent wind flow created by a structure extending vertically twice the height of the structure, turbines should be placed at a distance of at least twenty times the height of any man made structure or vegetation upwind of the project [5].

To estimate the wind resource at the candidate site, there are several approaches used which include ecological methods, the use of wind atlas data, computer modeling, statistical methods, and long term site specific data collection. Ecological methods are most useful during initial site selection and in geographical areas with very little available wind data and works best in coastal regions, mountainous terrain, and river valleys and gorges exhibiting strong channeling of wind. Ecological methods are based on the deformation of vegetation by high average winds which are used to estimate the average annual wind speed and to compare candidate sites even when no wind data are available. The use of wind atlas data from a nearby site may be used to determine local long term

wind conditions. With the creation of computer modeling programs the local wind field of an area can be estimated and wind turbine layout in a wind farm can be optimized. These programs use topographical information and long term upper level meteorological data and nearby surface level wind data. Statistical methods use data from nearby sites to predict the wind resource at a candidate site. Site specific data collection is the most ideal and accurate approach to determining the wind resource but the most costly and time consuming. It measures the wind speed, wind direction, wind shear, turbulence intensity, and temperature at the exact location of interest [1 ,4].

2.2.2 Grid Connection of Traditional Wind Turbine

An electric grid can be separated into generation, transmission, distribution, and supplier feeders. Large wind turbines are most often connected to the distribution system whereas smaller wind turbines are connected into the feeder system. For the traditional means of producing electricity, generation has been provided by large synchronous generators powered by fossil or nuclear fuel or hydroelectric turbines. The synchronous generators respond to load variations, keep the system frequency stable and adjust the voltage and power factor at the generating station as needed. Power is produced at high voltage by these generators which feed current into a high voltage transmission system used to distribute the power over large regions. The transmission systems use high voltage to reduce the losses in the power transmission lines. Local distribution systems operate at lower voltage, distributing the power to local neighborhoods. The voltage is reduced further and the power is distributed through feeders to one or more consumers.

To connect and disconnect the wind turbine to an existing electrical grid requires the use of a switchgear. A switchgear consists of large contactors controlled by electromagnets and should be designed for fast automatic operation. To ensure that turbine problems do not affect the grid or vice versa, protection equipment should be added. Provision should be made for rapid disconnection in case of a short circuit or overvoltage in the wind farm. The wind farm should also be disconnected from the grid

in case of a deviation of the grid frequency from the rated frequency due to a grid failure or a partial or full loss of one of the phases in a three-phase grid. Electrical conductors also connect the wind turbine to the grid as well as being used for transformers and dissipate power because of their electrical resistance. These losses reduce system efficiency and can damage if wires and cables get too hot. Transformers, located at substations, are used to connect electrical circuits at different voltage levels. Grounding equipment protects against lightning damage and short circuits to ground.

Turbine-grid interactions are contingent on the electrical behavior of the turbines under consideration and the electric grids to which the turbines are connected. Introducing a wind turbine to a distribution grid can limit the magnitude of wind power or it can help to support and stabilize a local grid. The four main concerns are steady state voltages, flickering, harmonics, and islanding. Steady state voltage changes can occur in the connected grid system when there is a change in the mean power production and reactive power needs of the turbine or a wind farm. If the grid is weak, there will be an increase in the voltage fluctuations. Flickering take place when there is a disturbance to the network voltage that occurs faster than steady state voltage changes. These changes are fast enough and of a large enough magnitude that there is a noticeable change in the brightness of the lights. Flickers are caused by the connection and disconnection of wind turbines to a grid, the changing of generators, and by torque fluctuations in fixed-speed turbines as a result of turbulence, wind shear, tower shadow, and pitch angles. Variable speed turbines do not usually impose rapid voltage fluctuations on the network but may cause flickering when connected and disconnected. Sinusoidal voltages and currents are created in the distribution system at frequencies that are multiples of the grid frequency by the power electronics in variable wind turbines. The isolation of a self-supporting section of an electric grid is referred to as islanding. Though it poses a low risk, islanding can cause current to flow into a grid fault from a disconnected section of the grid, endangering repair personnel and causing synchronization problems upon reconnection of the islanded grid to the main grid.

2.3 Variability of Wind Energy

The variability of wind in wind generation is a critical factor that makes it difficult to predict the power that will be produced during a given time span. A wind turbine only produces when wind is available. Wind speed varies with the time of day, season, and location above ground making it easier to forecast energy production than power.

2.3.1 Wind Fluctuation

There are several methods in which to determine the variations of wind speed in time. Atmospheric motions vary over a wide range of time scales (seconds to months) and space scales (meters to kilometers). Long-term variability or inter-annual variations in wind occur over a time scale greater than one year[1]. Inter-annual variations have a large effect on long term wind turbine production and are almost as important as estimating the long term mean wind at a site. It has been concluded by meteorologists that it takes 30 years of data to determine long term values of weather or climate and that it takes at least five years to arrive at a reliable average annual wind speed at a given location. Yet one year of record data is generally sufficient to predict long term seasonal mean wind speeds within an accuracy of 10% with a confidence level of 90% [1, 4].

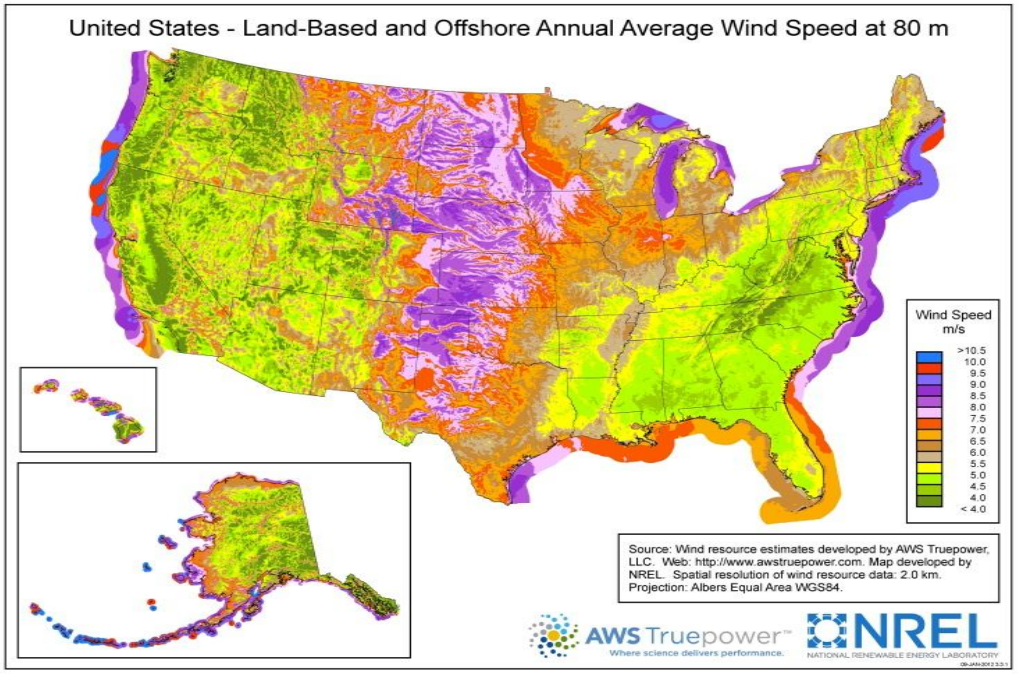

Figure 2.2 Land Based and Offshore Annual Average Wind Speed at 80 m (United States) [6]

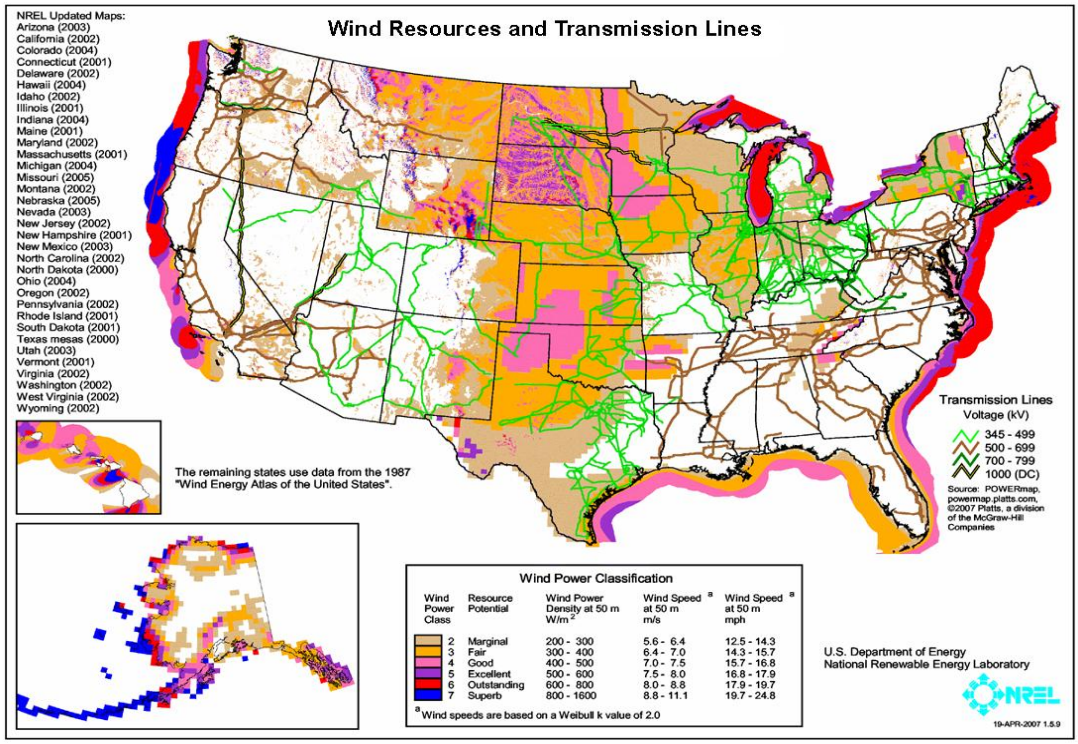

Figure 2.3 Wind Resources and Transmission Lines [6]

Seasonal and monthly variability, or annual variations, have wind speeds that vary from season to season. These changes are common over most of the world. The measure of seasonal variation in the wind at a given site depends on latitude and position with respect to specific features such as land masses and water. Mid latitude continental locations that are well exposed will experience higher winds in the winter and spring, primarily because of large scale storm activity. However mountain passes in coastal areas may experience strong winds in the summer when cool maritime air moves into a hot interior valley. Within a given season, time variations in the wind over periods of one to several days can be caused by disturbances in the overall flow pattern such as cyclonic storms in temperate latitudes and traveling wave systems in the tropics. The above disturbances are capable of causing the output of a wind power station to cycle between zero and rated power several times a month [4].

Wind variations can occur on a diurnal or daily time scale in both the tropical and temperate latitudes and is triggered by the differential heating of the earth's surface during the daily radiation cycle. There is an increase in wind speed during the day created by the variations in radiation flux with the wind speeds lowest during the night. For tropical latitudes, the variations are more pronounced over land areas and during dry seasons when the humidity content of the air is very low and the skies are cloudless. Temperate latitudes have prominent variations over flat land areas. Diurnal variation in wind speed may vary with location and altitude above sea level but generally have the largest changes during the spring and summer and the smallest throughout the winter [1, 4].

Turbulence and gusts cause short term variations in wind speed. Short term variations deal with time intervals of ten minutes or less. Turbulence can be defined as the mixing of cold and warm air in the atmosphere by wind. It can be thought of as random wind speed fluctuations imposed on the mean wind speed which occurs in the direction of the wind, perpendicular to the wind, and vertical to the wind. A gust is a sudden burst of high speed wind and is a discrete event within a turbulent wind field [1].

2.3.2 Power Available from Wind

Power from the wind can be measured in wind power density and is proportional to the area swept by the rotor, density of the air, and the cube of the wind velocity. Power production potential of a wind turbine must take into account the fluid mechanics of the flow passing through a power producing rotor, and the aerodynamics and efficiency of the rotor/generator combination. In practice a maximum of 45% of the available wind energy is harvested by the best modern horizontal axis wind turbines [1].

Available wind power is given by the following equations. The mass flow rate of air $\frac{dm}{dt}$ can be determined through the rotor disk of area *A*. The mass flow rate is a function of air density, ρ, from the continuity equation of fluid mechanics and air velocity *U*.

$$\frac{dm}{dt} = \rho A U \tag{1}$$

To calculate the kinetic energy per unit time, or power of the flow is given by:

$$P = \frac{1}{2}\frac{dm}{dt}U^2 = \frac{1}{2}\rho A U^3 \tag{2}$$

The wind power per unit area, $\frac{P}{A}$ or wind power density is:

$$\frac{P}{A} = \frac{1}{2}\rho U^3 \tag{3}$$

2.4 Components of a Hydraulic Turbine

A gearless hydraulic wind energy harvesting and transfer system is comprised of several components that when assembled, harvest energy by a low speed-high torque wind turbine connected to a high displacement hydraulic pump, which provide hydraulic fluid to a central generation unit composed of hydraulic motors. This system has no

gearbox unlike the traditional wind turbine configurations. Figure 5 illustrates how these components are constructed to harvest energy from the wind.

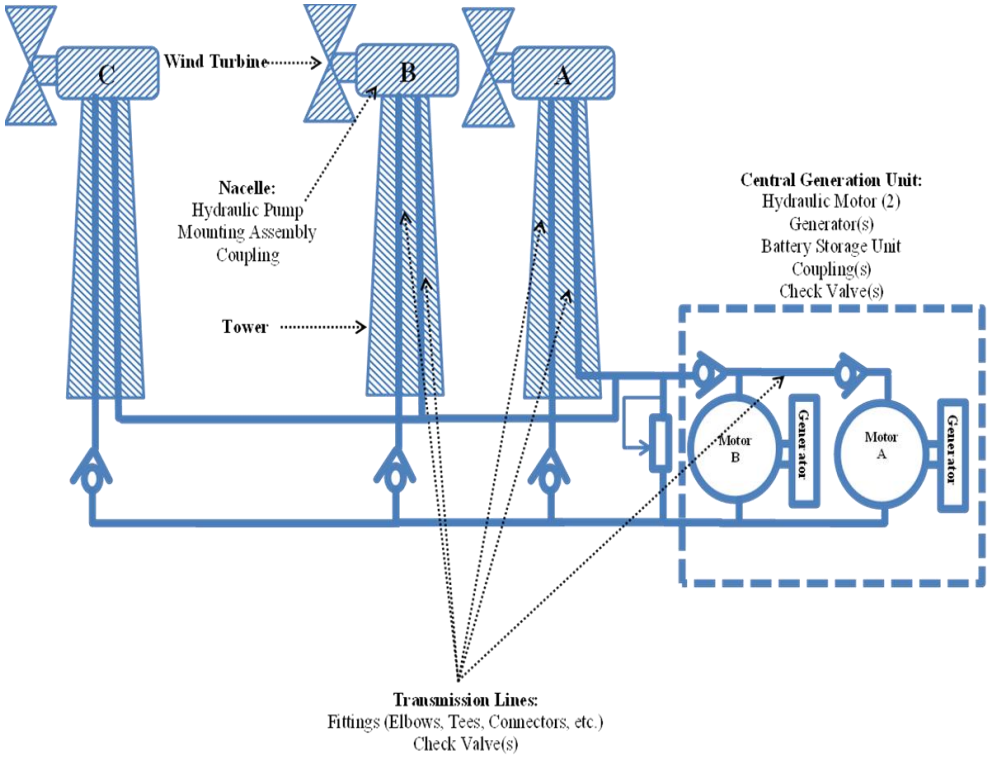

Figure 2.4 A gearless hydraulic wind energy harvesting and transfer system

2.4.1 Hydraulic Pump/Motors

A hydraulic pump converts mechanical energy into hydraulic energy and behaves as the heart of the system. The mechanical energy is delivered to the pump through a prime mover or wind turbine for this application and causes a partial vacuum at the inlet of the pump. This enables atmospheric pressure to force the fluid through the inlet line and into the pump. The pump then pushes the fluid into the hydraulic system. For fluid power applications, a positive displacement pump or fixed displacement proves to be more beneficial than a dynamic or non-positive displacement pump due to its high pressure capabilities, small compact size, high volumetric efficiency, and great flexibility of performance [7]. The amount of fluid discharged per revolution cannot be varied.

Of the various types of positive displacement pumps, an internal gear pump has been chosen for this research. An internal gear pump is comprised of an internal gear, a large exterior gear, a crescent shaped seal, and an external housing. When hydraulic fluid inters the inlet of the pump, the motion of the gears draw fluid from the hydraulic system and forces it around both sides of the crescent seal which acts as a seal between the suction and discharge ports. When the teeth of the gears mesh together on the side opposite of the crescent seal, the fluid is forced to enter the discharge port or outlet of the pump [7].

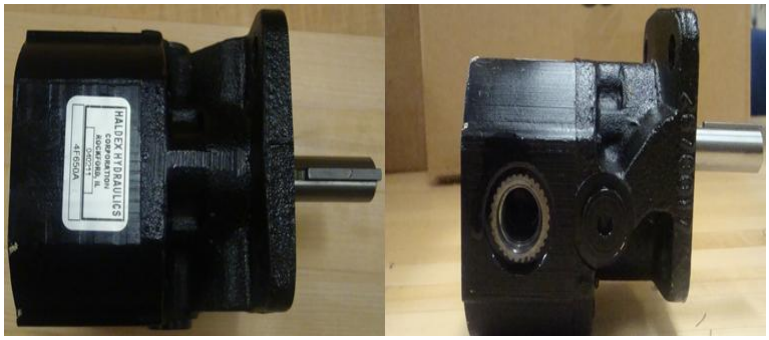

Figure 2.5 Top and side view of hydraulic pump/motor

The hydraulic motor has a similar configuration to the hydraulic pump mentioned above. Like the pump, it is of positive displacement. Motors are driven by the hydraulic fluid while the pumps drive the fluid. This action causes the motor to develop torque and produce continuous rotary motion. Torque is generated due to the hydraulic pressure acting on the surfaces of the gear teeth [7]. Depending on the direction of fluid flow, the gear motor can reverse its direction of rotation. At the inlet of the motor there is high pressure while the motor outlet delivers low pressure creating a large load on the shaft.

2.4.2 Hydraulic Lines/Fittings

Hydraulic lines are used to distribute pressurized fluid through the hydraulic system from hydraulic pump to hydraulic motor. Pipe, seamless tubing and hose are the most frequently used. It is important that the sizing of these lines be designed around the

maximum fluid velocity and the maximum working pressure of the system which is set by the pressure relief valve setting.

Pipes and pipe fittings are designed by the ANSI standard into nominal size and schedule number. The nominal size is neither the outside diameter nor the inside diameter but indicates the thread size for the mating connections. Pipes are designed with male tapered threads to connect to hydraulic components. Pipe joints are sealed by an interference fit between male and female threads, or metal to metal contact, as the pipes are tightened causing one of the major drawbacks with using piping. The pipe must be tightened further to reseal once taken apart. Teflon tape helps in the resealing of pipe joints. Pipes are not the ideal option for bending around obstructions and require numerous types of fittings to make end connections and change direction. The addition of these fittings increases the opportunity for leakage in the hydraulic circuit [7, 8].

Hydraulic tubing has a thinner wall when compared to hydraulic piping and is specified by its outside diameter and for this reason there are other methods than threading that have been developed to connect tubing. These methods include specific types of fittings. It can be bent into almost any shape, reducing the amount of fittings necessary in a hydraulic system and can be reused without any sealing problems. Tubing is sealed through flared or flareless fittings. The three categories of flared fittings include two piece, three piece, and inverted flare. A two piece flare is used to connect lines for lower pressure applications but can weaken the tubing by twisting it as the fitting is tightened. A three piece flare fitting is used for high pressure applications and utilizes a sleeve that is placed on the tubing before it is flared. When the flare nut is tightened, the sleeve absorbs the twisting friction produced by the nut so that only the axial forces are exerted against the flared tube. The inverted flare fitting uses the same concept of the three piece flare but is designed with a male thread on the compression nut. As the wall thickness of the tubing increases to produce tubing with a higher pressure rating, flaring more becomes difficult. For a flareless fitting, a ferrule is pressed against the tubing and

sits into the surface where it cannot be removed. Flareless fittings are subject to leak if under tightened or over tightened [7, 8].

Hose is used when hydraulic components are subject to vibration and movement and is reinforced with either fabric or wire. The fabric reinforced hose has a plastic (rubber) inner tube covered by one or more layers of woven fabric with an outer surface protected by a rubber or plastic covering. The wire reinforced hose has a synthetic rubber outer coating to protect the wire. Pipe and steel tubing should not be connected directly to a hydraulic pump due to the natural vibration of the pump. Over time the vibration can damage the connections and amplify the pump noise. By using hose, the oil's pulsations can be dampened [7].

2.4.3 Hydraulic Valves

Hydraulic circuits are primarily controlled through the use of valves. The three basic types of valves are pressure control valves, directional control valves, and flow control valves.

2.4.3.1 Pressure Relief Valve

Pressure relief valves are utilized to protect the hydraulic system against overpressure due to a valve closing, equipment failure or excessive loading on the motor. The pressure relieve valve is the most commonly used valve and can be found in practically every hydraulic system and is generally the first component downstream from the pump. Its function is to limit the pressure to a specified value, the cracking pressure, by diverting pump flow back to the tank in an open system and to the pump in a closed system. When the hydraulic system reaches the cracking pressure, the resulting hydraulic force exceeds the spring force and the poppet is forced off its seat. Flow is then permitted to travel through the outlet to the tank or pump as long as the high pressure level is maintained.

As the fluid is diverted the pressure inside the system will decrease causing the poppet to be reseated and the valve to close.

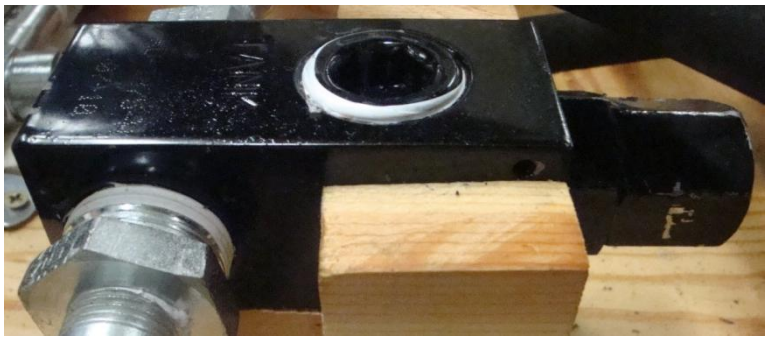

Figure 2.6 Pressure Relief Valve

2.4.3.2 Check Valve

A check valve is a two port directional control valve with one port for fluid entry while the other port is for the fluid to exit. The main purpose of a check valve is to permit free flow in one direction and prevent any flow in the opposite direction. They are analogous to a diode in electric circuits. It is designed with a spring that holds a poppet flush to a seat in the closed position. As fluid passes between the seat and poppet of the valve, the fluid pressure overcomes the spring force. If fluid attempts flow in the opposite direction, the fluid pressure pushes the poppet in the closed position allowing no flow.

Figure 2.7 Check Valve

2.4.3.3 Electronically Adjustable Proportional Flow Control Valve

A proportional flow control valve is an electrically controlled valve that uses a solenoid that produces a force proportional to the current in the coils. By controlling the current in the solenoid coil, the position of the spring-loaded and compensator spool can also be controlled [7]. Both directional and flow control are centralized in a single valve. As hydraulic fluid enters the valve, flow is manipulated to compensate for the load disturbance and to keep speed of the motor as close to the set point as possible.

2.4.4 Hydraulic Transmission System

A Hydraulic Transmission System (HTS) can be defined as a 'pump-controlled motor'. In general, it consists of a fixed displacement pump driven by the prime-mover and one or more either fixed or variable-displacement motors [9]. For this renewable energy application, the prime mover will be a wind turbine. The hydraulic transmission uses the pump to convert the inputted mechanical energy into pressurized fluid through hydraulic hoses and deliver and distribute the motor(s) to convert the potential energy back to mechanical energy [10] without the use of gear boxes. These transmissions can be used to transmit power in applications where the design of a geared drivetrain may be undesirable or impossible [11]. The overall hydraulic system is a closed loop.

A HTS is identified as an exceptional means of power transmission when variable output velocity is required in engineering applications in the fields of manufacturing, automation, and heavy duty vehicles [12]. They offer fast response times, maintain precise velocity under varying loads [13], including high durability and the ability to produce large forces at high speeds [14]. HTS are known for having low inertia of its rotating members permitting fast starting and stopping with smoothness and precision and infinitely variable speed and torque in either direction and over the full speed and torque ranges [7]. It also offers a more decoupled dynamic allowing for multiple input/multiple output configurations not permitted by its electrical counterpart but has had a slow transition into the powering of wind turbines due to lower energy efficiency,

leakage, and noise [15]. The disadvantages associated with a HTS include the decrease in efficiency from the use of a set of gears for the same task, and there is a much softer transmission of power than a mechanical gear train [11]. It is important that the dynamic contribution of the transmission be considered.

A hydraulic transmission system can transfer large amount of power and has more flexibility than a mechanical and electrical system. However, this configuration of hydraulic power transmission has already been tested for wind and resulted in low efficiency. Power transfer efficiency in a hydraulic transmission system is evaluated by examining the pressure losses through a fixed displacement hydraulic pump coupled to a fixed displacement hydraulic motor and generator by way of high pressure hydraulic piping. There are many variables that significantly affect the behavior of a hydraulic transmission system [16], including 1) the pressure differential across the pump and motor, 2) the rotational speed of the pump, motor and prime mover, 3) volumetric displacement of pump and motor, and 4) density, effective bulk modulus, and dynamic viscosity of the fluid. Conventional variable speed hydraulic drives exhibit the ruggedness, weight and controllability required for large wind turbines; however, HTS' generally have acceptable efficiency at full load and drop efficiency as the loading changes, typically having a peak around 60%, as a result of the loss mechanisms internal to pumps and motors [17, 18, 19]. HT's offer an infinite speed ratio range, while gearboxes, though readily available, have the drawback of only offering fixed speed ratios [18].

2.5 System Sensor

2.5.1 Flow Sensor

To observe the amount of flow passing through the hydraulic system, flow sensors can be inserted into the system at designated components. A Hall Effect flow rate sensor

consists of a magnetic multi bladed free spinning rotor mounted inside at right angles to the flow. As flow passes through the sensor, the turbine spins due to the force of the flow. A square wave pulse is generated from magnets embedded in the blades of the rotor each time it passes the Hall Effect sensor. The Hall Effect sensor has a built in pre-amplifier and works well with lower flow rates.

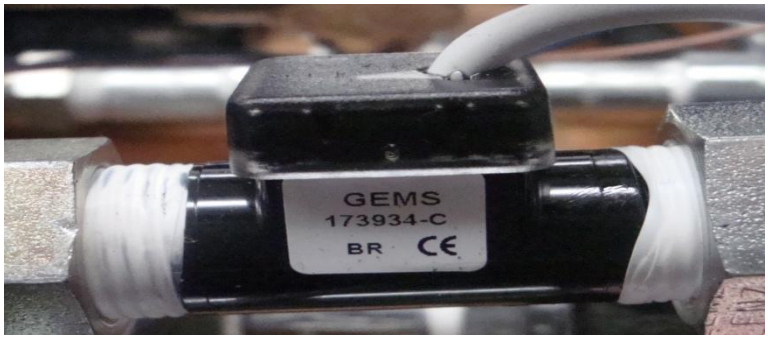

Figure 2.8 Flow Sensor

2.5.2 Pressure Sensor

A pressure sensor produces a signal as a function of the pressure imposed. Acting as a transducer, pressure is converted into an analog electrical signal such as voltage. The conversion of pressure into an electrical signal is achieved by the physical deformation of strain gages which are fused with high temperature glass to a stainless steel diaphragm. A deflection occurs in the diaphragm which introduces strain to the gages when pressure is applied to the sensor. The strain produces an electrical resistance change proportional to the pressure. Detecting is done without the sensor coming in contact with the object eliminating mechanical wear on both.

Figure 2.9 Pressure Sensor

2.5.3 Speed Sensor

A geartooth Hall effect sensor is used to detect the shaft speed of the hydraulic pump and motor. This type of sensor detects the variation in flux found in the air gap between a magnet and passing ferrous gear teeth. In order to detect the passing gear teeth with a Hall Effect sensor, a magnetic source is needed. By arranging a permanent magnet such that the axis of magnetization is pointing toward the surface of the gear teeth this can be accomplished. As a tooth moves across the surface of the magnet the flux will become attracted to the lower reluctance path provided by the ferrous steel structure. When this occurs the flux density measured by the Hall element between the face of the sensor and the gear tooth increases [20]. The change in the magnetic flux produces a square wave pulse which is emitted as a voltage.

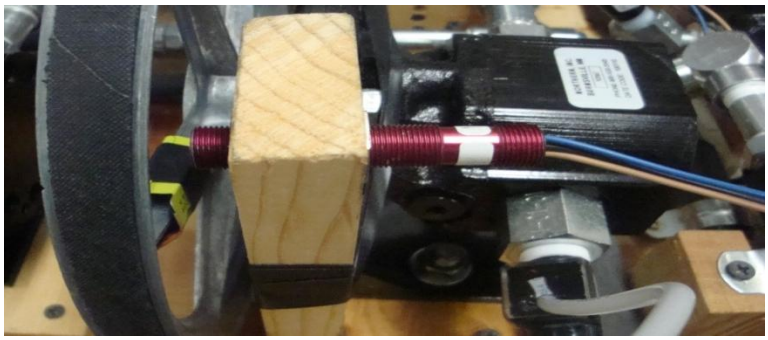

Figure 2.10 Speed Sensor

2.6 Energy Storage

To provide energy storage to this system, a hydraulic accumulator has been integrated. This device is a pressure storage reservoir in which a non-compressible hydraulic fluid is held under pressure by an external source, compressed gas. In a compressed gas accumulator there are two chambers that are separated by an elastic diaphragm. The top chamber contains the compressed gas that provides the compressive force on the hydraulic fluid while the bottom chamber houses the hydraulic fluid and is connected to a hydraulic line in the system. As the volume of the compressed gas changes, the pressure of the gas (and the pressure on the fluid) changes inversely [21]. For example as the pressure increases, the volume of the gas decreases, causing energy to be stored.

An accumulator can maintain system pressure for periods of slight leakage, aid the hydraulic pump in delivering power to the system and absorb pressure interruptions by smoothing out pulsations. However its main function in this system will be to store energy during low demand periods and to respond immediately to temporary demand. A hydraulic accumulator is defined by [7] as device that stores potential energy by means of either gravity, mechanical springs, or compressed gases. The stored potential energy in the accumulator acts as a quick secondary source of fluid power capable of doing useful work as required by the gearless energy transfer system. In this system a compressed gas accumulator has been chosen for further study. Compressed gas accumulators, or hydro-pneumatic accumulators, provide the system with a lightweight energy storage option, the ability to accept both high frequencies and high rates of charging/discharging [22], immediate failure, simple maintenance, and it is not susceptible to contamination. The disadvantages include sizing constraints, sudden failure allowing gas to escape into the system, and difficulties operating at high flow rates. From an environmental standpoint, the use of an accumulator as energy storage proves to be fuel free and has low impact on the environment [23].

The compressed gas accumulator operates in accordance with Boyle's law of gases [7]. Boyle's law states that the pressure of a gas is inversely proportional with its volume if the temperature is held at a constant and is defined by the following equation:

$$pV^n = k \tag{4}$$

where p is system pressure, V is the volume of the gas, and k is a constant. When a change has been introduced to the system, the resulting equation is used to determine pressure or volume of an ideal gas:

$$p_1 V_1^n = p_2 V_2^n \tag{5}$$

p_1 and V_1 are the original pressure and volume and p_2 and V_2 are the pressure and volume resulting from the change.

$$V_2 = V_1 (\frac{p_1}{p_2})^{\frac{1}{n}} \tag{6}$$

$$\Delta V = V_1 - V_2 \tag{7}$$

$$\Delta V = V_2 [1 - (\frac{p_1}{p_2})^{\frac{1}{n}}] \tag{8}$$

Typically the pressure in the gas chamber is equal to the pressure in the fluid chamber but if the pressure at the accumulator inlet drops below the accumulator's precharge value, the gas chamber gets isolated from the system. In this case the pressure in the gas chamber remains constant and equal to the precharge value, while the pressure at the inlet depends on the pressure in the system to which the accumulator is connected. If the pressure at the inlet builds up to the precharge value or higher, the chamber starts interacting again [24].

3. SYSTEM LOSS AND EFFICIENCY

Power transfer efficiency in a hydraulic transmission system (HTS) is evaluated by examining the pressure losses through a fixed displacement hydraulic pump coupled to a fixed displacement hydraulic motor and generator. The wind turbine is of variable speed which offers increased efficiency in capturing the energy from the wind over a wider range of wind speeds. [25]. The power transferred from the wind turbine to the generator is important to maintaining the system's power balance and droop frequency control when connected to a network and to ensure that the maximum [26, 27] output power is obtained for a certain wind speed.

3.1 Energy Equation

The Bernoulli equation is one of the most useful and referred to as the most fundamental relationship of fluid mechanics [7, 28, 29]. It is the sum of the piezometric pressure and kinetic pressure and is derived by applying Euler's equation, or the conservation of energy law, along a streamline. There are several restrictions that apply when using Bernoulli's equation and can only be applied to certain flow conditions. These assumptions include a flow that is steady, frictionless and inviscid (zero viscosity). The fluid must perform no work and has no work performed on it, and is incompressible. Euler's equation can be defined as the sum of the forces acting on a fluid element to the element's acceleration according to Newton's second law. To derive Euler's equation a cylindrical element is considered in an arbitrary direction l with cross sectional areal ΔA in a flowing fluid. The element oriented at an angle α with respect to the horizontal plane. The element has been isolated from the flow field and is being treated as a "free body" where the presence of the surrounding fluid is replaced by pressure forces acting

on the element which is being accelerated in the *l*-direction. Utilizing Newton's second law in the *l*-direction [30]:

$$\sum F_l = ma_l \tag{9}$$

$$F_{pressure} + F_{gravity} = ma_l \tag{10}$$

where the mass of fluid element is

$$m = \rho \Delta A \Delta l \tag{11}$$

and the net force due to pressure in the *l*-direction is

$$F_{pressure} = p\Delta A - (p + \Delta p)\Delta A = -\Delta p \Delta A \tag{12}$$

The piezometric pressure is represented by p, and ρ is the fluid density. The force due to gravity with the component of weight in the negative *l*-direction can be written as

$$F_{gravity} = -\Delta W_l = -\Delta W \sin\alpha \tag{13}$$

$\sin\alpha = \frac{\Delta z}{\Delta l}$ illustrates the relationship between angle α, Δz and Δ*l*. $F_{gravity}$ then becomes

$$F_{gravity} = \Delta W \frac{\Delta z}{\Delta l} \tag{14}$$

The weight of the element is $\Delta W = \gamma \Delta l \Delta A$. Specific weight, γ, is the gravitational force per unit volume of fluid or simplified weight per unit volume. Substituting the mass of the element and the forces on the element into Equation (10) yields:

$$-\Delta p \Delta A - \gamma \Delta l \Delta A \frac{\Delta z}{\Delta l} = \rho \Delta l \Delta A a_l \tag{15}$$

Dividing through by ΔAΔ*l*, Equation (7) becomes

$$-\frac{\Delta p}{\Delta l} - \gamma \frac{\Delta z}{\Delta l} = \rho a_l \tag{16}$$

The differential equation for acceleration in the *l*-direction is determined by taking the limit as Δ*l* approaches zero

$$-\frac{\partial p}{\partial l} - \gamma \frac{\partial z}{\partial l} = \rho a_l \tag{17}$$

Since γ is constant for an incompressible flow, then

$$-\frac{\partial}{\partial l}(p + \gamma z) = \rho a_l \tag{18}$$

Taking Euler's Equation (18) and replacing direction *l* with *s*, the distance along a path line, and replacing acceleration a_l with a_t, this equation is transformed into

$$-\frac{\partial}{\partial s}(p + \gamma z) = \rho a_t \text{ where } a_t = V\frac{\partial V}{\partial s} + \frac{\partial V}{\partial t} \tag{19}$$

The local acceleration is zero for a steady flow making the path line a streamline. For a streamline, the properties only depend on *s*. The partial derivatives are then converted into ordinary derivatives

$$-\frac{d}{ds}(p + \gamma z) = \rho V \frac{dV}{ds} = \rho \frac{d}{ds}(\frac{V^2}{2}) \tag{20}$$

Moving all the terms to one side and integrating yields the Bernoulli's equation with C being a constant

$$p + \gamma z + \rho \frac{V^2}{2} = C \tag{21}$$

When (21) is divided by the specific weight, an equivalent form the Bernoulli's equation is formed where $\frac{p}{\gamma}$ is the pressure head, *z* is the elevation head (potential) and $\rho \frac{V^2}{2g}$ is the velocity head (kinetic)

$$\frac{p}{\gamma} + z + \frac{V^2}{2g} = C \tag{22}$$

To illustrate the flow through a pipe with two distinct locations (Subscripts 1 and 2) in the flow the following equation is used

$$z_1 + \frac{p_1}{\gamma} + \frac{\upsilon_1^2}{2g} = z_2 + \frac{p_2}{\gamma} + \frac{\upsilon_2^2}{2g} \tag{23}$$

System behavior can be determined for ideal conditions and used to target maximum performance.

In a hydraulic system, the pipes as well as other components such as valves and pipe fittings create frictional losses. To take into account these frictional losses, the Bernoulli Equation (23) was extended. The extended Bernoulli's equation or energy equation is expressed as:

$$z_1 + \frac{p_1}{\gamma} + \frac{\upsilon_1^2}{2g} = z_2 + \frac{p_2}{\gamma} + \frac{\upsilon_2^2}{2g} + \sum h_{losses} \tag{24}$$

For a system containing a pump to supply energy to maintain a specific amount of flow or to extract energy through the use of a motor, additional terms must be added

$$z_1 + \frac{p_1}{\gamma} + \frac{\upsilon_1^2}{2g} + \sum H_{pump} = z_2 + \frac{p_2}{\gamma} + \frac{\upsilon_2^2}{2g} + \sum H_{motors} + \sum H_{losses} \tag{25}$$

where H_p is the pump head, H_m is the motor head, and H_L is the head loss. All other components of this equation will be discussed in detail later in Section 3.2 of this chapter.

The Energy equation is similar to the Bernoulli equation but is not the same equation in that the Energy equation is applied to an inlet section and an outlet section in a pipe and then terms are equated as they apply to the pipe and for a steady, viscous, incompressible flow in a pipe. The Bernoulli's equation is applied by selecting two points on a streamline and then equating terms at these points and is for a steady, incompressible, inviscid flow [30]. Figure 3.1 displays how the energy equation would be applied between two points throughout a double turbine hydraulic system performing a complete energy analysis, determining frictional losses in valves and fittings, and head losses in pipes, pumps and motors. Table 3.1 provides a breakdown of points on the streamline and the components on each streamline.

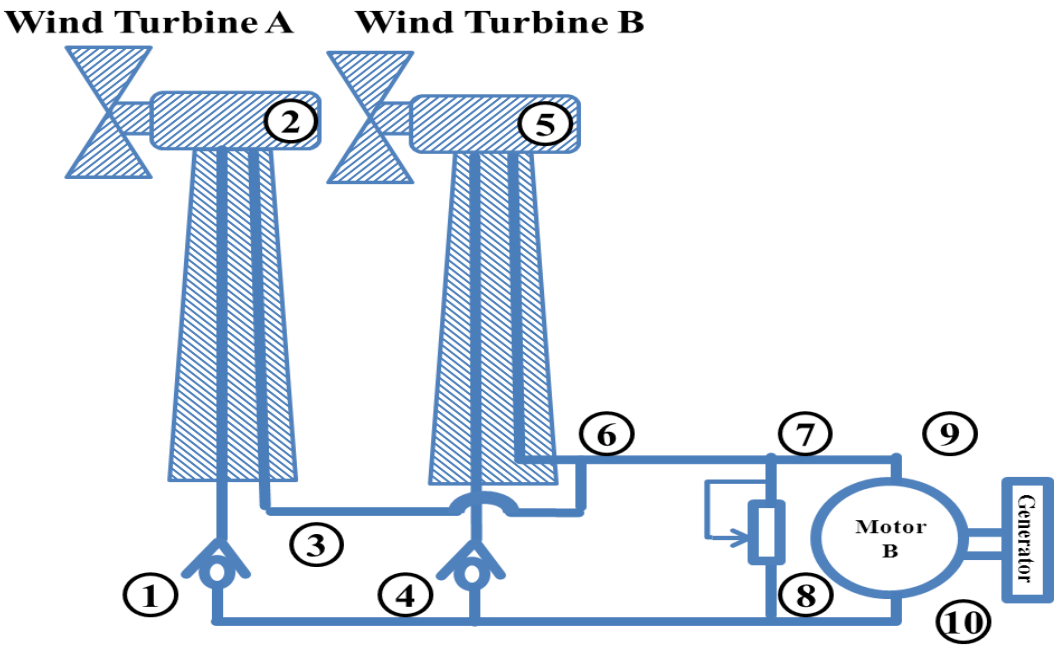

Figure 3.1 Schematic for the calculations of frictional losses in a hydraulic system

Table 3.1 Energy equation points on streamline

Points on Streamline	Components along Streamline
1-2	Check Valve, Pipeline, Hydraulic Pump
2-3	Pipeline, Bend
3-6	Pipeline, Bend
4-5	Check Valve, Pipeline, Hydraulic Pump
5-6	Pipeline, Bend
6-7	Pipeline
7-8	Pipeline, Pressure Relief Valve
7-9	Pipeline, Bend
9-10	Hydraulic Motor
10-1	Pipeline

3.2 Loss Modeling

The main cause of energy losses in fluid power systems is produced by friction. For this research friction can be defined as the resistance to flow which is a measure of the viscosity of fluid. The greater the viscosity of fluid, the less readily it flows and the more energy needed to move the fluid. This energy loss is transferred into heat (wasted energy), which dissipates into the surrounding air. It results in a loss of potential energy and surfaces as a loss in pressure or head [7].

The loss in head is the decline in the overall head or pressure (sum of the elevation head, velocity head, and pressure head) of the fluid as it moves through a fluid system. Head associates the energy in an incompressible fluid to the height of an equivalent static column of that fluid. Head loss is separated into two main components, losses in pipes and losses in valves, bends, and fittings [7]. Head loss in pipes can be computed with the use of the Darcy-Weisbach equation. The Darcy-Weisbach illustrates how head loss is the related to the friction factor, pipe length to diameter ratio, and velocity. It can be utilized for both laminar and turbulent flow that is fully developed and steady through round or non-round pipes.

The Darcy-Weisbach equation is derived by assuming a fully developed and steady flow in a round tube of a constant diameter D. A cylindrical control volume of diameter D and length ΔL is placed inside the pipe. A radial coordinate in the r-direction and an axial coordinate in the stream wise direction, s-direction, is also defined. Applying the momentum equation to the fully developed and steady flow in a round tube gives

$$\sum F = \frac{d}{dt}\int_{cv} v\rho dV + \int_{cs} v\rho \mathrm{V} \bullet dA \tag{26a}$$

(Net forces) = (Momentum accumulation rate) + (Net efflux of momentum) (26b)

Both the momentum accumulation term and the net efflux of momentum is zero when analyzing each of the above three terms in the s-direction thus reducing Equation 26a and 26b to $\sum F = 0$. Summing the forces in the s-direction results in:

$$F_{pressure} + F_{shear} + F_{weight} = 0 \tag{27a}$$

$$(p_1 - p_2)(\frac{\pi D^2}{4}) - \tau_0(\pi D \Delta L) - \gamma[(\frac{\pi D^2}{4})\Delta L]\sin\alpha = 0 \tag{27b}$$

Considering $\sin\alpha = \frac{\Delta z}{\Delta l}$,

$$(p_1 + \gamma z_1) - (p_2 + \gamma z_2) = \frac{4\Delta L \tau_0}{D} \tag{28}$$

Applying the energy Equation 25 to the cylindrical control volume and recognizing that $H_p = H_m = 0, V_1 = V_2$, and $\alpha_1 = \alpha_2$, the energy equation reduces to

$$(p_1 + \gamma z_1) - (p_2 + \gamma z_2) = \gamma H_l \tag{29}$$

Combining Equations 28 and 29 and replace ΔL by L yields

$$H_l = \frac{4L\tau_0}{D\gamma} \tag{30}$$

Rearranging the right side Equation (30) results in

$$H_l = (\frac{L}{D})(\frac{4\tau_0}{\rho V^2/2})(\frac{\rho V^2/2}{\gamma}) = (\frac{4\tau_0}{\rho V^2/2})(\frac{L}{D})(\frac{V^2}{2g}) \tag{31}$$

$$f = \frac{\tau_0}{\rho V^2/2} \tag{32}$$

$$H_L = f\left(\frac{L}{D}\right)\left(\frac{V^2}{2g}\right) \tag{33}$$

where *f* is the frictional factor, τ_0 is the sheer stress applied to the pipe wall, ρ is the fluid density, L is the length of pipe, D is the pipe inside diameter, V is the average fluid velocity, and g is the acceleration of gravity. Head loss is the conversion of useful mechanical energy to waste thermal energy through viscous action between fluid particles [30]. Frictional factor *f* is a dimensionless quantity that is used to illustrate the frictional losses in pipe flow. It is associated with the shear stress applied to the walls of the pipe [28].

When a real fluid flows through the interior of a pipe, the velocity profile presents a maximum at the center as a consequence of the viscosity. The shear stress of the pipe wall is directly proportional to the velocity gradient [28, 30, 31]:

$$\tau_0 = -\mu\frac{dV}{dr} \tag{34}$$

$$-\mu\frac{dV}{dr} = \frac{r}{2}\left(-\frac{dp}{dz}\right) \tag{35}$$

$$\frac{dp}{dz} = \frac{p_2 - p_1}{L} = \frac{\Delta p}{L} \tag{36}$$

$$\int_0^V dv = -\frac{1}{2\mu}\left(-\frac{dp}{dz}\right)\int_a^r r dr \tag{37}$$

$$V = \frac{1}{4\mu}\left(-\frac{dp}{dz}\right)\left(a^2 - r^2\right) = \frac{-\Delta p}{4\mu L}\left(a^2 - r^2\right) \approx \frac{Q}{A} \tag{38}$$

where μ is the viscosity of the fluid, *r* is any radial location, *L* is a finite length of pipeline, *p* is the pipe pressure, *a* is the radius of the pipe, A is the area of the pipe, and *Q* is the volumetric flow rate. It can be concluded that the smaller the pipe diameter, the larger the value of fluid velocity.

The volumetric flow rate, *Q*, is the volume of fluid that passes through an area per unit time. It is based on a constant flow velocity over the cross-sectional area [30] and can be obtained by determining the cross section of the pipe and integrating:

$$dQ = VdA = 2\pi rVdr \tag{39}$$

$$Q = \int_0^Q dQ = 2\pi \int_0^a \frac{1}{4\mu}\left(-\frac{dp}{dz}\right)\left(a^2 - r^2\right)rdr \tag{40}$$

$$Q = \frac{\pi a^4}{8\mu}\left(-\frac{dp}{dz}\right) = \frac{\pi a^4}{8\mu}\frac{p_1 - 2}{L} = \frac{\pi a^4(-\Delta p)}{8\mu L} \tag{41}$$

The above equation is a relation for pipe flow known as the Hagen-Poiseuille law.

The friction factor *f* can also be determined through the use of the Reynolds Number (RE) $f = \frac{64}{RE}$. It is the ratio between inertial forces and viscous forces and is dimensionless. The Reynolds Number is utilized to determine the conditions governing the transition from laminar flow to turbulent flow [7] or vice versa. A change from laminar flow to turbulent flow takes place approximately at 2000. A flow with a Reynolds Number greater than 2000 and less than 4000 is unpredictable and is considered transitional because it changes between laminar and turbulent states. Turbulent flow has a Reynolds Number greater than 4000.

$$RE = \frac{V\rho D}{\mu} = \frac{VD}{\nu} = \frac{4Q}{\pi D\nu} \tag{42}$$

where μ is, the absolute viscosity, and ν is the kinematic viscosity. Table 3.2 illustrates how the flow is characterized based on the value of the Reynolds Number [28].

Table 3.2 Dependence of pipe flow regime on the Reynolds Number

Approximate Value of Reynolds Number	Flow Regime	Pressure Gradient is Proportional to
< 2,000	Laminar	Q
2,000 - 4,000	Transition	Variable
> 4,000	Turbulent	$Q^{1.8} - Q^2$

Laminar flow occurs when adjacent fluid layers move smoothly with respect to each other and has a smooth, parabolic velocity distribution. Turbulent flow is unsteady and characterized by intense cross-stream mixing. A near uniform velocity distribution occurs across the pipe because the high velocity fluid at the pipe center is transported by turbulent eddied across the pipe to the low velocity region near the wall. Unsteady flow causes fluctuations at any point in the pipe with time [30]. It is assumed that if the Reynolds number lies within the transition or critical zone, the flow is considered as turbulent. Turbulent flow results in a larger amount of losses, therefore hydraulic systems are generally designed to operate in a laminar flow region as in this case. Table 3.2 also indicates that the when there is restriction in the flow, there is a pressure drop across the component that depends on the geometry of the restriction and has been observed to be proportional to the flow rate squared [31].

The main source of energy loss in system occurs in valves and fittings. This is due to the change in the cross section of the flow path and in the change in the direction of the flow [7]. The head losses in fittings and valves are proportional to the square of the velocity of the fluid [7, 32].

$$H_L = K\left(\frac{V^2}{2g}\right) \tag{43}$$

$$K = \frac{\Delta h}{(\frac{V^2}{2g})} = \frac{\Delta p}{(\frac{\rho V^2}{2})} \tag{44a}$$

$$K = \frac{drop\_in\_piezometric\_head\_across\_component}{velocity\_head} = \frac{pressure\_drop\_due\_to\_component}{kinetic\_pressure} \tag{44b}$$

where K is the loss coefficient of the fitting or valve. The loss coefficient accounts for the loss in mechanical energy caused by viscous effect on a flowing fluid through a partially open valve or pipe bend. With the use of the Darcy-Weisbach equation it can be illustrated that the head loss in a pipe is proportional not only to the square of the fluid but also to the length of the pipe due to fluid friction. This length of a pipe is regarded as the equivalent length of a particular fitting or valve. For the equivalent length technique the head loss for a fitting or valve is set equal to the head loss of the pipe:

$$H_{L(valveorfitting)} = H_{L(pipe)} \tag{45}$$

$$K\left(\frac{V^2}{2g}\right) = f\left(\frac{L_e}{D}\right)\left(\frac{V^2}{2g}\right) \tag{46}$$

$$L_e = \frac{KD}{f} \tag{47}$$

where L_e is the equivalent length or entrance length. The entrance length is the distance required for flow to develop in a pipe and depends on the shear stress that acts on the pipe wall. Until a flow is fully developed it is called a developing flow and is defined as the region in which the velocity distribution changes in the stream wise direction as viscous effects cause the plug type profile to gradually change into a parabolic profile. Once the

parabolic distribution is attained, the flow becomes fully developed. Near the pipe entrance, the radial velocity gradient is high creating large shear stress for laminar flow. As the velocity profile progresses to a parabolic shape, the velocity gradient and the wall shear stress decrease until a constant value is achieved. The entry length is defined as the distance at which the shear stress reaches to within 2% of the fully developed value [30].

Pump head or motor head can be determined using the following equation. H_p, pump head, represents the energy per pound of fluid added by the pump, while H_m, motor head, represents the energy per pound of fluid removed by the hydraulic motor

$$H_p = H_m = \frac{HydraulicPower(W)}{Q(m^3/s)*\gamma} = \frac{3950*(HHP)}{Q(gpm)*\gamma} \tag{48}$$

The loss in pressure for each component of head loss can be determined with the following:

$$p_L = \gamma H_L = (SG*\gamma_{H2O})*H_L \tag{49}$$

where SG is the specific gravity of the fluid, and γ_{H2O} is the specific weight of water.

3.3 Hydraulic Power

Hydraulic power or fluid power is the use of pressurized fluid to generate, transmit and control power. Fluid is sent to a hydraulic motor through way of a hydraulic pump that converts hydraulic power into a mechanical output capable of doing work on a load. Both pump and motor lose energy due to mechanical friction, viscous dissipation, and leakage [30]. Hydraulic power can be defined as the following

$$Hydraulic\_Power = HHP = pQ \tag{50}$$

where p is pressure in PSI and Q is the volumetric flow rate in gallons per minute (GPM). In this research, there will be the use of electrical power, hydraulic power, and mechanical power which are all typically involved in hydraulic systems. This is illustrated in Figure 3.2. This flow chart indicates how the power created by an electric motor can be used to rotate the shaft of a hydraulic pump creating pressure and a flow of fluid to produce a hydraulic power that is then delivered to a hydraulic motor. The hydraulic power is then converted to mechanical power and is applied to an external load.

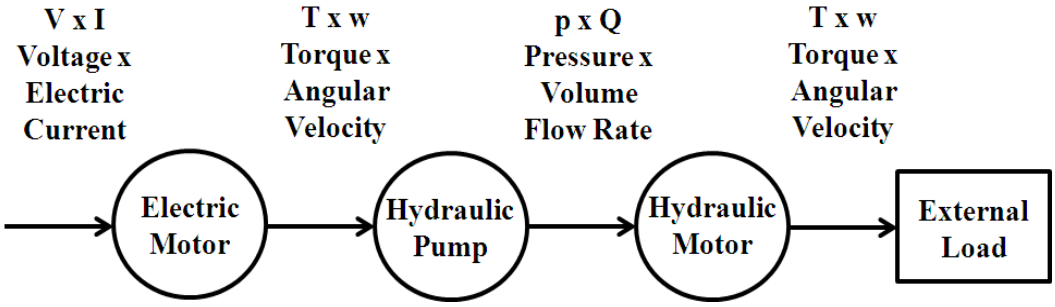

Figure 3.2 Conversion of power from input electrical to mechanical to hydraulic to output mechanical in hydraulic system [7]

Figures 3.3 and 3.4 demonstrate how power is distributed throughout a single-wind turbine hydraulic system and a double turbine hydraulic system.

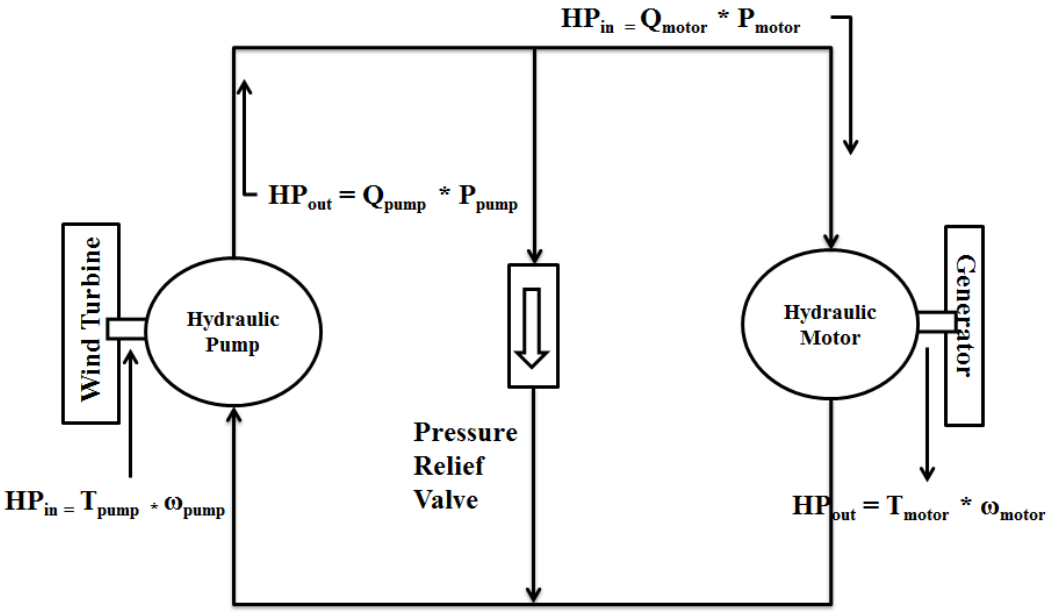

Figure 3.3 Power transfer of single-wind turbine

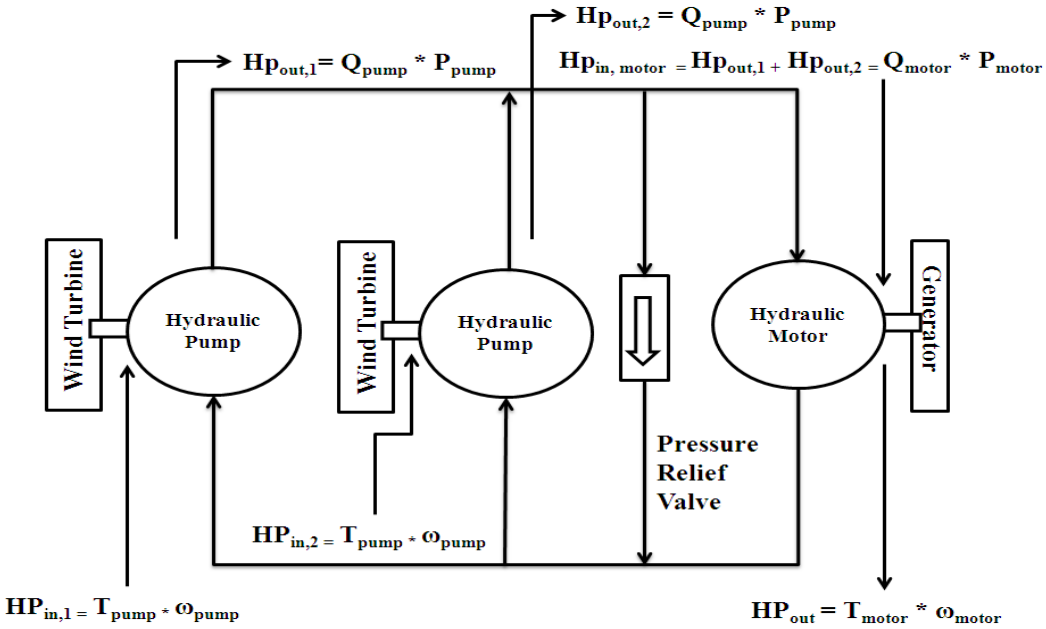

Figure 3.4 Power transfer of double-wind turbine

3.4 System Efficiency

Efficiency is equal to the output power divided by the input power. It is used to calculate power loss in a hydraulic system and is always less than 100%. Efficiency determines the amount of power that is actually delivered in comparison to the power received [7]. The overall efficiency of the system seen in Figures 3.3 and 3.4, are related to mechanical loss and volumetric loss which is due to the fluid's viscosity. Volumetric losses take place when there is internal leakage as the fluid travels through the gear teeth of a pump or motor. Volumetric efficiency for a gear pump or motor typically ranges from 80% to 90%. Mechanical efficiency accounts for the mechanical losses caused from gears, bearings, and mating parts. There is a reduction in the power transferred from the shaft to the fluid in the pump or from the shaft of the motor to the pump. The efficiency of a pump or motor can be calculated as follows:

$$\eta_{overall} = \eta_{vol} * \eta_{mech} = \frac{HP_{output}}{HP_{input}} * 100 \tag{51}$$

where η_{vol} is the volumetric efficiency and η_{mech} is the mechanical efficiency. The hydraulic system used in this research converts mechanical energy from a prime mover into fluid flow and pressure causing work to be performed on an external load by a motor. Pressure is generated due to the restriction of flow in the hydraulic system.

4. MATHEMATICAL MODELING OF SYSTEM

A mathematical model of the system is required to consider the system dynamics which can be used in control system development. With the mathematical model of this system, an enhanced understanding of the hydraulic transmission system through analysis can be gained. It can be determined which factors are of greater importance in the system and how different parts of the system are related.

4.1 One Wind Turbine/One Central Generation Unit

The schematic diagram of the hydraulic transmission system being considered for this work is given in Figure 4.1. The fixed displacement pump, driven by a wind turbine, is coupled to a fixed displacement hydraulic motor to which it supplies hydraulic power. A pressure relief valve is used to protect the system from excessive pressure.

4.2 Multiple Wind Turbine/One Central Generation Unit

Figure 4.2 provides an illustration of the second configuration being investigated to increase system efficiency. A second hydraulic pump, also driven by a wind turbine, has been added to the configuration in Figure 4.1.

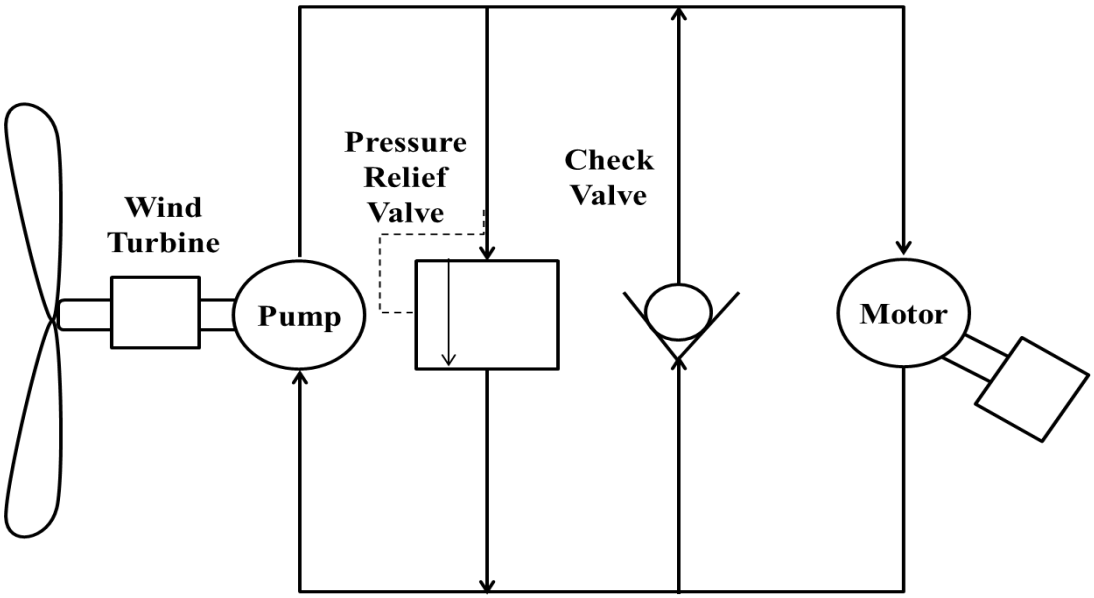

Figure 4.1 Hydraulic wind power transmission system, single-wind turbine schematic

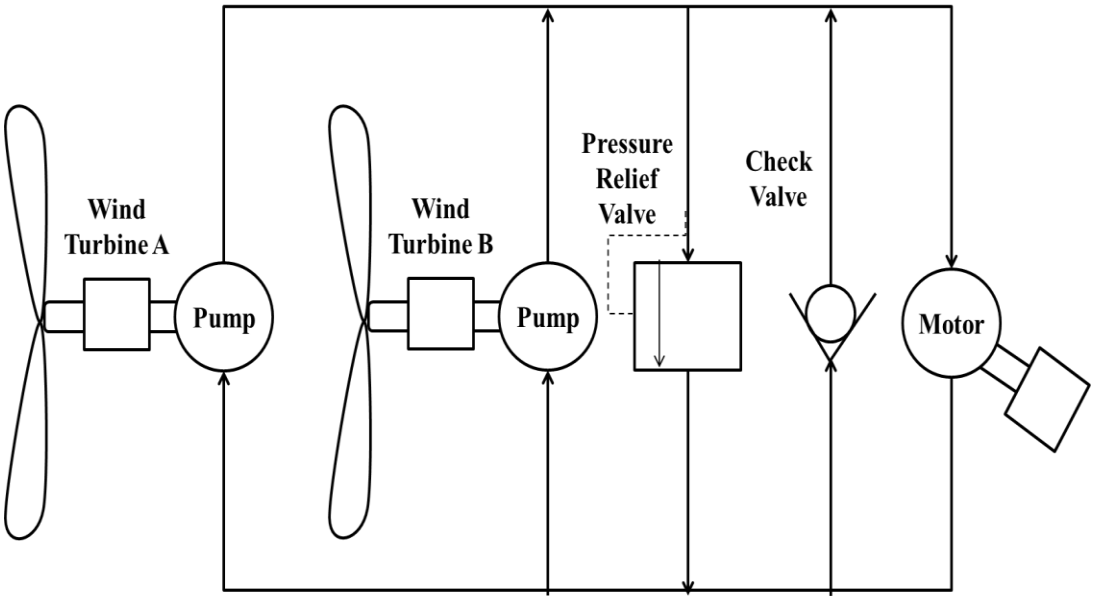

Figure 4.2 Hydraulic wind power transmission system, double-wind turbine schematic.

4.3 Mathematical Modeling of Components

The components of the hydraulic power transfer circuit and their governing equations are illustrated below.

4.3.1 Fixed Displacement Pump

In the hydraulic transmissions, shown in Figure 4.1 and Figure 4.2, the output shaft velocity of the hydraulic motors is controlled by the flow rate of the hydraulic fluid, which is supplied from the hydraulic pump(s) [10]. As mentioned earlier, the pump is driven by a wind turbine. In this model, the flow rate is being controlled by varying the shaft velocity of the fixed displacement pump(s).

The flow that a fixed displacement pump generates is modeled as a function of pump displacement, shaft velocity, and the leakage coefficient [33] as

$$Q_p = D_p \omega_p - k_{leak} P \tag{52}$$

$$k_{leak} = \frac{k_{HP}}{\nu \rho} \tag{53}$$

$$k_{HP} = \frac{D \omega_{nom} (1 - \eta_v) \upsilon_{nom} \rho}{p_{nom}} \tag{54}$$

where Q_p is the pump flow rate, D_p is the pump displacement, ω_p is the angular velocity of the pump, k_{leak} is the leakage coefficient, P is the system pressure, and k_{HP} is the Hagen-Poiseuille coefficient which is calculated using the following parameters: nominal angular velocity (ω_{nom}), nominal fluid kinematic viscosity (υ_{nom}), nominal pressure (p_{nom}), fluid density (ρ), and *as* volumetric efficiency (η_v).

4.3.2 Pressure Relieve Valve

The pressure relieve valve is modeled as a close/open valve energized at a preset pressure value. The valve is open if the pressure exceeds the preset value, and for pressures below this value, the valve is closed. The following two equations are given for passing flow rate through the pressure relieve valve:

$$Q_v = k_{zb}(P - P_b) \qquad \text{if } P > P_b \tag{55}$$

$$Q_v = 0 \qquad \text{if } P \le P_b \tag{56}$$

where Q_v is the flow rate through the valve, k_{zb} is the flow discharge coefficient, and P_b is the valve preset pressure setting.

4.3.3 Fluid Compressibility

In connecting the wind turbine to the motors in our prototype, we have used flexible hoses. The dynamics of these pressurized hoses are modeled as volume with a fixed bulk modulus. The fluid compressibility [13, 34] relation can be illustrated as

$$\frac{dP}{dt} = \frac{\beta}{V}(Q_p - Q_m - Q_v) \tag{57}$$

where β is the fluid bulk modulus and V is the fluid volume subjected to pressure effect.

This equation also provides the resultant pressure at a given flow rate. It is assumed that pressure drop in the hydraulic hose is negligible.

4.3.4 Hydraulic Motor and Load

Like hydraulic pumps, the governing equation of a motor is a function of displacement factor, leakage coefficient, and flow rate and is expressed as [35]

$$Q_m = D_m \omega_m + k_{leak} P \tag{58}$$

where Q_m is the pump flow rate, D_m is the pump displacement, and ω_m is the angular velocity of the motor.

The motor's moment of inertia, damping coefficient, and the load connected to the motor's shaft determine the torque dynamics, and can be expressed as

$$T_m = I_m \dot{\omega}_m + B_m \omega_m + T_l \tag{59}$$

$$T_m = \frac{D_m P}{2\pi} \tag{60}$$

where T_m is the torque produced by the motor, I_m is the inertia moment of motor, B_m is the damping coefficient of motor, and T_l is the load torque.

The output shaft velocity of the motor under loading condition (speed drop due to loading) in the mathematical modeling of the system can be determined using Equation (59) as

$$I_m \dot{\omega}_m = T_m - B_m \omega_m - T_l \,, \tag{61}$$

$$\dot{\omega}_m = \frac{T_m - B_m \omega_m - T_l}{I_m} \tag{62}$$

4.3.5 Hydraulic Transmission System

The HTS comprises of a combination of the mathematical model of the system components mentioned above. The mathematical expression of the overall system can be obtained from the block diagram shown in Figure 4.3 and Figure 4.4 for above configurations. Equations (57) and (62) are the structure for which the mathematical model of the HTS system is built. We have used Matlab/Simulink to carry out the simulation results and to solve these nonlinear equations.

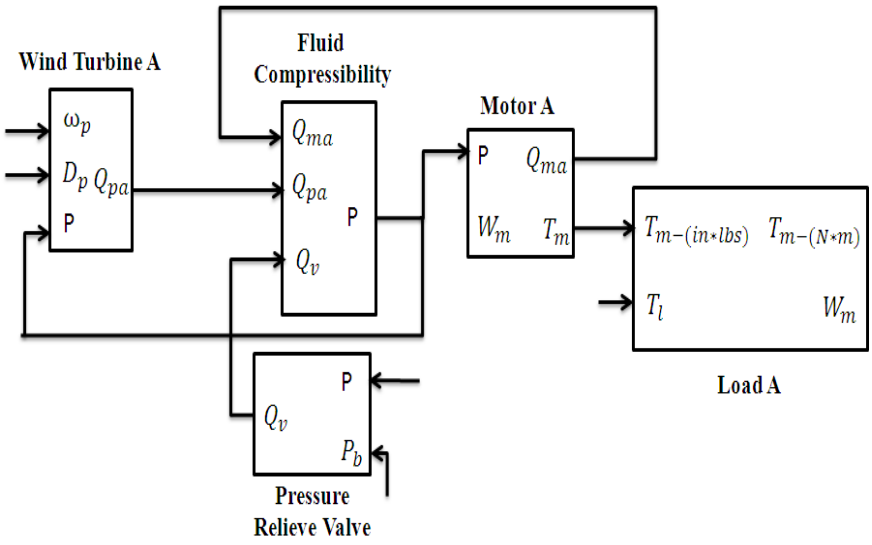

Figure 4.3 Mathematical Model Block Diagram
(One Pump, One Motor) of Hydraulic Power Transfer System

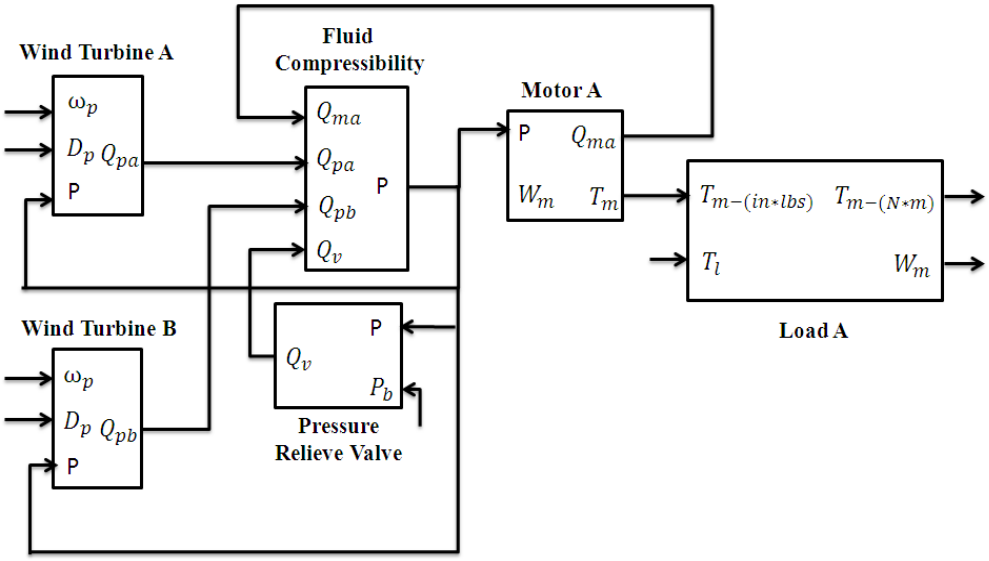

Figure 4.4 Mathematical Model Block Diagram
(Two Pumps, One Motor) of Hydraulic Power Transfer System

5. VALIDATION OF MODELING USING SIMULATION SOFTWARE

5.1 SimHydraulics Toolbox

To validate the mathematical model presented in Chapter 4, a hydraulic system was created with Matlab's SimHydraulics toolbox. SimHydraulics is a tool used for modeling and simulating hydraulic power and control systems in the Matlab/Simulink environment. It provides an extensive library of hydraulic components and building blocks that can be connected to behave as physical networks. SimHydraulics uses block modeling with each block being defined by inserting manufacturing specifications of each component. Sensors in SimHydraulics return the pressure differential, flow of the hydraulic fluid, and shaft velocity of the pump and motor. Figure 5.1 and 5.2 illustrates how the hydraulic components are assembled to represent the wind turbine hydraulic power transfer system of a single wind turbine and multi-wind turbine system.

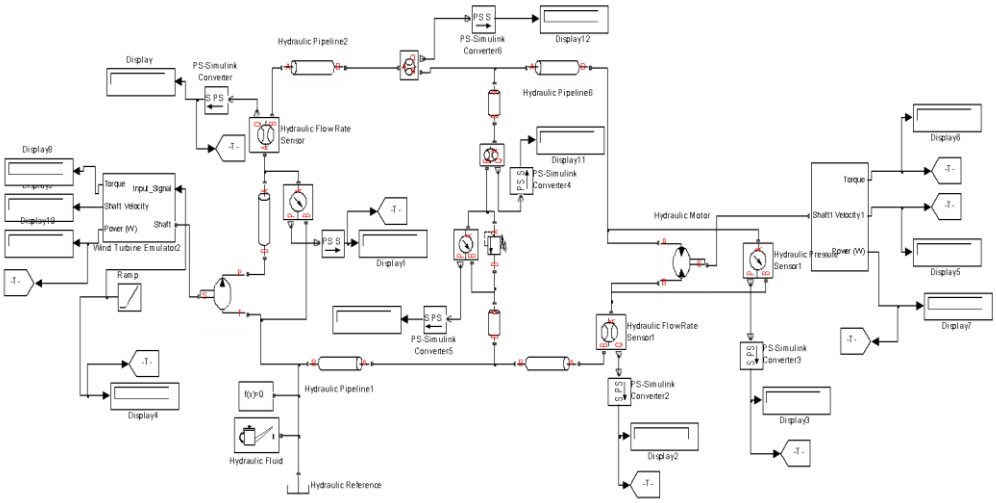

Figure 5.1 Single-wind turbine SimHydraulics schematic

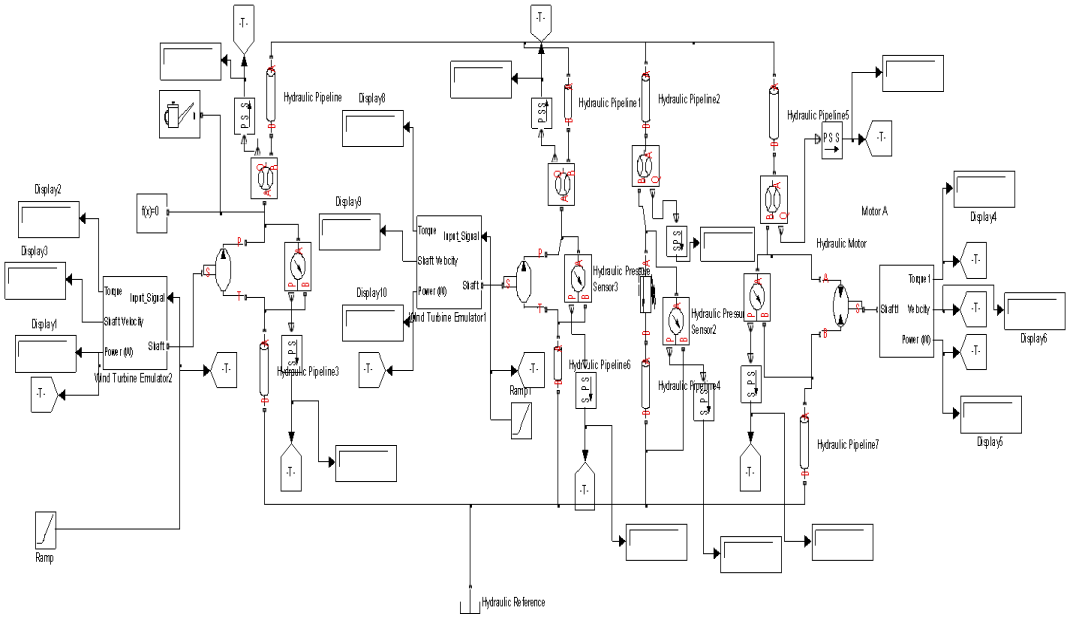

Figure 5.2 Multi-wind turbine SimHydraulics schematic

A wind turbine velocity was applied to the shaft of the SimHydraulic model as well as the Mathematical model to determine if both systems behaved similarly and to demonstrate the quality of power transfer from high torque/low speed wind turbine to a main and auxiliary high speed generator. Validation of the mathematical model is important because it considers the system dynamics and can be used in control development. With the mathematical model of this system, an enhanced understanding of the HTS through analysis can be gained. It can be determined which factors are of greater importance in the system and how different parts of the system are related.

5.2 Model Validation

As verification to our mathematical modeling, the HTS was also simulated using SimHydraulics, a hydraulics toolbox provided by Matlab and Simulink®, and compared to the mathematical model obtained in Chapter 4. The following assumptions were considered to develop the model [35]:

1. The hydraulic fluid is assumed incompressible.

2. No loading is considered on pump and motor shafts (i.e. inertia, friction, spring and etc.).

3. Leakage inside the pump and motor are assumed to be linearly proportional to their respective pressure differential [36].

Single-Wind Turbine: In the first simulation, a fixed displacement pump with a displacement of 0.517 in^3/rev provided hydraulic fluid to a main motor (Motor A) with a displacement of 0.097 in^3/rev . As Figure 5.3 demonstrates, the wind turbine velocity was increased from 200 RPM to 650 RPM in 15 seconds creating a motor velocity of 0 RPM to 2451 RPM in the SimHydraulics model. The motor velocity reached 2338 RPM in the Mathematical model, which verifies the accuracy of mathematical model in the speed calculations. It can be seen that the same system dynamics are produced for both models.

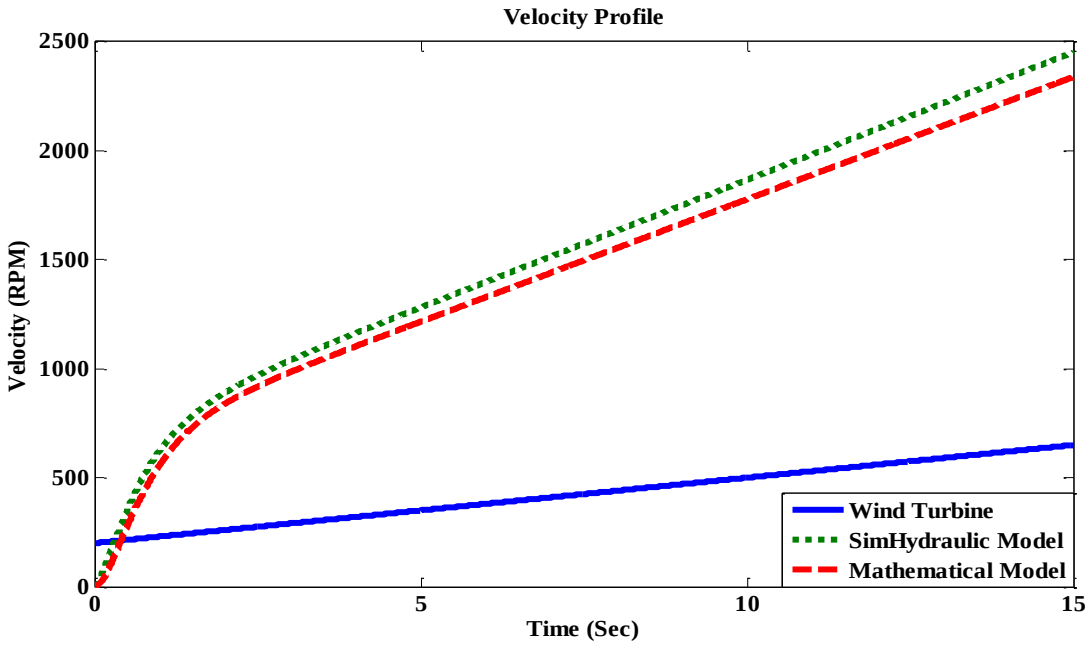

Figure 5.3 Velocity profile of a single-wind turbine hydraulic power transfer system

Figure 5.4 shows the flows in the hydraulic system. As the figure illustrates, a flow of 0 GPM to 1.216 GPM flows through the hydraulic pump while the motor experiences a flow of 0 GPM to 1.215 GPM. The mathematical model also produces a similar flow to the SimHydraulic model with a pump flow of 0 GPM at 200 RPM to 1.1 GPM while the motor flow was observed to be 0 GPM to 1.099 GPM at 650 RPM. Figure 5.4 verifies the mathematical model predictions with the simulations created using SimHydraulics.

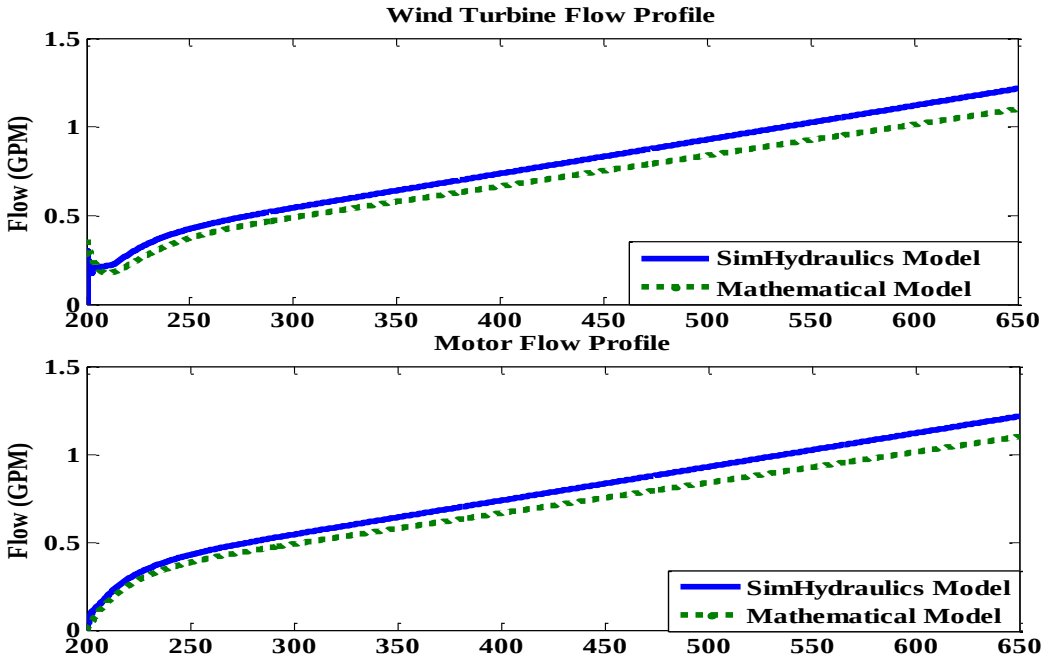

Figure 5.4 Flow profile of a single-wind turbine hydraulic power transfer system

Double-Wind Turbines: In the second simulation, two fixed displacement pumps (as seen in Figure 5.2) with similar displacements of 0.517 in^3/rev generated hydraulic fluid to the main motor A with a displacement of 0.097 in^3/rev . Wind turbine A was driven at a constant velocity of 400 RPM while wind turbine B was varied from 200 RPM to 650 RPM to measure the effect of rotational speed on power transfer efficiency. The motor of the SimHydraulics model produced a velocity of 0 RPM to 3670 RPM whereas the motor of the Mathematical model reached a high of 3582 RPM. There is little variance, 88 RPM, in the velocities produced by the motors of the SimHydraulics model and the Mathematical model (Figure 5.5).

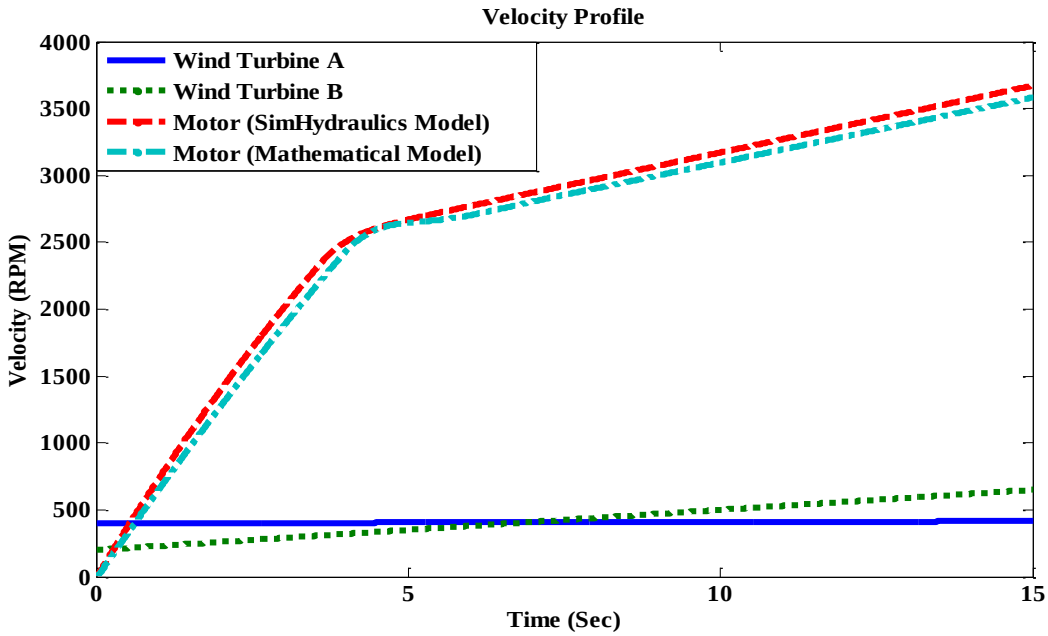

Figure 5.5 Velocity profile of a double-wind turbine hydraulic power transfer system

Figure 5.6 illustrates the flows of pumps A and B, and motor A. Since pump A generates a constant velocity, a steady flow of 0.7905 GPM for the SimHydraulics Model and 0.7341 GPM for the Mathematical model are generated. As the input speed to pump B is varied, it generated a range of flows from 0 GPM to 1.008 GPM (SimHydraulics Model) and 0 GPM to 0.9302 GPM (Mathematical Model) causing the motor to experience a flow increase from 0 GPM to 1.798 GPM (SimHydraulic Model) and 0 GPM to 1.664 GPM (Mathematical Model).

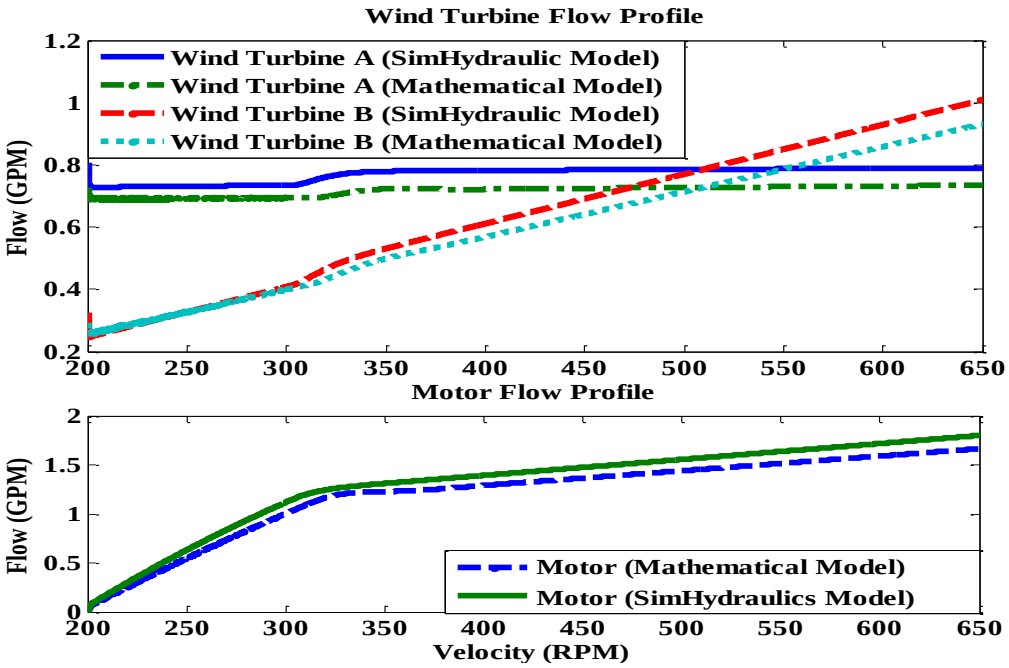

Figure 5.6 Flow profile of a double-wind turbine hydraulic power transfer system

It can be observed from Figure 5.6 that as the velocity of wind turbine B is increased the variation between the SimHydraulic Model and Mathematical Model increases. The slight difference in flow calculations is originated from the leakage factor that is set as affixed number in Mathematical Model, but is obtained from system operating conditions in the SimHydraulics Model.

5.3 System Loss and Efficiency Validation

Single-Wind Turbine: The overall system efficiency of the single turbine simulation (Figure 5.7) was 80.01% from the SimHydraulic model while the mathematical model yielded an efficiency of 85.67%. The difference is originated from the hose dynamics and losses associated with joints and connections which has not been represented in the Mathematical Model.

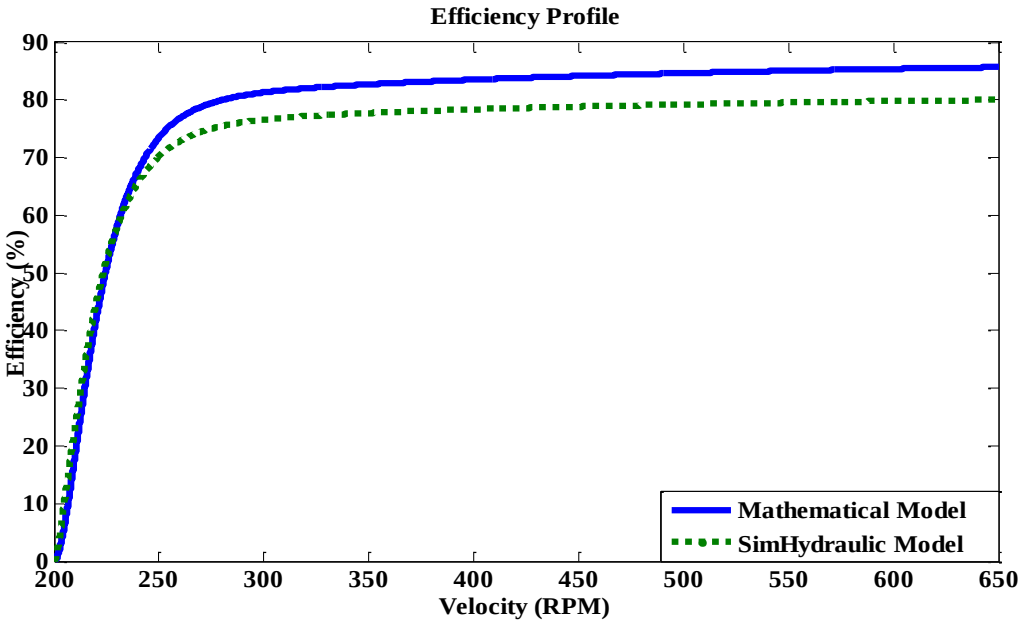

Figure 5.7 System efficiency of a single-wind turbine hydraulic power transfer system

Double-Wind Turbines: The system overall power transfer efficiencies obtained from mathematical model and SimHydraulics are shown in Figure 5.8. Because of changes in parameter calculation and slight dynamic differences in the math model and that of SimHydraulics, the overall efficiencies of the systems deviated by maximum 3.5%. It can be observed from Figure 5.8 that by increasing the number of wind turbines, the overall system efficiency will increase. The overall system efficiency of the double turbine simulation was 90.95% from the SimHydraulic model while the mathematical model yielded an efficiency of 87.75%.

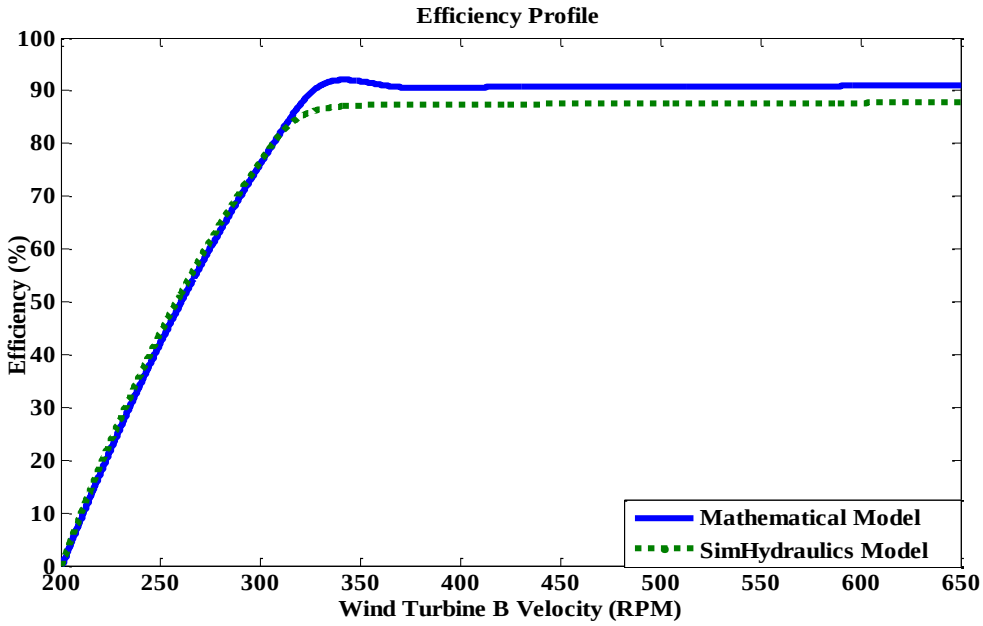

Figure 5.8 System efficiency of a double-wind turbine hydraulic power transfer system

The power transfer efficiencies obtained from the Mathematical and SimHydraulics model in single-and double-wind turbine power plants are compared in Figure 5.9. By increasing the number of wind turbines to the hydraulic system, there was an increase in the overall efficiency.

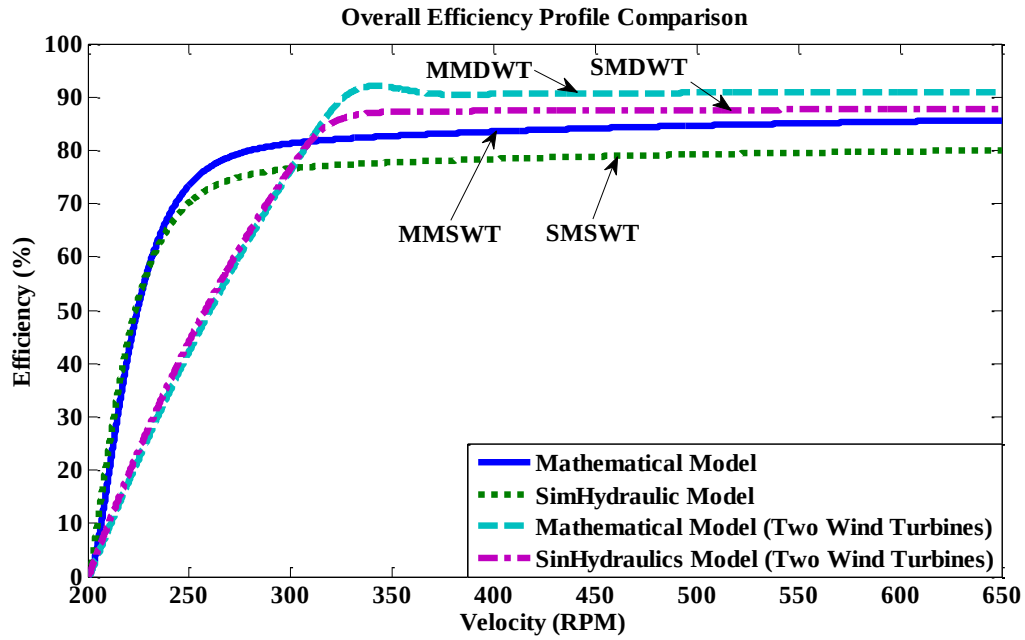

Figure 5.9 System efficiency comparison of single-wind and double-wind turbine hydraulic power transfer system.

5.4 Results and Discussion

As the figure illustrates, the mathematical model shows an efficiency increase of 5.28% in average when double-wind turbines are operated in parallel in a hydraulic wind power plant reaching maximum of 90.95%. SimHydraulics predicted an increase of 7.74% when double-wind turbines operated reaching the maximum of 87.75%. The difference in prediction is originated from the level of details considered in calculations. The simulation results proved that double-wind turbines generate higher efficiencies than a single-wind turbine in a hydraulic power transfer system.

6. DESIGN AND FABRICATION OF GEARLESS POWER TRANSFER SYSTEM

6.1 Design Specifications

For a traditional wind power generation system to harvest wind energy and produce electric power, the required components include a wind turbine, gearbox, and a generator. These components, the gearbox specifically, are expensive, bulky, and require regular maintenance, which makes the wind energy production expensive. To reduce the cost, time for maintenance and weight on top of the tower, the gearbox will need to be eliminated. Traditional wind power generation systems do not allow for the connection of wind turbines in a central power generation unit. Each wind turbine requires it's on power generator. By replacing the gearbox with a hydraulic transmission system (HTS), a central generation unit can be used to harvest the wind energy and send it to the electric grid from multiple wind turbines. This reduces the number of power converters as well as the number of power generators needed. Reducing the amount of power electronics is important because the cost of the power electronics are expensive and the efficiency of the power that a small induction generator can harvest from the prime mover is less than what a large central synchronous machine can provide. Heavy equipment can be removed from the towers reducing weight and increasing the efficiency of the towers.

The end goal of this research is to hydraulically connect wind turbines to a central generation unit that controls the flow of high pressure fluid.

6.2 Experimental Setup

To emulate wind power and velocity variations, a transformer (Figure 6.1) is connected to an electric motor whose shaft is coupled to a hydraulic pump. Each electric

motor and hydraulic pump combination makes up a wind turbine. Wind turbine A consists of hydraulic pump A and a split phase AC motor (Figure 6.2). Split phase AC motors provide a greater starting torque and when powered both the running and the starting windings draw about four to five times their normal full load current. The heat loss in these windings is up to 25 times higher than normal. To prevent overheating of the windings the starting period must be instantaneous.

Figure 6.1 Transformers used to vary wind velocity

Wind turbine B consists of hydraulic pump B and a direct current permanent magnet motor (Figure 6.3). As the transformer transfers electric power through magnetic induction from one winding to another winding by varying magnetic field produced by alternating current, the velocity measured as the shaft of each hydraulic pump can be varied. Wind turbine A varies from 350 RPM to 415 RPM while Wind Turbine B varies from 200 RPM to 650 RPM.

Figure 6.2 AC Motor connected coupled to shaft of Pump A

Figure 6.3 DC Motor coupled to the shaft of Pump B and Motor A

Hydraulic pumps A and B are then connected to check valves to ensure that the movement of fluid is sent in the correct direction toward the hydraulic motor. Flexible piping is used as connections with a number of fittings that include tees and elbows. A pressure relief valve is added to the system to ensure over pressuring. Fluid is diverted between Motor A and Motor B using an electronically adjustable proportional flow control valve. With this valve and the use of a PI controller flow can be sent to either Motor A or Motor B or split between both motors. For this research, hydraulic fluid was transferred through two system configurations. Figure 6.4 illustrates both of these. Following the red arrows shows the fluid flow for a single turbine wind power transfer

system while the arrows in yellow show the fluid flow for a double wind turbine wind power transfer system.

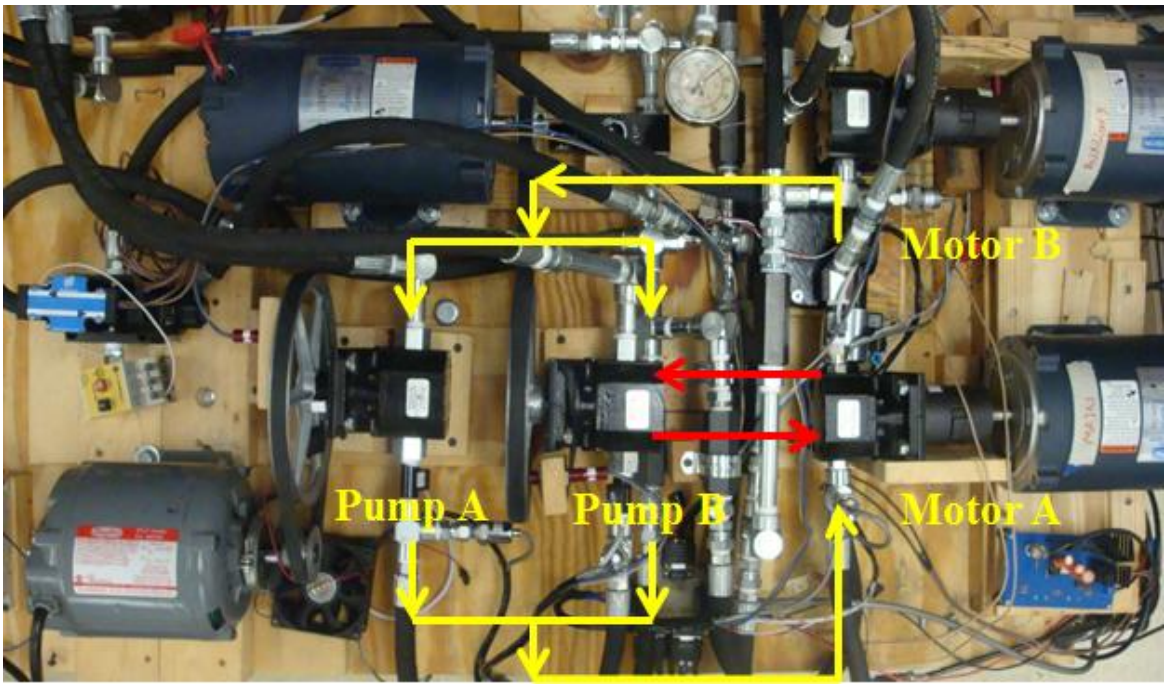

Figure 6.4 Hydraulic Test Bed

Sensors were strategically placed in the system to measure the velocity at the shaft of each pump and motor, the pressure at each pump and motor and the flow passing through each pump and motor. This data was collected as signals and sent to DSPACE to be converted into values with units of flow (GPM), velocity (RPM), and pressure (PSI) where they were recorded in a spreadsheet.

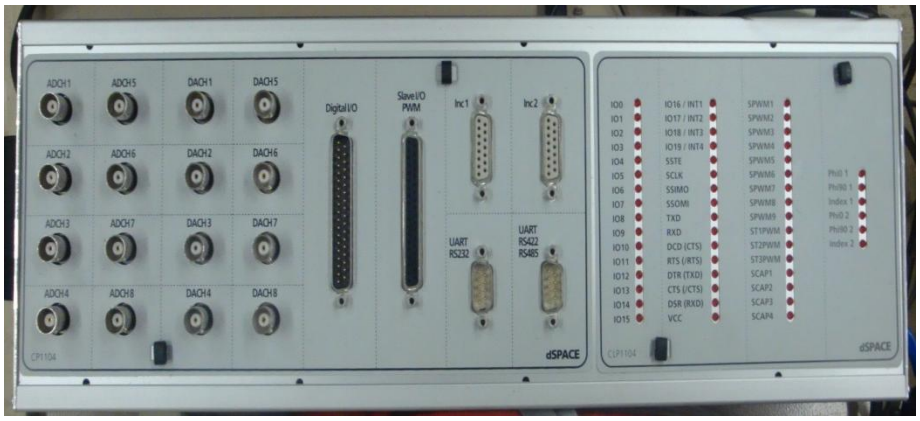

Figure 6.5 DSPACE

Through this research it was discovered that there was a discrepancy in the manufacture's rated pump and motor displacement and the displacement calculated from the measured flow and measured velocity. For Pump A and Pump B the manufacture's displacement is 0.517 in^3/rev while the manufacture's rated displacement for Motor A and Motor B is 0.097 in^3/rev . When flow is traveling from one pump to one motor the calculated displacement for the pump is 0.466 in^3/rev and the calculated displacement for the motor is 0.111 in^3/rev. The displacements for the motor are close in value but there is a large difference in the displacements of the pump (Table 6.1).

Table 6.1 Calculated Displacement

	Flow Meter (GPM)	Velocity (RPM)	Calculated Displacement (in^3/rev)	Flow With Given Displacement (GPM)
Pump A	0.65	400	0.375	0.895238
Motor A		1558	0.096374	0.0654225
Pump A	0.65	400	0.375	0.895238
Motor A		1558	0.096374	0.0654225
Pump B	0.62	307	0.466	0.6871
Motor A		1290	0.111	0.541688
Pump B	1.08	526	0.474	1.17724
Motor A		2307	0.10814	0.96874
Pump A	1.04	397	0.375	0.888524
Pump B		241	0.373817	0.538381
Motor A		2264	0.106113	0.950684
Pump A	1.49	389	0.375	0.87069
Pump B		500	0.38808	1.11905
Motor A		3333	0.103	1.39957

When selecting a hydraulic fluid its compressibility factor and viscosity are greatly important. Compressibility is measured by the amount of volume reduction due to pressure expressed by bulk modulus. The compressibility increases with pressure and temperature and has significant effects on high pressure fluid systems. Viscosity is considered the most important characteristic of a hydraulic fluid. It plays a significant impact on the operation of a hydraulic system. If the viscosity is too high, friction, pressure drop, power consumption, and heat generation increases. If the viscosity is to low, increased internal leakage may result under high operating temperatures. Some of the primary properties of a quality hydraulic fluid include oxidation stability, rust prevention, foam resistance, water separation, and antiwear properties. Many of these are achieved through the use of additives.

7. EXPERIMENTAL RESULTS AND DISCUSSION

7.1 Experimental Procedure

The efficiency enhancement was experimentally measured through a laboratory test bed. Two experiments were conducted to demonstrate the efficiency enhancement in the hydraulic wind power transfer system. In experiment 1, a single-wind turbine generated high-pressure flow to transfer the energy from wind turbine to a generator. In the second experiment, a second wind-driven hydraulic pump was added to the system and the energy was measured at the hydraulic motor output shaft for experiment 2. The voltage provided by the transformer simulates the wind captured by the wind turbine and is translated into velocity measured in revolutions per minute (RPM) at the shaft of the pump. The transformer can provide a range of velocities from 350 to 415 RPM for Pump A and 200 RPM to 700 RPM for Pump B. As the voltage produced by the transformer is increased or decreased, the pressure and torque created at the shaft generates the flow of hydraulic fluid through a closed loop hydraulic power system. The sensors connected to each pump and motor collect system pressure as well as flows of the hydraulic fluid flowing through each pump and motor, and the velocity at the shaft of each pump and motor.

During the experiment it was observed that: 1) The pump ramp speed created a ramp response at the motor, 2) It was determined that the flow rate sensor used at the motor could not detect any flow rate for pump velocities below 115 rpm, and 3) The accuracy of the flow readings diminished at velocities lower than 200 rpm. Therefore, experiments were conducted at pump speeds higher than 200 rpm.

7.2 One Wind Turbine/One Central Generation Unit

7.2.1 Velocity Applied to the Shaft of the Pump and Motors

Experiment 1: Single-Wind Turbine. In Experiment 1, one pump provided hydraulic fluid to one motor in the setup show in Figure 7.1. Figure 7.2 illustrates the velocity profiles of the pump and motor. A ramp velocity was applied at the input shaft of a hydraulic pump so that the system power transfer and velocity responses at the hydraulic motor could be observed. The input velocity ranged from 200 RPM to 650 RPM for the duration of 15 seconds.

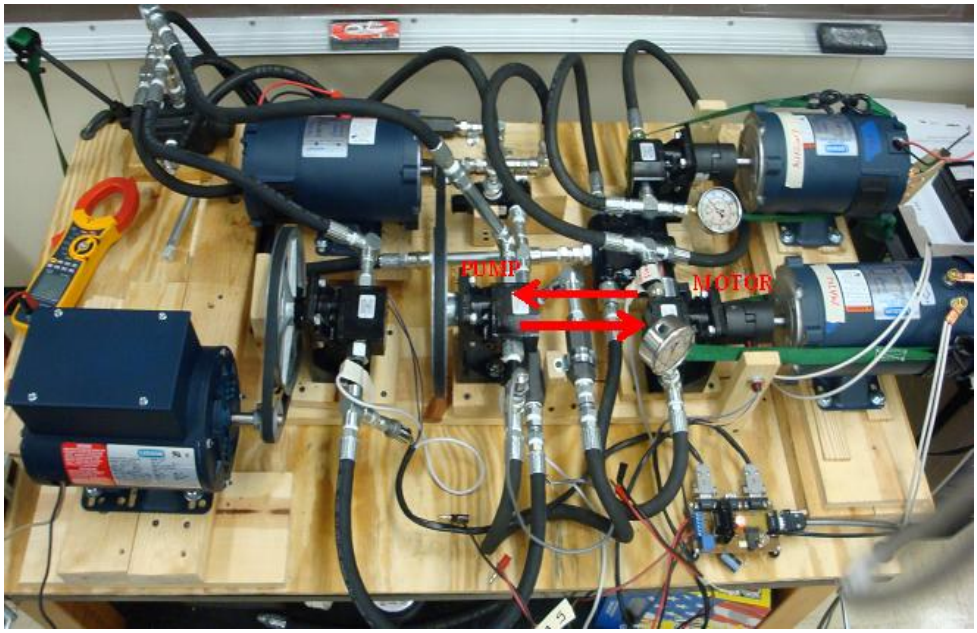

Figure 7.1 Experimental Setup (One Wind Turbine)

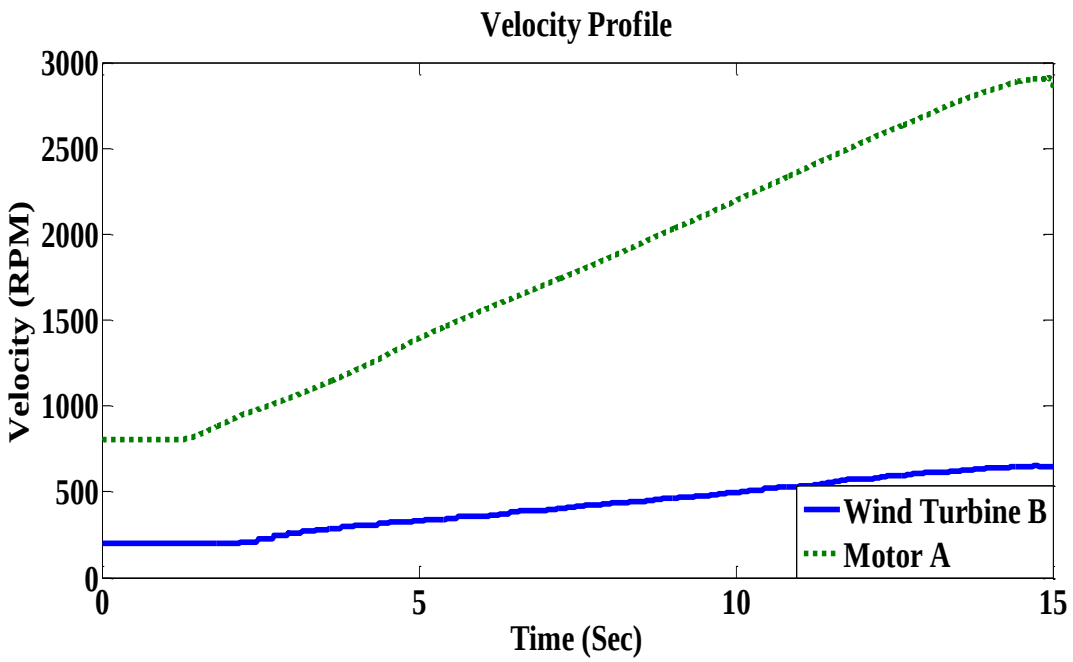

Figure 7.2 Experimental velocity measurement in a single-wind turbine hydraulic power transfer setup

The velocity seen at the shaft of the hydraulic pump will determine the flow of the hydraulic fluid in the system as well as the overall system pressure. Velocity also directly affects the torque and horse power applied to the pump shaft.

7.2.2 Overall System Flow Rate and System Pressure

With a ramp increase in the velocity applied to the input shaft of the hydraulic pump, the pump generated a linearly proportional flow (Figure 7.3). The flow rate for the hydraulic pump spanned from 0.45 GPM to 1.45 GPM, while the motor flow rate ranged from 0.34 GPM to 1.21 GPM. As the hydraulic fluid travels through the hydraulic pump to the motor, losses occur. As the flow increases there is a greater gap that appears between the flow of the pump and the flow of the motor. These losses are due to the leakage that takes place in the pump and motor, and the friction in the fittings and flexible piping.

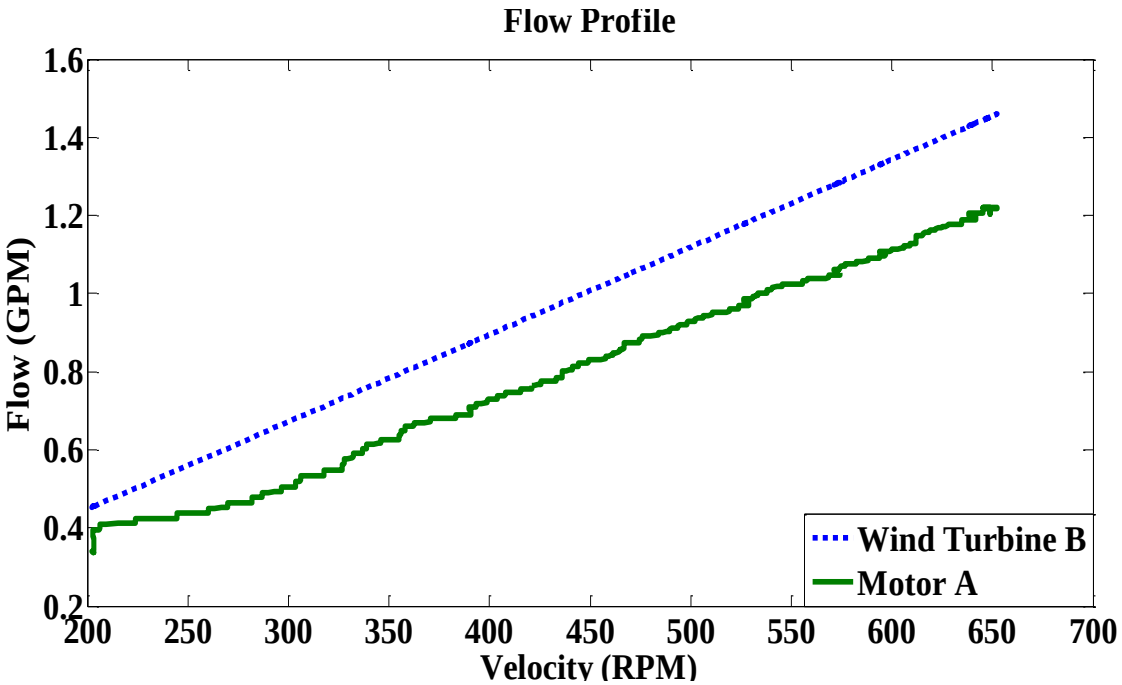

Figure 7.3 Experimental flow measurement in a single-wind turbine hydraulic power transfer setup

The pressure in the gearless wind power transfer system was recorded at two locations for the single turbine experiment. These locations include Wind Turbine B and Motor A. As the velocity at the shaft of the hydraulic pump increased from 200 RPM to 650 RPM, the pressure increased as well as seen in Figure 7.4. Figure 7.4 illustrates how the relationship between the velocity of Wind Turbine B and the overall system pressure is linear. Figure 7.5 illustrates the relationship between the fluid flow of the system and the overall system pressure. Again the relationship is linear. From Figures 7.4 and 7.5, it can be observed that Motor A recorded a slightly higher pressure than Wind Turbine B. This is due to the Direct Current (DC) Permanent Magnet Motor coupled to the shaft of the motor. It has a higher rated horsepower (HP) of ¾ HP than the DC Permanent Magnet Motor, which only has a rated HP of ½, connected to the shaft of the hydraulic pump. A higher HP requires a larger force to move the shaft which in turns creates more pressure at that location. The overall system pressure range is 260 PSI to 587 PSI.

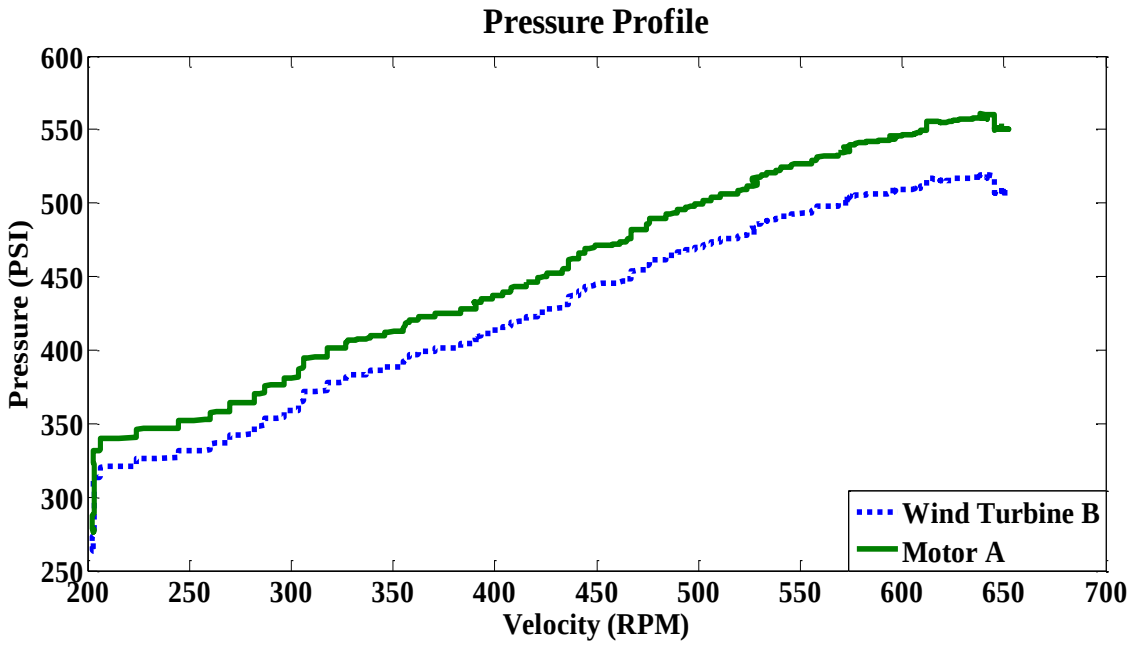

Figure 7.4 Experimental pressure measurement in a single-wind turbine hydraulic power transfer setup (Pressure vs Velocity)

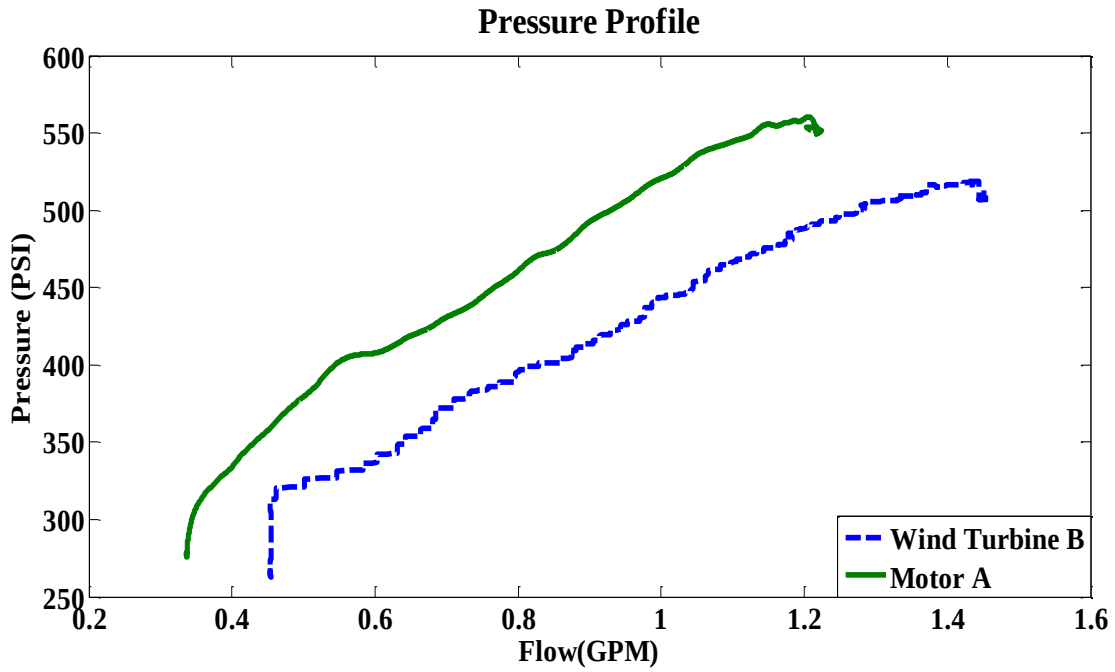

Figure 7.5 Experimental pressure measurement in a single-wind turbine hydraulic power transfer setup (Pressure vs Flow)

7.2.3 Horse Power and Efficiency of System

Figure 7.6 illustrates the horsepower of the single-wind turbine in hydraulic power transmission system. The system can generate and transfer around 0.6 HP. The figure illustrates a linear increase of power generated and transmitted through hydraulic system from 0.1 HP at 200 RPM to around 0.47 HP at 650 RPM.

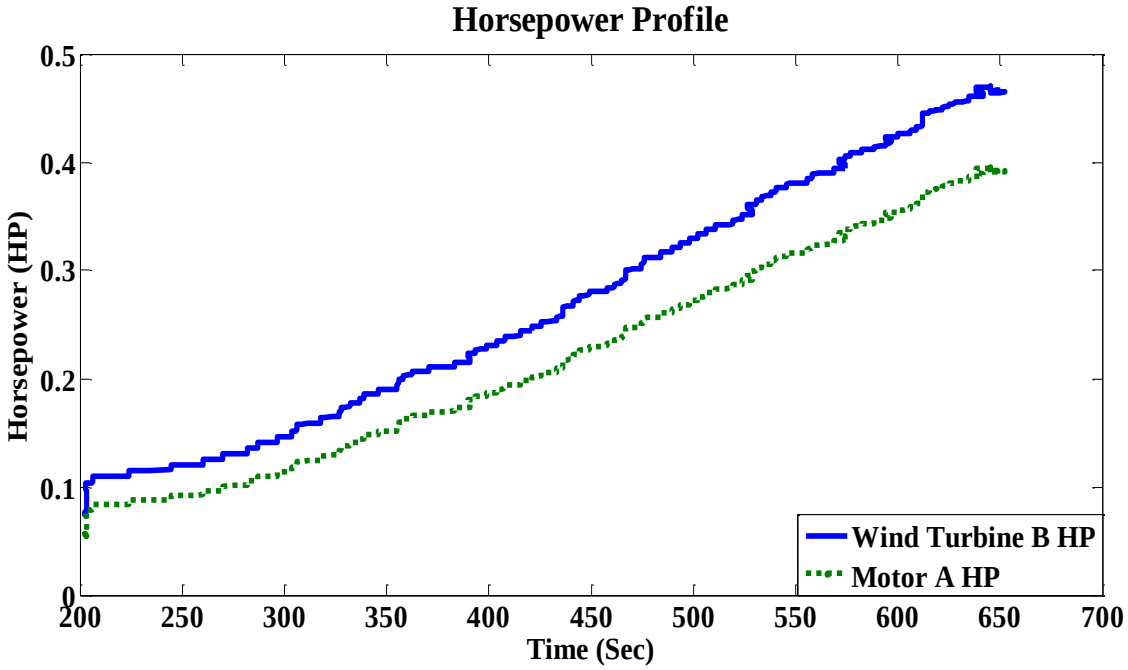

Figure 7.6 Experimental horsepower measurement in a single-wind turbine hydraulic power transfer setup.

Figure 7.7 illustrates the efficiency of the power transfer system when single-wind turbine was used. The pressure and flow rate were used to determine the horsepower generated by the pump and transferred to the motor. The efficiency of the system was then calculated from these values. At 200 RPM the efficiency of the system was 74%. As the velocity of the wind turbine was gradually increased to 650 RPM, the efficiency increases to its maximum value of 83%. The recorded system efficiency and the averaged efficiency are shown in Figure 7.8. The efficiency of power transfer system increases as the speed increases. For the single turbine hydraulic wind power system that eliminated

the gearbox, variable wind speed cannot be regulated which consequently results in lower overall system efficiency.

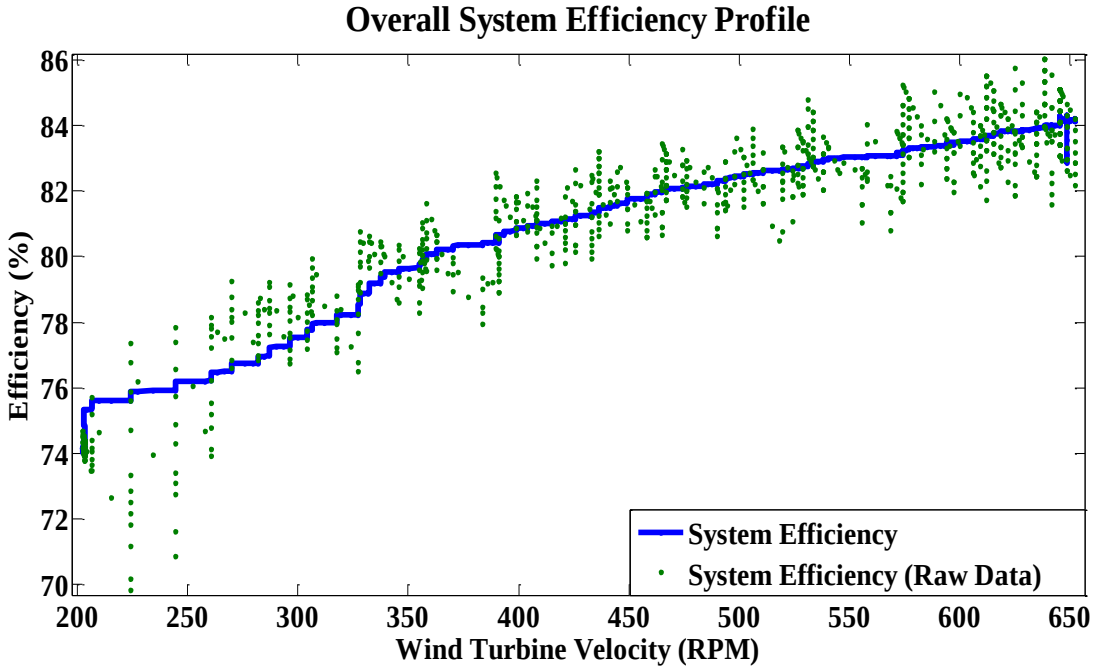

Figure 7.7 Experimental overall efficiency measurement in a single-wind turbine hydraulic power transfer setup.

7.3 Multiple Wind Turbines/One Central Generation Unit

7.3.1 Velocity Applied to the Shaft of the Pump and Motors

To make the system operation economic and highly efficient, there will be need for more wind turbines to pump high-pressure fluid to the system. That way the efficiency of overall power-transfer system is increased. The second experiment is designed to demonstrate and experimentally prove that as more wind-turbines are connected to the system, the overall efficiency is increased and this can be obtained at lower pump speeds. Experimental setup and flow directions of double-wind turbines are shown in Figure 7.8.

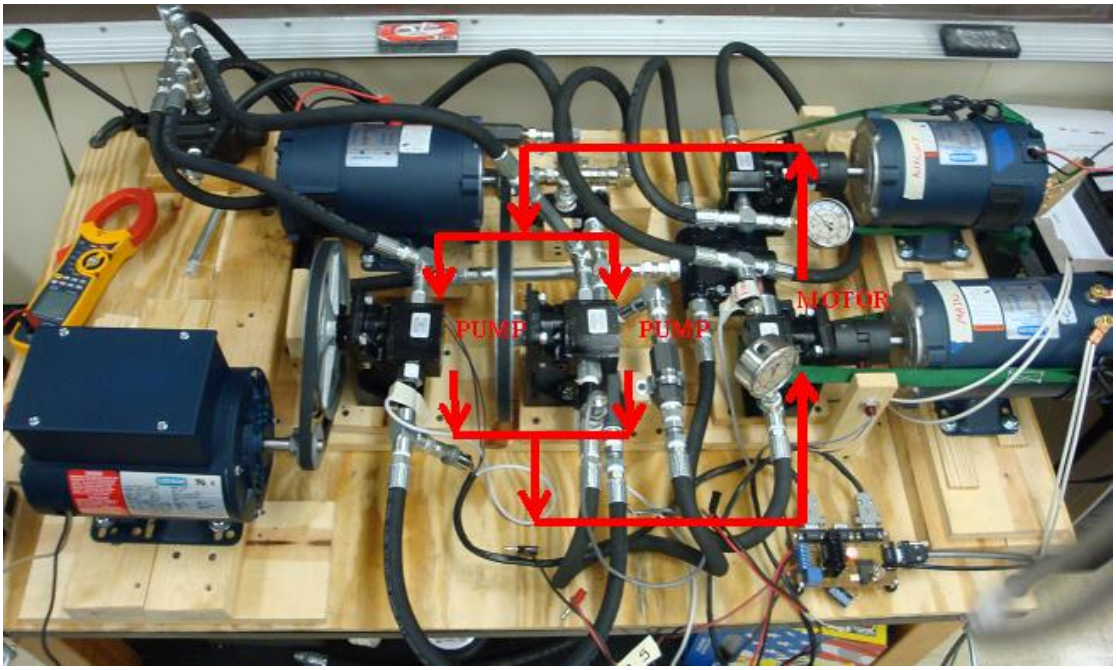

Figure 7.8 Experimental setup of double-wind turbine configuration

Experiment 2: Double-Wind Turbine Configuration. During this experiment, the flows of two wind-driven hydraulic pumps were integrated and directed to one hydraulic motor. The speed of one pump (pump A) was held constant with an average velocity of 389.04 RPM, while velocity of pump B varied from 185 RPM to 560 RPM in 15 seconds. With an additional pump to this experiment, the shaft velocity of the hydraulic motor jumped at a much higher value of 2069 RPM versus the 800 RPM in single turbine experiment, and reached a maximum velocity of 3333 RPM as shown in Figure 7.9.

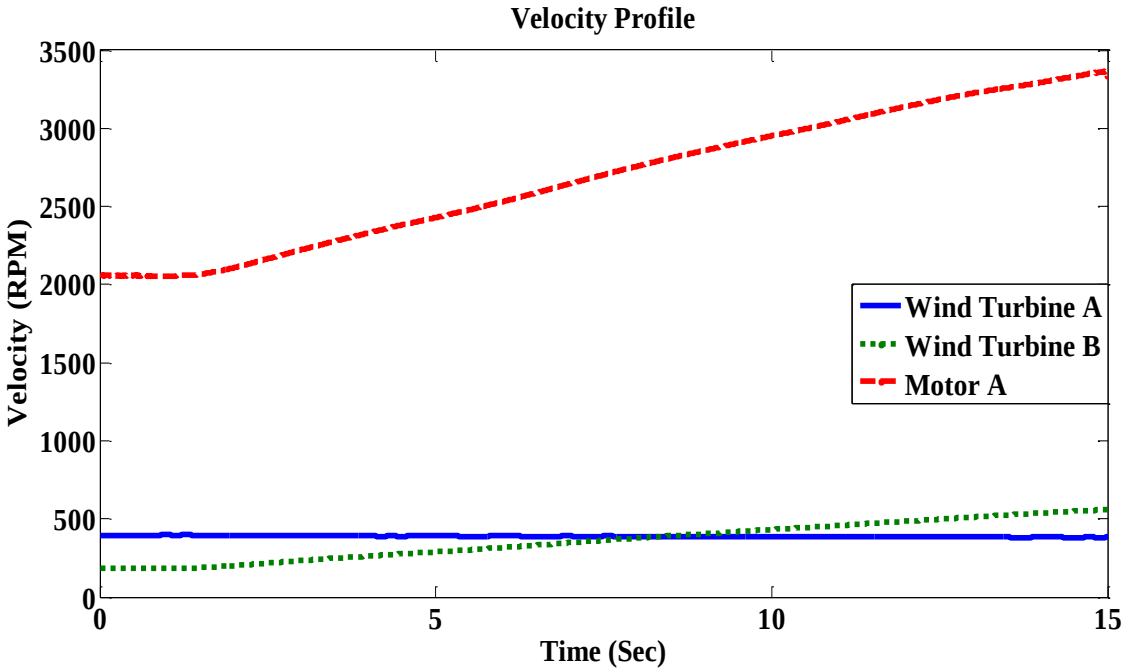

Figure 7.9 Experimental velocity measurement in a double-wind turbine hydraulic power transfer setup.

7.3.2 System Flow Rate and Overall System Pressure

The flows of wind turbines A and B, and their combination passing motor A are illustrated in Figure 7.10. As the pump speed increased, the flows of wind turbine B and motor A increased linearly. As motor B spun at higher velocity, the output pressure of their point of common coupling (PCC) increased. Therefore, motor A could pump less fluid at a constant speed. This effect has shown on Figure 7.10 with a slight decline in flow generation of wind turbine A. Wind turbines A and B provided a combined flow of 1.00 GPM to 1.76 GPM as the velocity of motor B increase from 200 to 550 RPM. The hydraulic motor's flow sensor measured 0.99 GPM to 1.60 GPM for the same range of speed.

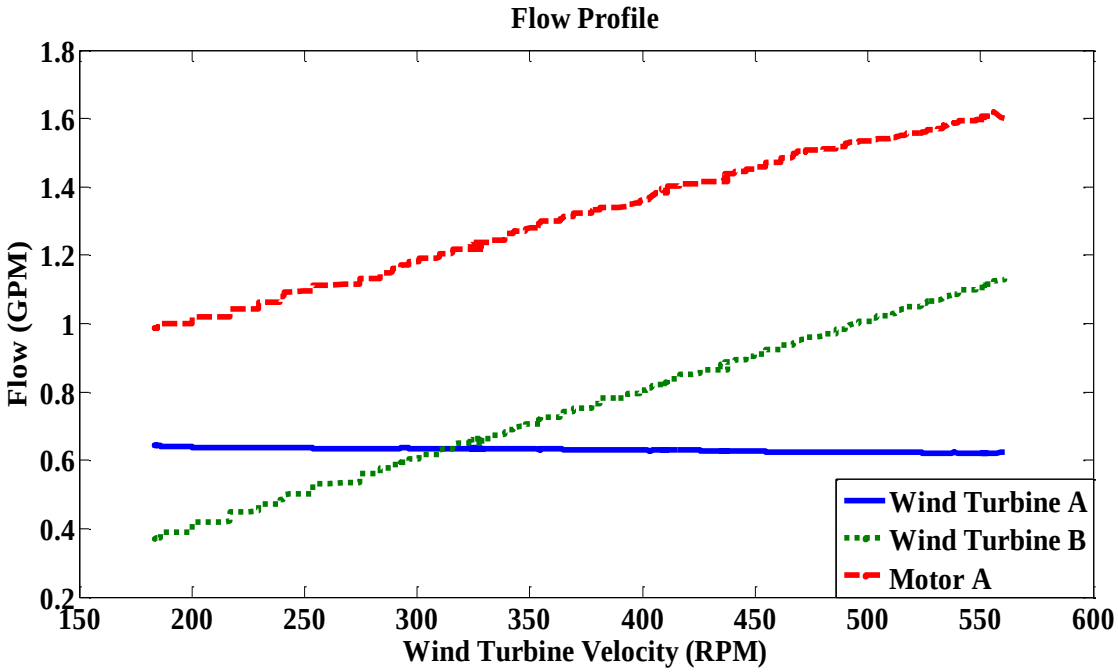

Figure 7.10 Experimental flow measurement in a double-wind turbine hydraulic power transfer setup.

Experiment 2 measured the pressure of the system at Wind Turbine A, Wind Turbine B, and Motor A. The relationship between velocity and pressure for the multi-turbine experiment is presented in Figure 7.11. The pressure for Wind Turbine A and Motor A are close in value while the pressure of Wind Turbine B is lower. Similar to Experiment 1, Motor A is attached to a DC Permanent Magnet Motor that has a higher rated horsepower of ¾ HP. Wind Turbine A is connected to a split phase AC motor that requires high resistance to operate. High resistance requires more driving force. In the Flow versus Pressure plot (Figure 7.12), Wind Turbine A produces a steady flow of about 0.64 GPM while the pressure increases from 393 PSI to 596 PSI. Motor A flow is a combination of the flow of Wind Turbine A and B and produces a pressure similar to that of Wind Turbine A. Because the system is closed loop, the pressure seen at all of the components increase collectively.

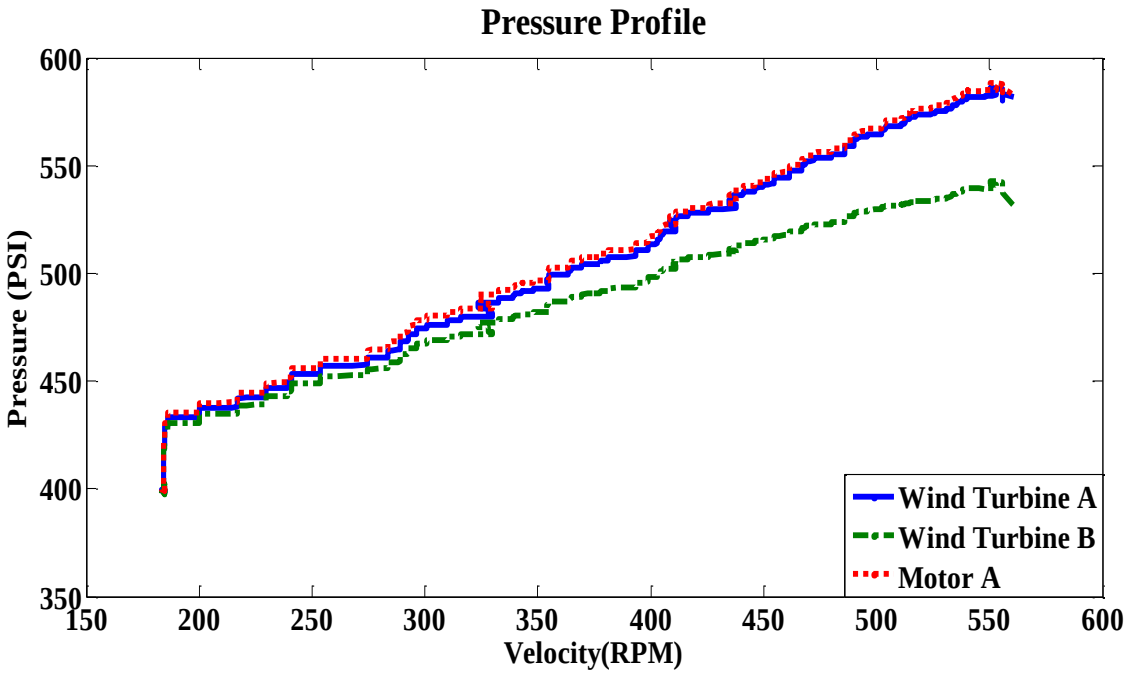

Figure 7.11 Experimental pressure measurement in a multi-wind turbine hydraulic power transfer setup (Pressure vs Velocity)

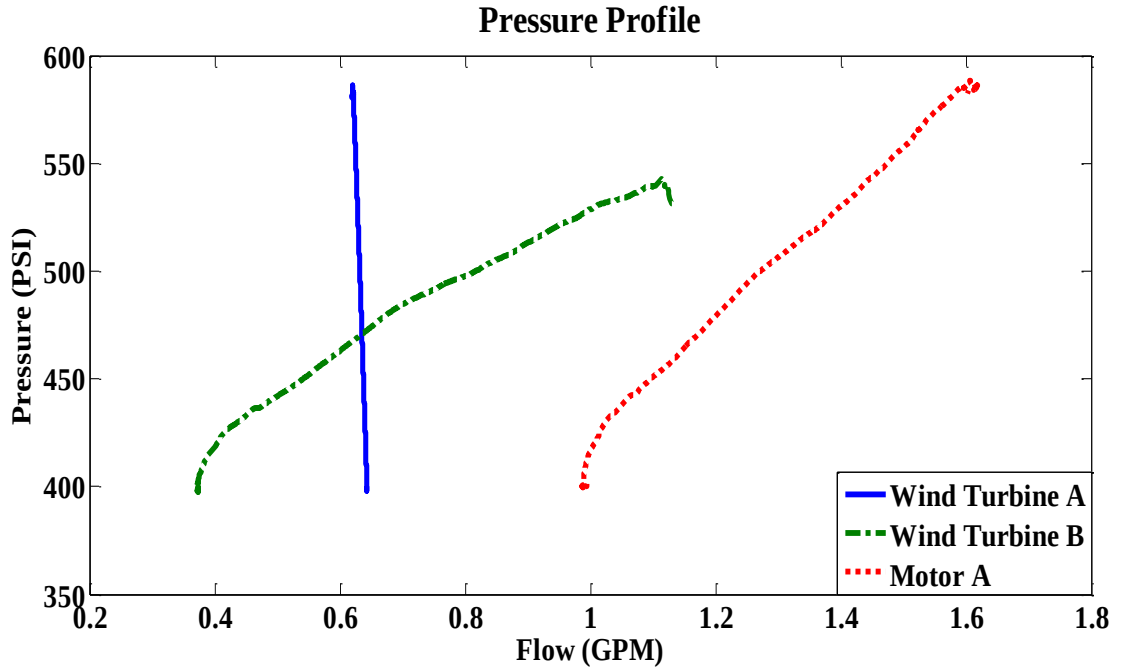

Figure 7.12 Experimental pressure measurement in a multi-wind turbine hydraulic power transfer setup (Pressure vs Flow)

7.3.3 Horse Power and Efficiency of System

The power generated by two integrated wind turbines and the power generated from the hydraulic motor are shown in Figure 7.13. As the figure illustrates, the output power increased as the speed of the wind turbine increased. Motor A required more power to keep up the flow generation. As the velocity of motor B increase, the output pressure of PCC increased, which received more power from wind turbine. The energy of wind turbines is used to increase the system pressure and circulate the fluid in the system.

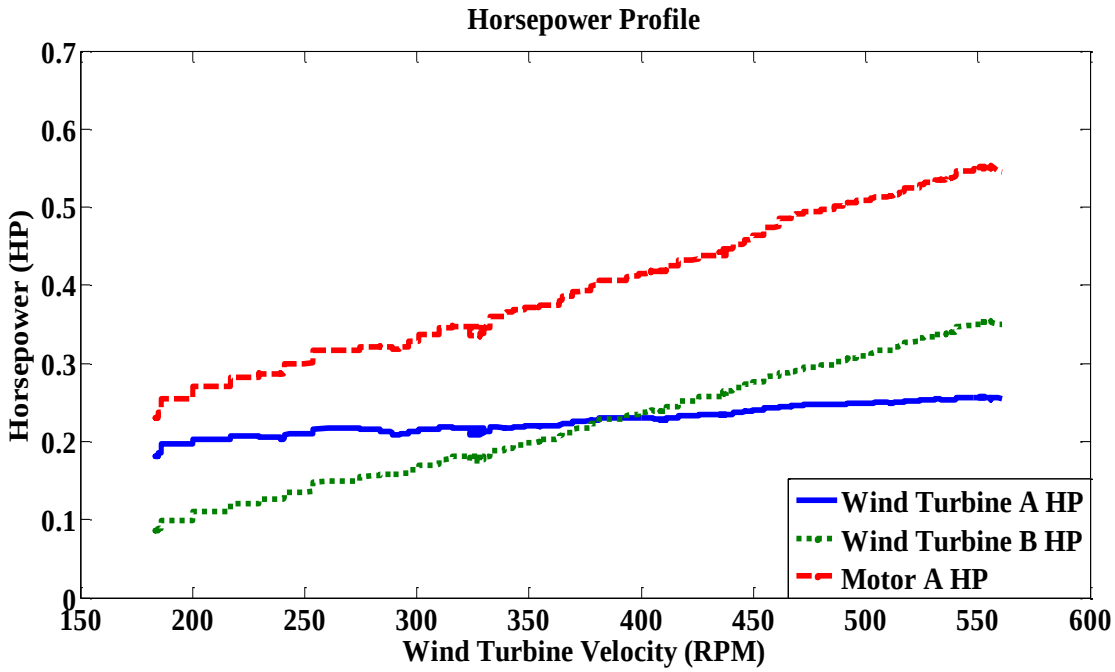

Figure 7.13 Experimental horsepower measurement in a double-wind turbine hydraulic power transfer setup

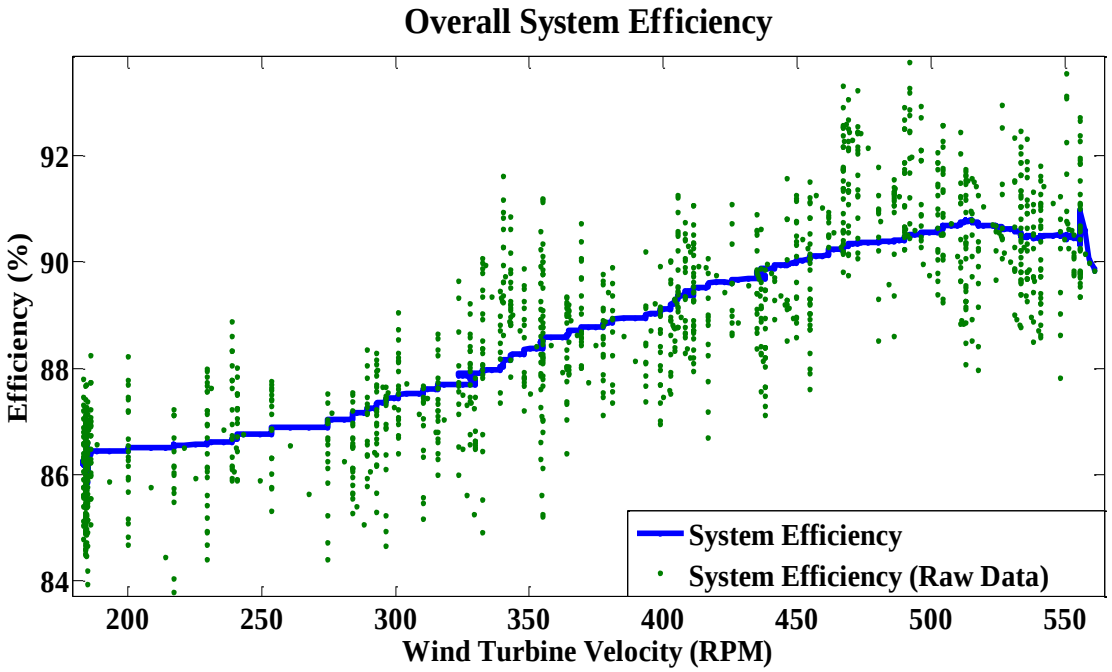

Figure 7.14 Experimental overall efficiency measurement in a double-wind turbine hydraulic power transfer setup.

The energy transfer efficiency of integrated wind turbines into one central energy generation unit is shown in Figure 7.14. As the figure illustrates, the overall efficiency of the double-wind turbine system started at efficiency of 86% at 185 RPM, and increased as the wind turbine velocity increased reaching a maximum of 90.7% at around 510 RPM. The single-wind turbine hydraulic power transfer could only reach maximum of 83.31% at 650 rpm. With an average velocity of 389.04 RPM being produced by wind turbine A, and wind turbine B starting with an rpm of 185, the overall system efficiency reached 89.83% while the overall efficiency of single turbine hydraulic wind power transfer reached 78%. These experiments demonstrate two important observations: 1) The maximum efficiency of double-wind turbine system reached 90.7% at a lower speed. 2) At low rotational speeds the efficiency of double-wind turbine system increased by 17%.

7.4 Results and Discussion

A comparison of system speed dependent efficiencies in a single turbine and double turbine system is shown in Figure 7.15.

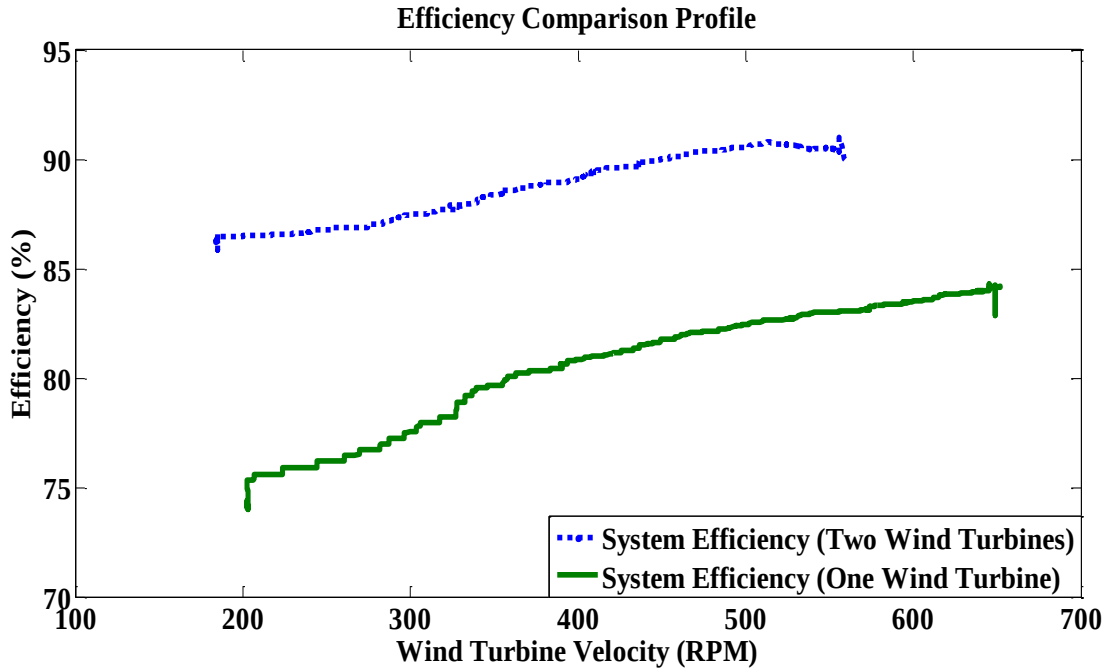

Figure 7.15 Experimental system efficiency measurement comparison of single-wind turbine and double-wind turbine hydraulic power transfer setups

The set of experiments proved that by increasing the number of wind turbines in a hydraulic energy transfer system increased the power transfer efficiency. The increased efficiency occurred at lower rotational velocities suggesting strong prove for elimination of variable speed gearbox from wind turbine drivetrain and high efficiency of multiple-turbine hydraulic wind power transfer. A novel efficiency enhancement of hydraulic energy transfer system was introduced. It was observed that the addition of one wind turbine-driven hydraulic pump will increase the efficiency by 17%. It was observed that the addition of one wind-driven hydraulic pump would decrease the required rotational velocity at which the maximum efficiency occurred. The multi-turbine system can run at lower speeds and still produce a higher efficiency requiring the system to do less work.

Since the system will perform less work, there is also opportunity to integrate energy storage with the energy not being used to operate the system.

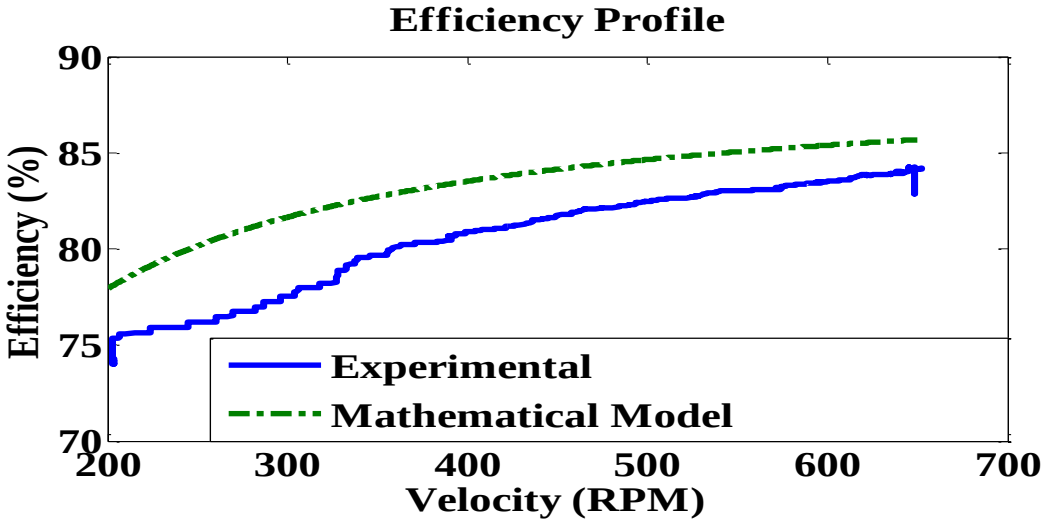

Figure 7.16 Efficiency profile of single-wind turbineconfiguration comparing the efficiency of the following-Mathematical Model, and Experiment

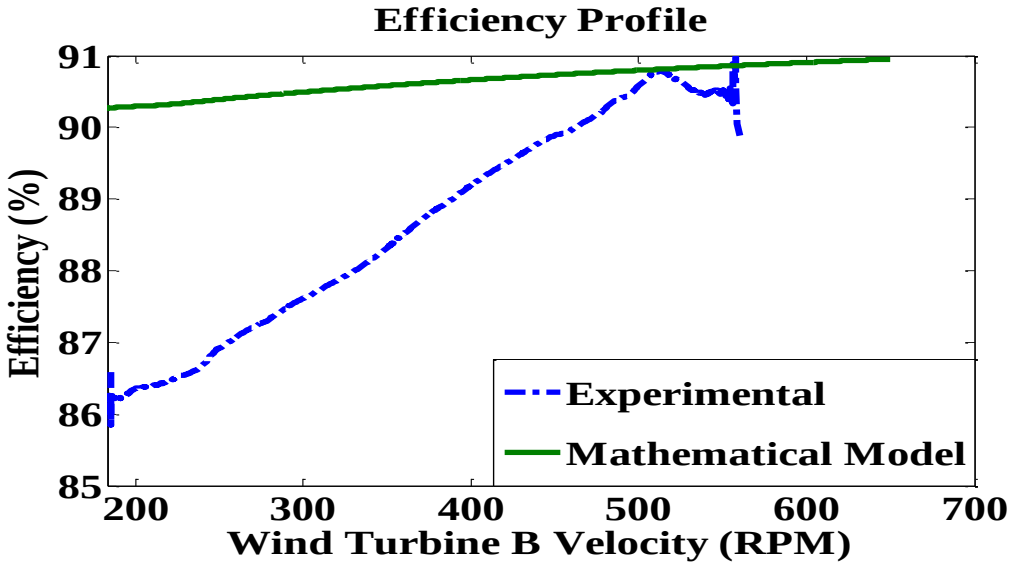

Figure 7.17 Efficiency profile of double-wind turbine configuration comparing the efficiency of the following-Mathematical Model, and Experiment

To determine how the efficiency of the experimental setup compared to the SimHydraulics and Mathematical Models, Figure 7.16 is provided for the single-wind turbine configuration and Figure 7.17 is provided for the double-wind turbine configuration. It can be observed that there is small variation between the two models/setups for the overall efficiency of each hydraulic system configuration. It can also be observed that the efficiency outputted by the experimental setup is closer in value to the mathematical model for each configuration as well. Figure 7.18 illustrates how the addition of one turbine can increase the efficiency in both the mathematical model as well as in the experiment.

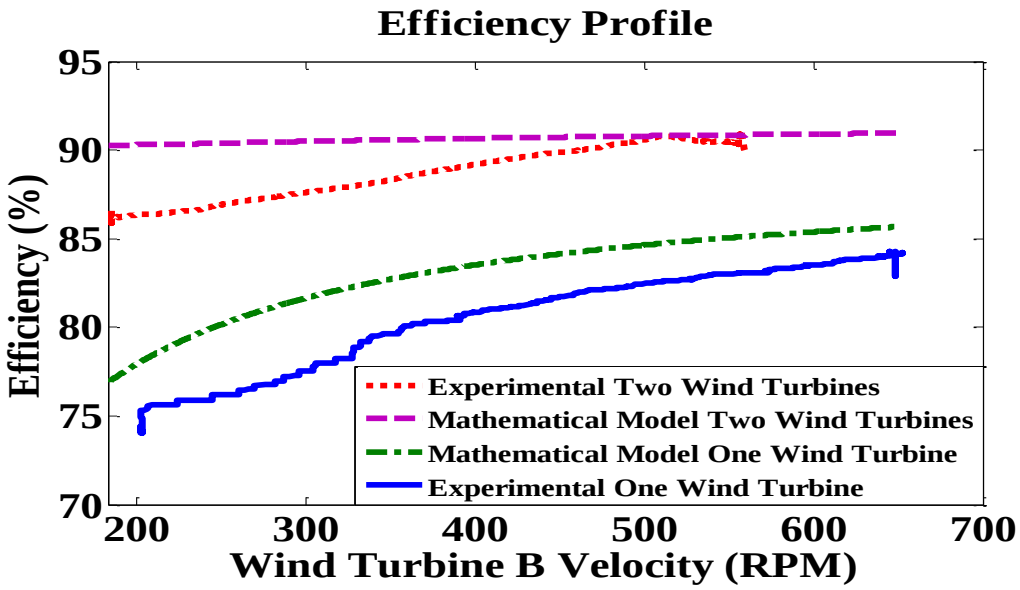

Figure 7.18 Efficiency profile of both single-wind turbine and double-wind turbine configuration

8. CONCLUSION AND RECOMMENDATIONS

8.1 Conclusions

The focus of this research was to determine the efficiency of a gearless wind power transfer system and to prove that a multi-turbine gearless wind power system was more efficient than a single turbine system. To accomplish this, a single turbine system was designed, simulated, fabricated and constructed. Sensors provided key measurements such as velocity (RPM), pressure (PSI) and flow (GPM) to calculate the power transferred from the shaft of the pump to the shaft of the motor. Afterwards, another wind turbine was added making the system a multi-turbine system. Again the power transferred from the shaft of two pumps to the shaft of one motor was calculated. The efficiencies of both systems were observed. The multi-turbine system did provide higher efficiency and delivered more of the power created at the shaft of the hydraulic pumps to the shaft of the motor.

Using SimHydraulics, a Matlab/Simulink toolbox, a single wind turbine wind energy power transfer system was designed. The system was also modeled using mathematical equations. These systems were compared to validate the mathematical model needed to later create controls. A 0.517 in^3/rev hydraulic pump was affixed to a 0.097 in^3/rev hydraulic motor to transfer high pressure hydraulic fluid through the system. A pressure relieve valve protected the system against overpressure. As the velocity the pump was increased, and fluid was pushed through the motor, the velocity at the shaft of the motor was observed. It was also important to measure the overall system pressure as well as the flow moving through key hydraulic components. It was verified that for a single-wind turbine system, the mathematical model behaved as the model built using SimHydraulics.

The overall efficiency of the system paralleled that of the efficiency of a standard hydraulic pump.

One additional hydraulic pump was added to the model built in SimHydraulics as well as the mathematical model making the system a double-wind turbine system. Two fixed displacement pumps with displacements of 0.517 in^3/rev transferred hydraulic fluid to the main motor A with a displacement of 0.097 in^3/rev . Wind Turbine A was held at a constant velocity while the velocity of Wind Turbine B varied drastically to measure the effect of rotational speed on power transfer efficiency. Since the velocity of Wind Turbine A was held constant, the flow created was also constant. The flow of Motor A was a combination of the flow of Wind Turbine A and B. It was noted that there was a slight difference in the flows measured from the SimHydraulic model and the mathematical model due to the leakage factor that is set as an affixed number in the math model but varies from the system operating conditions in SimHydraulics. The system's overall power transfer efficiencies obtained from mathematical model and SimHydraulics deviated slightly because of changes in parameter calculation and slight dynamic differences. The double-wind turbine system provided higher efficiency than a single turbine system proving that wind turbines working in parallel would increase the overall system efficiency.

After validating the mathematical model with simulations, the wind power transfer system was constructed. Testing began on the test and two experiments were performed. Experiment 1 was done on the single turbine configuration (one hydraulic pump and one hydraulic motor). A ramp velocity was applied at the input shaft of a hydraulic pump for a given time period so that the system power transfer and velocity responses at the hydraulic motor could be observed. The velocity seen at the shaft of the hydraulic pump determined the linearly proportional flow of the hydraulic fluid in the system as well as the overall system pressure. It was monitored that as the hydraulic fluid traveled through the system losses occurred showing up as a decrease in the flow seen at the motor. These

losses were caused by the leakage that takes place in the pump and motor, and the friction in the fittings and flexible piping.

The pressure in the gearless wind power transfer system was recorded at two locations in Experiment 1, Wind Turbine B and Motor A. As the velocity at the shaft of the hydraulic pump increased, the pressure increased as well. In the provided pressure profiles (Chapter 7) it was recorded that the relationship between pressure and flow, and pressure and wind turbine velocity is linear. Motor A recorded a slightly higher pressure than Wind Turbine B due to the Direct Current (DC) Permanent Magnet Motor a higher rated horsepower coupled to the shaft of the motor. The pressure and flow rate were used to determine the horsepower generated by the pump and transferred to the motor. The efficiency of the system was then calculated from these values. As the velocity of the wind turbine was gradually increased, the efficiency also increased. For the single turbine hydraulic wind power system that eliminated the gearbox, variable wind speed cannot be regulated which consequently results in lower overall system efficiency.

To validate that the addition of another wind turbine would increase the efficiency of the system Experiment 2 was performed. It is important to make this system economical and to increase efficiency at lower operational velocities. During this experiment, the flows of two wind-driven hydraulic pumps were integrated and directed to one hydraulic motor. The speed of one Wind Turbine (A) was held constant providing a constant flow while velocity of Wind Turbine B varied for a given time period. As the pump speed increased, the flows of Wind Turbine B and Motor A increased linearly. As Wind Turbine B spun at a higher velocity, the output pressure of their point of common coupling (PCC) increased allowing Motor A to pump less fluid at a constant speed. In Experiment 2 the pressure of the system at Wind Turbine A, Wind Turbine B, and Motor A was measured. The pressure for Wind Turbine A and Motor A are close in value while the pressure of Wind Turbine B is lower. Similar to Experiment 1, Motor A is attached to a DC Permanent Magnet Motor that has a higher rated horsepower of ¾ HP. Wind

Turbine A is connected to a split phase AC motor that requires high resistance requiring more driving force to operate.

The output power increased as the speed of the wind turbine increased. Motor A required more power to keep up the flow generation. As the velocity of Wind Turbine B increased, the output pressure of PCC increased, which received more power from the wind turbine. The energy of the wind turbines were used to increase the system pressure and circulate the fluid in the system. The overall efficiency of the double-wind turbine system proved to be more efficient than a single wind system and at a lower velocity. This is strong proof that the variable speed gearbox used in a tradition wind turbine drivetrain can be eliminated.

8.2 Recommendations

For further research on the transfer of gearless wind power, the addition of a third wind turbine to this system should be implemented. With the addition of the third wind turbine, it can be determined how many wind turbines can be connected to a central generation unit before efficiency saturation will be attained.

To provide a better range of velocities to wind turbine A, a variable speed drive can be utilized. A variable speed drive is a device that regulates the speed and rotational force, or torque output of an electric motor. In the current setup, the wind turbine A is connected to an AC motor that only allows a velocity range of 350 RPM to 415 RPM to be applied to the shaft of the hydraulic motor. This does not create much variation and places limits on the real wind characteristics trying to be achieved.

8.3 Future Work

Energy Storage: To provide energy storage to this system, a hydraulic accumulator can be integrated. This device is a pressure storage reservoir in which a non-

compressible hydraulic fluid is held under pressure by an external source, compressed gas [7]. Compressed gas accumulators can provide the system with a lightweight energy storage option, the ability to accept both high frequencies and high rates of charging/discharging [22]. The main function of the accumulator will be to store energy during low demand periods and to respond immediately to temporary demand. An accumulator can also maintain system pressure for periods of slight leakage, aid the hydraulic pump in delivering power to the system and absorb pressure interruptions by smoothing out pulsations. The stored potential energy in the accumulator acts as a quick secondary source of fluid power capable of doing useful work as required by the gearless energy transfer system.

Speed (Frequency) Control: The fluctuation of frequency can be minimized or even eliminated through the use of frequency (speed) droop control. Frequency droop control is used to match generation to load to achieve the desired system frequency. Speed droop is the decline in speed or frequency of a prime mover in proportion to the load that is applied to it. As the load is increased, the speed or frequency droops. When introducing wind generated electricity into an existing electric system, difficulties can arise. It is important to preserve the balance between generated and demanded power to operate and control electric power systems [37, 38]. The amount and location of wind generation, wind turbine technology, and the size and characteristics of the electricity system all play an important role [25]. System inertia, having the greatest affect, determines the system frequency sensitivity to supply demand imbalances [25, 39]. It will be investigated how several wind speeds and loading conditions will affect the droop characteristics of the hydraulic energy transfer system.

LIST OF REFERENCES

LIST OF REFERENCES

[1] J. F. Manwell, J. G. McGowan and A. L. Rogers, *Wind Energy Explained: Theory, Design and Application*, The Atrium, Southern Gate, Chichester, West Sussex: John Wiley & Sons Ltd, pp. 3-7, 2002.

[2] "Brand Hydraulics," [Online]. Available: http://www.brand-hyd.com/efc/catalog.pdf. [Accessed January 2013].

[3] D. A. Spera, "Introduction to Modern Wind Turbines," in *Wind turbine Technology: Fundamental Concepts of Wind Turbine Engineering*, New York, NY, ASME Press , pp. 47-103, 2009.

[4] W. Frost and C. Aspliden, "Characteristics of the Wind," in *Wind Turbine Technology: Fundamental Concepts of Wind Turbine Engineering*, New York, ASME Press, pp. 467-541, 2009.

[5] N. SEED, "Northwest Community Energy," Groundwire, www.nwcommunityenergy.org/wind/resource-assessment/turbine-micro-siting. [Accessed 18 July 2012].

[6] U. D. o. Energy, "National Renewable Energy Laboratory," http://www.nrel.gov. [Accessed August 2012].

[7] A. Esposito, *Fluid Power with Applications*, Upper Saddle River, New Jersey: Pearson Prentice Hall, Inc., 2009.

[8] J. S. Cundiff, *Fluid Power Circuits and Controls: Fundamentals ans Applications*, Boca Raton, FL: CRC Press LLC, 2002.

[9] J. Cidras and C. Carrillo, "Regulation of Synchronous Generators by Means of Hydrostatic Transmissions," *IEEE Transactions on Power Systems,* vol. 15, no. 2, pp. 771-778, May 2000.

[10] e. a. K. Wu, "Modelling and identification of a hydrostatic transmission hardware-in-the-loop simulator," *International Journal of Vehicle Design,* vol. 34, pp. 52-64, 2004.

[11] N. D. Manring and G. R. Luecke, "Modeling and Designing a Hydrostatic Transmission With a Fixed-Displacement Motor," *Journal of Dynamic Systems, Measurements, and Control,* vol. 120, pp. 45-49, March 1998.

[12] K. Dasgupta, "Analysis of a hydrostatic transmission system using low speed high torque motor," *Mechanism and Machine Theory* , vol. 35, pp. 1481-1499, October 2000.

[13] A. V. Akkaya, "Effect of bulk modulus on performance of a hydrostatic transmission control system," *Sadhana-Academy Proceedings in Engineering Sciences,* vol. 31, pp. 543-556, Oct 2006.

[14] G. A. Sohl and J. E. Bobrow, "Experiments and simulations on the nonlinear control of a hydraulic servosystem," *IEEE Transactions on control Systems Technology,* vol. 7, pp. 238-247, March 1999.

[15] S. Habibi and A. Goldenberg, "Design of a new high-performance electrohydraulic actuator," *IEEE-ASME Transactions on Mechatroncs,* vol. 5, pp. 158-164, June 2000.

[16] M. Ijas and E. Mäkinen, "Improvement of Total Efficiency of Hydrostatic Transmission by Using Optimized Control," in *7th JFPS International Symposium on fluid Power*, Toyama, 2008.

[17] W. Rampen, *Gearless Transmission for Large Wind Turbines - The History and Future of Hydraulic Drives,* Artemis IP Ltd, Scotland.

[18] G. S. Payne, A. E. Kiprakis, M. Ehsan, W. H. S. Rampen, J. P. Chick and A. R. Wallace, "Efficiency and dynamic performance of Digital Displacement hydraulic transmission in tidal current energy converters," in *Power and Energy*, 2006.

[19] R. Herderson, "Design, simulation, and testing of a novel hydraulic power take-off system for the Pelamis wave energy converter," in *Renewable Energy 31*, Edinburgh, Scotland, UK, 2006.

[20] M. M. I. Systems, "Melexis Microelectronic Systems," 1998-2011. http://www.melexis.com/Assets/Hall-Effect-Geartooth-Sensor--3721.aspx. [Accessed August 2012].

[21] A. Pourmovahed and D. R. Otis, "An Expereimental thermal time-Constant corelation for Hydraulic Accumulators," *Transactions of ASME Journal of Dynamic Systems, Measurements, and controls,* vol. 112, pp. 116-121, March 1990.

[22] B. Wu, C.-C. Lin, Z. Filipi, H. Peng and D. Assanis, "Optimization of Power Management Strategies for a Hydraulic Hybrid Medium Truck," in *Proceedings of the 2002 Advanced Vehicle Control Conference*, Hiroshima, Japan, September 2002.

[23] S. Lemofouet and A. Rufer, "A Hybrid Energy Stroage system Based on compressed Air and supercapacitors With Maximum Efficiency Point tracking (MEPT)," *IEEE Transaction on Industrial Electronics,* vol. 53, no. 4, pp. 1105-1115, August 2006.

[24] N. U. Haq, "Design and Modelling of a Piston Accumulator for Rock Drill and its Fatigue Strength," Sweden, 2010.

[25] G. Lalor, A. Mullane and M. O'Malley, "Frequency Control and Wind Turbine Technologies," *IEEE Transactions on Power Systems,* vol. 20, no. 4, pp. 1905-1913, 2005.

[26] K. Pandiaraj, P. Taylor, N. Jenkins and C. Robb, "Distributed Load Control of Autonomous Renewable Energy Systems," in *IEEE Transactions on energy Conversion,* 2001.

[27] Z. Miao, L. Fan, D. Osborn and S. Yuvarajan, "Wind Farms With Hvdc Delivery in Inertial Response and Primary Frequency Control," in *IEEE Transactions of Energy Conversion,* 2010.

[28] J. O. Wilkes, *Fluid Mechanics for Chemical Engineers,* Upper Saddle River, New Jersey: Prentice-Hall, Inc., 1999.

[29] C. E. Synolakis and H. S. Badeer, "On combining the Bernoulli and Poiseuille equation-A plea to authors of college physics text," *American Association of Physics Teachers,* pp. 1013-1019, 1988.

[30] C. T. Crowe, D. F. Elger, B. C. Williams and J. A. Roberson, *Engineering Fluid Mechanics*, Hoboken, NJ: John Wiley & Sons, Inc., 2009.

[31] M. E. Saleta, D. Tobia and S. Gil, "Experimental study of Bernoulli's equation with losses," 2004.

[32] J. S. Cundiff, Fluid Power *Circuits and Controls: Fundamentals and applications*, Boca Raton, Florida: CRC Press LLC, 2002.

[33] http://www.mathworks.com/help/toolbox/physmod/hydro/ref/fixeddisplacemen tpump.html Fixed Displacement Pump.

[34] R. Z. a. A. Alleyne, "A Mdeol Reference Load Controller with Adaptation Using a two Stage Pressure Relieve Valve," *Proceedings of the Amercian Control Conference*, pp. 3949-3954, 2001.

[35] http://www.mathworks.com/help/toolbox/physmod/hydro/ref/hydraulicmotor. html,"Hydraulic Motor.".

[36] A. van Kooten, "Wind Power Delvelopment: Economics and Policies" in Policy Working Paper 4868," *T.W.B.D.R.G.E.a.E. Team, Ed., ed*, March 2009.

[37] N. A. Cutululis, A. Vigueras-Rodríguez, P. Sørensen, E. L. Jensen, J. Hjerrild, M. H. Donovan and H. Madsen, "Power Fluctuations From Large Wind Farms," *IEEE Transaction on Power Systems*, vol. 22, no. 3, pp. 958-965, 2007.

[38] L. Jin, S. Yuan-zhang, P. Sorensen, L. Xiong and L. Guo-jie, "Frequency Modeling of Wind Power Fluctuation and the Application on Power Systems," in *2010 International Conference on Power System Technology*, Hangzhou, 2010.

[39] S. Sharma, S.-H. Huang and N. Sarma, "System Inertial Frequency Response Estimation and Impact of Reneable Resources in ERCOT Interconnection," in *Power and Energy Society General Meeting*, 2011.

[40] J. Layton, "How Stuff Works," 2006.: http://science.howstuffworks.com/environmental/green-science/wind-power.htm. [Accessed April 2012].

[41] "Energy Works: Engineering Construction Procurment," Energy Works US, LLC, http://www.solar-wind-nature-energy.com/win_turbines_hz.html. [Accessed August 2012].

[42] P. Sorensen, A. D. Hansen, K. Thomsen, H. Madsen, A. H. Nielsen, N. K. Poulsen, F. Iov, F. Blaabjerg and B. K. Okkels, "Simulation and optimisation of wind farm controllers".

[43] E. Cam, "Application of fuzzy logic for load frequency control of hydrolectrical power plants," *Energy Conversion and Managament*, vol. 48, pp. 1281-1288, 2007.

[44] "Gems Sensors and Controls," http://www.gemssensors.com/Products/Flow/Electronic-Flow-Sensors/Turbo-Flow/FT-110-Series-Flow-Sensor. [Accessed January 2013].

[45] "Cherry Corp, "http://www.cherrycorp.com/english/sensors/Speed_Direction/gs1005_1009.htm. [Accessed January 2013].

[46] "Measurement Specialites, Inc.," http://www.meas-spec.com/product/t_product.aspx?id=2888. [Accessed January 2013].

[47] "Prince Measurement Corporation," http://www.princehyd.com/Portals/0/products/valves/catalog/ValvesRd1809.pdf. [Accessed January 2013].

[48] "Concentric," http://www.concentricab.com/Hydraulics2.asp?cat=4&subcat=41&subsubcat=411. [Accessed January 2013].

[50] "Northman Fluid Power," http://www.northmanfp.com/. [Accessed January 2013].

APPENDIX

Toubleshooting Chart

SYMPTOM	POSSIBLE CAUSE(S)	CORRECTIVE ACTION
Pump does not develop full pressure	1. System relief valve set too low, or leaking 2. Oil temp is too high 3. Pump is worn out 4. Double acting cylinder piston seals are cut or worn out	1. Check system relief valve for proper setting with pressure gauge in outlet line 2. Let oil cool below 140°F 3. Replace worn parts or pump 4. Replace or repair cylinder
Motor won't start	1. Loose connection 2. Circuit breaker tripped 3. Voltage drop 4. Seized pump 5. Start up load is higher than motor torque capability	1. Check wiring 2. Reset circuit breaker 3. Use heavier gauge wire 4. Replace pump 5. Use larger motor or reduce operating pressure
Will not pump oil (Motor runs but cylinder does not move, or moves slowly)	1. No oil in reservoir 2. Motor rotating wrong direction 3. Oil level low 4. Suction strainer is clogged 5. Double acting cylinder piston seals are cut or worn out 6. Reservoir breather is dirty or clogged 7. Bi-rotational check valve leaking	1. Check oil level, refill 2. Change rotation of prime mover or reverse inlet and outlet hoses 3. Add oil as needed 4. Clean suction strainer 5. Replace or repair cylinder 6. Clean reservoir breather and reinstall 7. Remove check valve on pressure side. Clean and reassemble.
Pump motor unit is noisy	1. Low oil level 2. Air in system 3. Suction strainer or inlet filter is clogged	1. Add oil as needed 2. Bleed air from highest fitting in system by loosening fitting very slightly and operating unit until bubbling of air stops, then tighten 3. Clean suction strainer or inlet filter
Motor operating slow or stalling	1. Excessive slipping of gears due to overheating of oil 2. Excessive wear on the sides of gear housing due to oil contaminants	1. Check system. Add oil if needed. Oil cooler may be necessary to keep oil at normal operating temperatures 2. Check condition of oil and replace if contaminated
Motor speed is erratic	1. Motor operating below minimum recommended speed of 750 RPM 2. Air in system	1. Increase minimum operating speed to 750 RPM or more 2. Bleed air from system

Figure A.1 Data sheet for hydraulic pump [48]

CONCENTRIC OPERATING INSTRUCTIONS & PARTS MANUAL

HYDRAULIC GEAR PUMPS/MOTORS

MODELS 10561 THRU 10567

Concentric P/N 2690163 revised 07/21/11

READ CAREFULLY BEFORE ATTEMPTING TO ASSEMBLE, INSTALL, OPERATE OR MAINTAIN THE PRODUCT DESCRIBED. PROTECT YOURSELF AND OTHERS BY OBSERVING ALL SAFETY INFORMATION. FAILURE TO COMPLY WITH INSTRUCTIONS COULD RESULT IN PERSONAL INJURY AND/OR PROPERTY DAMAGE! RETAIN INSTRUCTIONS FOR FUTURE REFERENCE.

Description

Our hydraulic pumps are highly efficient and specifically designed for bi-directional rotation. They utilize an external gear fixed displacement design and are of a durable cast iron construction. They incorporate an internally lubricated ball bearing on the drive shaft which will withstand up to 150 lb. side load.

They can be used for direct drive or for belt driven applications. Hydraulic pumps are suitable for use in a wide variety of material handling, agricultural, and construction equipment applications, in addition to machine tools, robotics, and other types of machinery.

Unpacking

Due to cast iron construction, very little damage can occur during transit. Do not remove the plastic shipping plugs from the ports until ready for installation. This will keep dirt or foreign material from entering the system.

Specifications

Cast iron hydraulic pump, bi-rotational, 4-bolt 4F17 mounting, 11 tooth gears, 1.50" shaft extension, 0.50" shaft diameter with 0.125" square x 1" drive key, side porting with SAE straight thread ports, internally lubricated ball bearing for side loads to 150 lbs.

Replacement Parts

Seal & Bearing Kit 2300780

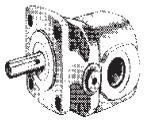

Figure 1

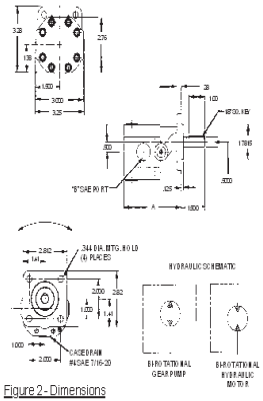

Figure 2 - Dimensions

PUMP/FLUID MOTOR DIMENSIONAL DATA

MODEL	DIMENSIONS A	B
10561	3.16"	9/16-18 SAE #6
10562	3.16"	9/16-18 SAE #6
10563	3.16"	3/4-16 SAE #8
10564	3.16"	3/4-16 SAE #8
10565	3.16"	3/4-16 SAE #8
10566	3.66"	7/8-14 SAE #10
10657	3.66"	7/8-14 SAE #10

⚠ WARNING! ⚠

General Safety Information

DISCONNECT POWER AND RELEASE ALL SYSTEM PRESSURE BEFORE SERVICING THIS EQUIPMENT.

1. Follow all local electrical and safety codes, as well as the National Electrical Code (NEC) and the Occupational Safety and Health Act (OSHA).
2. Never exceed the maximum operating speed or pressure.
3. When using AC motors, ground the motor properly by wiring with a grounded, metal-clad raceway system, using a separate ground wire connected to bare metal of the motor frame, or other suitable means.
4. Guard all moving parts.
5. Drain all liquids from the system before servicing.
6. Check hoses and connections for security before each use.
7. Periodically check the pump/fluid motor and system components.
8. Provide a means of pressure relief for pumps whose discharge line can be shut off or obstructed.
9. Wear safety glasses at all times when working with pumps/fluid motors.
10. Keep work area clean, uncluttered and properly lighted; replace all unused tools and equipment.
11. Keep visitors at a safe distance from the work area.
12. Make the workshop child-proof with padlocks, master switches, and by removing start keys.
13. Do not operate an engine in an enclosed area.
14. Do not spill gasoline on hot engine surfaces.
15. Store gasoline only in an approved container.
16. Keep dirty and oily cleaning rags in a tightly closed metal container.
17. Check engine oil level before operating the engine.
18. Familiarize yourself with the controls and emergency shutdown procedures.
19. Never operate the equipment when you are fatigued.
20. All system components pressure ratings should be greater than maximum system pressure.
21. Guard all moving parts.
22. Replace all guards when servicing is complete.

Assembly

Models 10561 through 10567 are packaged fully assembled and require no further assembly.

Installation

MOUNTING PUMP ASSEMBLY TO FLEXIBLE COUPLING DRIVE SYSTEMS

1. Assemble the flexible coupling half to the pump/fluid motor shaft.

⚠ CAUTION ⚠

Do not force coupling half onto drive shaft; it must be a slip fit for adjustment and to avoid internal damage.

2. Tighten the setscrew and insert rubber spider in coupling half.
3. Assemble the other coupling half loosely to the engine/motor shaft.
4. Bolt the pump/fluid motor loosely to the SAE type four bolt mounting pump adapter as furnished by the equipment manufacturer.
5. Align the shafts to make sure they are on center with each other.
6. Tighten the mounting bolts.
7. Mate the coupling halves together, allowing 1/16" gap between halves.
8. Check the alignment again.

IMPORTANT: THE GAP IN THE COUPLING HALVES IS TO PREVENT END LOADING OF THE PUMP/FLUID MOTOR DRIVE.

9. Tighten the setscrew in the mating coupling half.
10. Remove plastic shipping plugs from the inlet and outlet ports.
11. Squirt clean oil into pump for pre-lubrication and start-up.
12. Turn shaft coupling slowly to ensure proper shaft alignment and coupling installation.
13. Connect inlet and outlet lines with an SAE straight thread fitting and tighten.

⚠ CAUTION ⚠

Flush all lines and fittings of contamination.

⚠ WARNING! ⚠

THREADS ARE SAE, *NOT* NPTF. USING INCORRECT FITTINGS COULD DAMAGE THE HYDRAULIC COMPONENT OR CAUSE PERSONAL INJURY.

NOTE: Do not use teflon tape; the O-ring provides the seal and teflon tape is not required.

14. When using the assembly as a pump keep inlet hose short and of adequate size to avoid pump cavitation.

NOTE: Cavitation is recognized by excessive noise and foaming of hydraulic fluid.

⚠ CAUTION ⚠

Never run assembly without hydraulic oil.

15. At initial start-up, turn the drive shaft several times by hand to prime.
16. Bleed all air from the system to prevent erratic operation.
17. After several cycles, check the reservoir oil level and refill as necessary.

Figure A.1 Continued

STOCK NO.	DISP. CU.IN./REV.	Flowat* 1800 RPM	Flowat* 3600 RPM	MAX. PRESSURE CONT.	MAX. PRESSURE INTER.	Port Size SAE	
10561	0.065	0.5	1	3000	4000	9/16-18	SAE #6
10562	0.097	0.75	1.5	3000	4000	9/16-18	SAE #6
10563	0.129	1	2	3000	4000	3/4-16	SAE #8
10564	0.194	1.5	3	3000	4000	3/4-16	SAE #8
10565	0.258	2	4	2300	4000	3/4-16	SAE #8
10566	0.388	3	6	1600	2500	7/8-14	SAE #10
10567	0.517	4	8	1200	2000	7/8-14	SAE #10

* Flow based on 0 pressure and rated in Gallons per minute.

Installation (Continued)

NOTE: Be sure adequate cooling for the hydraulic oil is provided. Excessive temperatures can cause damage to oil and/or system components. Cooling of oil is especially important on systems where continuous operation is required. Cooling requirements must be based on: duty cycle, pressure/flow, ambient temperatures, oil and component maximum temperature specifications, and reservoir capacity. Systems operating at excessively high temperatures can be hazardous and may cause property damage and/or personal injury.

NOTE: When the ambient temperature is below 32°F, allow the pump to operate unloaded for several minutes to warm the oil in the reservoir.

Operation

1. At initial start-up, start and stop several times (jog) to allow the assembly to prime. After lines are full, the pump may be operated at full speed.
2. Bleed all air from hydraulic system to prevent erratic operation.
3. Recheck reservoir oil level after a few complete cycles of the hydraulic system and refill if necessary.

When using as a hydraulic motor

Do not exceed 20 psi at the outlet. If unit is going to be used in series or when outlet pressure exceeds 20 psi, case drain must be plumbed. The case drain port is a 7/16-20 SAE #4 port located on the bottom rear of the unit. Remove plug and run a 1/4" hydraulic line back to a vented reservoir.

⚠ WARNING! ⚠

BE SURE TO DISCONNECT POWER AND RELEASE ALL SYSTEM PRESSURE BEFORE SERVICING THIS EQUIPMENT.

Maintenance

1. Keep the reservoir filled with hydraulic fluid. Recommended Hydraulic Fluids: use a good grade of automatic transmission fluid (ATF).
2. Make frequent inspection of hydraulic fluid and change if contaminated.
3. To fill the reservoir with clean oil:
   Use a clean funnel fitted with a fine mesh wire screen. Do not use a cloth strainer. Most pump/fluid motor failure, valve malfunctions, and short unit life can be traced directly or indirectly to dirt or other foreign material (water, chips, lint, etc.) getting into, or already in, the hydraulic system.
4. Keep the unit clean of dirt and foreign materials.
5. Keep electrical connections clean.

Common Hydraulic Motor Formulas

$$\text{Torque / 100 psig (in./lbs.)} = \frac{\text{Fluid Motor Displacement (cu. in.)}}{0.0628}$$

$$\text{Speed} = \frac{231 \times \text{Flow Rate (GPM)}}{\text{Fluid Motor Displacement (cu.in.)}}$$

$$\text{Horsepower} = \frac{\text{Torque Output (in./lbs.)} \times \text{RPM}}{63025}$$

VALVES

MODEL RD-1800 PRESSURE RELIEF
MODEL RD-900 SELECTOR VALVE

MODEL RD-1800
BALL/SPRING TYPE
DIRECT ACTING RELIEF

The PRINCE valve model RD-1800 is a direct acting ball/spring type pressure relief. The valve is compact and simple in design. This type relief is fast opening and is well suited for pressure spike protection. The performance curves below indicate the low cracking pressure typical to ball/spring reliefs. Please refer to the model RV relief for a system pressure relief. The valve is available with a standard steel seat, model RD-1800S, or with a hardened seat, model RD-1800H. Both models are externally adjustable.

VALVE SPECIFICATIONS:
Capacity: 20 gpm max inlet flow
Pressure: 2500 psi max
Weight: 2 lb.
Adjustment Range: 1000 PSI to 2500 PSI

SYMBOL

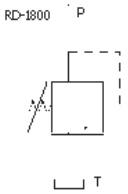

RELIEF VALVE CURVE
AT VARIOUS SET POINTS
110 SUS OIL AT 115°F.

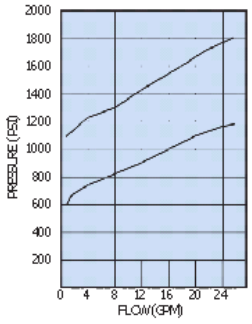

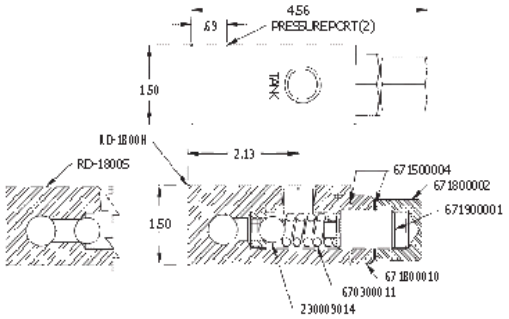

NOTE: Relief settings are 1500 PSI @ 12 GPM. For non-standard relief settings specify PSI in hundreds and GPM after model number.
EX: RD-1850S-**12-10** for **1200 PSI @ 10 gPM**

STANDARD MODELS AVAILABLE		
MODEL #	PORT SIZES	MAX FLOW
RD-1837S	3/8 NPTF	8 GPM
RD-1850H	1/2 NPTF	16 GPM
RD-1850S	1/2 NPTF	16 GPM
RD-1875S	3/4 NPTF	20 GPM

MODEL RD-900
SELECTOR VALVE

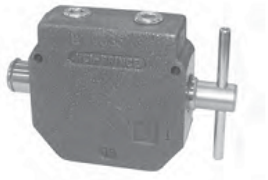

The PRINCE valve model RD-900 is a manual 3-way 2-position selector valve. This valve will allow one pump source to supply two separate circuits. Pushing the handle in diverts oil flow to port away from handle. Pulling the handle out diverts oil flow to port nearest handle

SYMBOL

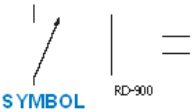

VALVE SPECIFICATIONS
Capacity: 30 gpm max inlet flow
Pressure: 3000 psi max
Weight: 7 lbs

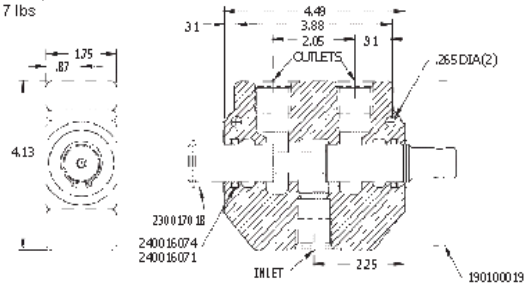

STANDARD MODELS	
MODEL #	PORT SIZES
RD-950 RD-975	1/2 NPTF 3/4 NPTF

SEAL KIT 660590025

PRINCE MANUFACTURING CORPORATION • P.O. BOX 7000 • NORTH SIOUX CITY, SOUTH DAKOTA 57049-7000
URL: www.princehyd.com • E-MAIL: prince@princehyd.com
O.E.M. CUSTOMER SERVICE: (605) 235-1220 • FAX (712) 233-2181 DISTRIBUTOR CUSTOMER SERVICE: PHONE (605) 235-1220 • FAX (712) 233-2181
SEE PAGE 23 OF THE STANDARD PRODUCT PRICE LIST FOR PRICING
CATV 66-09-04-0

Figure A.2 Data sheet for pressure relief valve [47]

DIRECTIONAL CONTROLS
IN LINE CHECK VALVE

SYMBOL

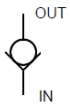

SPECIFICATIONS

MODEL	RATE FLOW LPM(GPM)	MAX. OPERATED PRESSURE KGF/CM^2 (PSI)	CRACKING PRESSURE KGF/CM^2(PSI)
CI-T03	30(7.9)	210(3000)	05: 0.35(5) 50: 3.5(50)
CI-T04	65(17.1)		
CI-T06	115(30.4)		
CI-T08	165(43.6)		
CI-T10	210(55.5)		

HOW TO ORDER

CI - T 03 - 05 - 10 - N

- NO CODE: PT PIPE THREADS
  N: NPT PIPE THREADS
- DESIGN NUMBE
- CRACKING PRESSURE
  05: 0.35KGF/CM^2 (5PSI)
  50: 3.5 KGF/CM^2 (50PSI)
- PORT SIZE
  03: 3/8"
  04: 1/2"
  06: 3/4"
  08: 1"
  10: 1 1/4"
- T: THREADED CONNECTIONS
- CI: IN-LINE CHECK VALVE

Figure A.3 Data sheet for check valve [50]

CI-T03

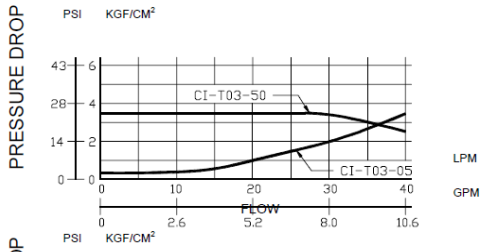

CI-T04

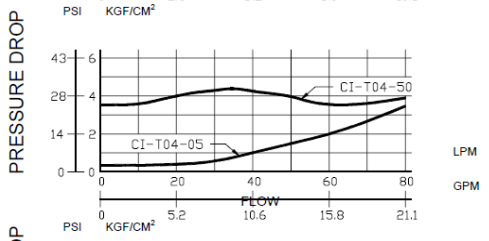

CI-T06

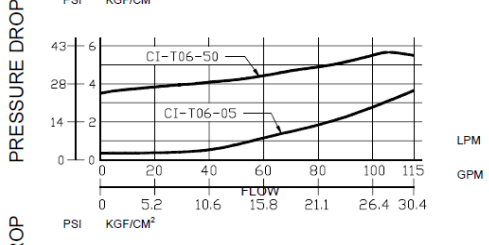

CI-T08

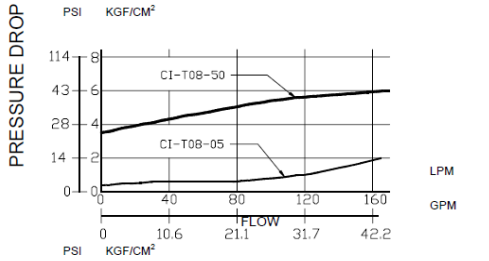

CI-T10

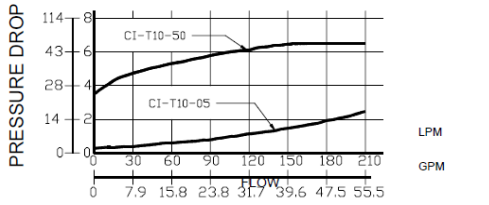

Figure A.3 Continued

INSTALLATION DIMENSIONS

UNIT： mm(inch)

CI-T03/04/06/08

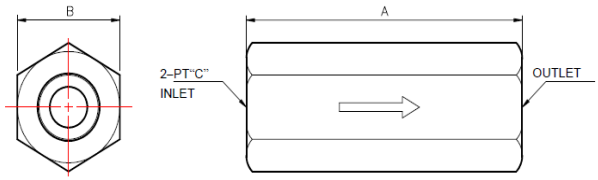

CI-T10

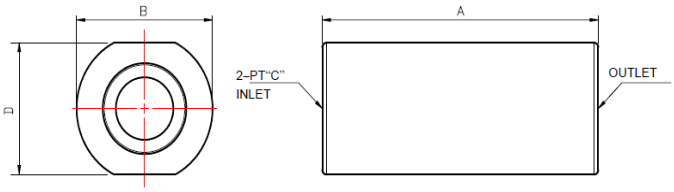

MODEL	A	B	C	D
CI-T03	70 (2.76)	26 (1.02)	3/8	– –
CI-T04	82 (3.23)	29 (1.14)	1/2	– –
CI-T06	91.5 (3.60)	35 (1.38)	3/4	– –
CI-T08	112 (4.41)	51 (2.01)	1	– –
CI-T10	132 (5.20)	65 (2.56)	1 1/4	58 (2.28)

Figure A.3 Continued

BRAND HYDRAULICS
Shipping: 2332 So 25th St (Zip 68105)
Mailing: P.O. Box #6069 (Zip 68106)
Omaha NE
Phone: (402) 344-4434
Fax: (402) 341-5419
HTTP://WWW.BRAND-HYD.COM
ISO 9001:2008 WITH DESIGN
Certificate #02.002.1

ELECTRONICALLY ADJUSTABLE PROPORTIONAL PRESSURE COMPENSATED FLOW CONTROL "EFC"

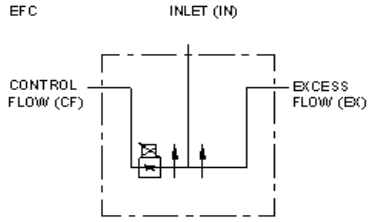

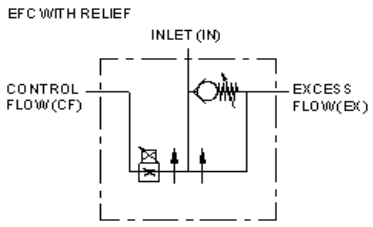

EFC12-10-12

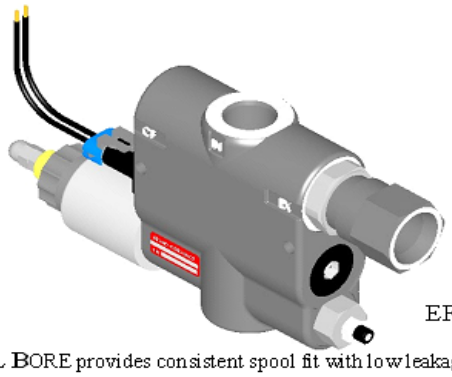

EFC12-15-12R22

FEATURES:

- DIAMOND HONED SPOOL BORE provides consistent spool fit with low leakage.
- O'RING PORTS to eliminate leakage.
- EVERY EFC IS TESTED for shutoff, linearity, max. flow, crack open and pressure compensation.
- STANDARD 3-PORT allows for pressure compensated flow out of the CF and EX ports.
- MANUAL OVERRIDE when electrical power is lost.
- OPTIONAL 2-PORT allows for pressure compensated flow out of CF port.
- OPTIONAL FREE REVERSE FLOW allows fluid to move from the CF port to the inlet.
- OPTIONAL HIGH LIFT RELIEF.

SPECIFICATIONS:

- See flow chart for capacity.
- 3000 psi (207 bar) rating.
- Weighs 8-1/2 lbs. (3.9 kg).
- Standard Port size #12SAE (1-1/16 – 12).
- 10-Micron Filtration Recommended.
- Pulse Frequency (90 to 115 hz).
- Coil

-12 VDC standard	(24 VDC).
-9.6 ohms	(48 ohms).
-15 watts	(15 watts).
-1.0 amp max	(0.5 amp max.).

- Response Time
  -0.035" Standard dashpot (375 ms).
  -0.020" Dashpot (900 ms).
  -0.093 Dashpot (175 ms to 350 ms depending on flow).
- Spool leakage (3.05 in^3/min. @ 1000 psi ((50 ml/min. @ 68.9 bar) on EX port).

MATERIALS:

- Ductile Cast Iron Body
- Heat Treated Steel Spools
- Buna N O'Rings
- Heat Treated Free Reverse Check Seat

Figure A.4 Data sheet for pressure compensated electronically controlled flow control valve [2]

BRAND HYDRAULICS

Electric Flow Control

EFC – GENERAL INFORMATION

The Brand, electronically adjustable proportional pressure compensated flow control is an electronically controlled version of the original FC51 style flow control valve. The EFC performance as a flow control is very similar to the FC51 because they both use the same spring and compensator spool. Thus, the control flow port (CF) and the excess flow port (EX) remain usable and pressure compensated.

The main advantage of the EFC over the FC51 is that the flow can be adjusted proportionally with a solenoid instead of manually. As the current to the solenoid increases the variable orifice moves proportionally similar to positioning the rotary side lever on the manual FC's. The solenoid is connected to our EC – series controls which can be sold with the EFC. We also give the choice of a dashpot size, which allows the customer to select a valve that responds to the control box at different rates. Other options are 2-port, free reverse flow and high lift ball spring relief.

2-PORT- The 2-port (2P) option is a modified version of the standard 3-port EFC. This option lets the customer use the control flow port while the excess port is plugged. A special compensator spool was designed to eliminate hunting that can occur between pressure compensated valves and pumps. To use the EFC 2-port a pressure compensated pump is required. The 2-port can be converted to a 3-port (by removing the EX plug), but it will not have the same characteristics as the standard 3-port. (See chart on next page for 2-port EFC)

FREE REVERSE FLOW- The free reverse flow option was designed to be used primarily where cylinders and motors are needed to go in reverse. The flow can only go in reverse from controlled flow (CF) to the inlet (IN). Flow is not metered when it goes in reverse. The steel ball seat inside the compensator spool is heat treated to assure a long life.

HIGH LIFT BALL SPRING RELIEF – The high lift ball spring relief (R) reduces plumbing and provides relief protection. Once the pressure on the inlet port increases above the relief setting the relief valve opens and diverts flow to the EX port while maintaining pressure on the IN port. The EX port must be plumbed back to tank for this relief to work. This relief does not chatter and the cracking pressure from low to high flow is virtually the same. The relief is easily adjustable by simply loosening the lock nut and turning the adjusting fitting. (See relief chart on next page)

EFC – EXAMPLES OF COMMON MODEL CODES:

EFC12-10-12..... 10 gpm (37.9 lpm) 3-port with 12 volt coil
EFC12-15-12R15..... 15 gpm (56.8 lpm) 3-port, 12 volt coil with 1500 psi (103.4 bar) relief
EFC12-10-122P..... 10 gpm (37.9 lpm) 2-port with 12 volt coil
CEP1000..... 10 gpm (37.9 lpm) 3-port with EC-12-01 control

EFC – CREATING A MODEL CODE FOR EFC'S:

E F C __ - __ - __

REVERSE FLOW:
C – Free reverse flow
Omit – No reverse flow

PORT SIZE:
12 - #12SAE (1-1/16 – 12)
** - Contact factory for others

FLOW SETTING:
05 – 0-5 gpm (18.9 lpm)
10 – 0-10 gpm (37.8 lpm)
15 – 0-15 gpm (56.8 lpm)
20 – 0-20 gpm (75.7 lpm)
25 – 0-25 gpm (94.6 lpm)*
30 – 0-30 gpm (113.6 lpm)*

OPTIONS:
2P – 2 port
R15 – Relief set at 1500 psi (103.4 bar) (specify pressure in 100 psi increments)*
.093 – 0.093 dashpot orifice
.020 – 0.020 dashpot orifice

COIL VOLTAGE & TERMINAL:
12 – 12 volt DC
24 – 24 volt DC
PF – Weather pack, female shroud with male pin
PM – Weather pack, male tower with female pin

* - 3 port only

Page B-12

Figure A.4 Continued

BRAND HYDRAULICS

Electric Flow Control

EFC WITH ELECTRONIC CONTROL:

C E P _ _ _ 0 0 _

REVERSE FLOW:
C – Free reverse flow
Omit – No reverse flow

CONTROLS:
D – EC-12-02 (Dashmount)
Omit – EC -12-01 (Weather proof box)

FLOW SETTING:
05 – 0-5 gpm (18.9 lpm)
10 – 0-10 gpm (37.8 lpm)
15 – 0-15 gpm (56.8 lpm)
20 – 0-20 gpm (75.7 lpm)
25 – 0-25 gpm (94.6 lpm)*
30 – 0-30 gpm (113.6 lpm)*

OPTIONS:
2P – 2 port
R15 – Relief set at 1500 psi (103.4 bar) (specify pressure in 100 psi increments)*
.093 – 0.093 dashpot orifice
.020 – 0.020 dashpot orifice
Omit – No options

* - 3 port only

EFC FLOW & SOLENOID CURRENT INFO FOR 2-PORT AND 3-PORT:

Flow vs. Solenoid Current for EFC 3-Port

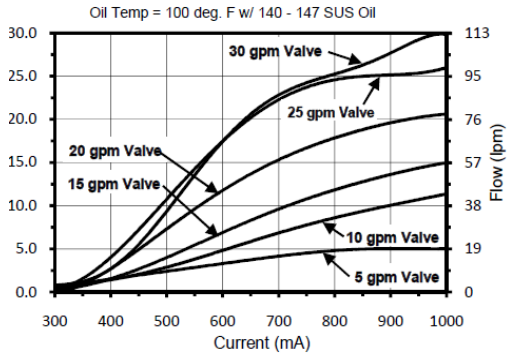

Flow vs. Solenoid Current for EFC 2-Port

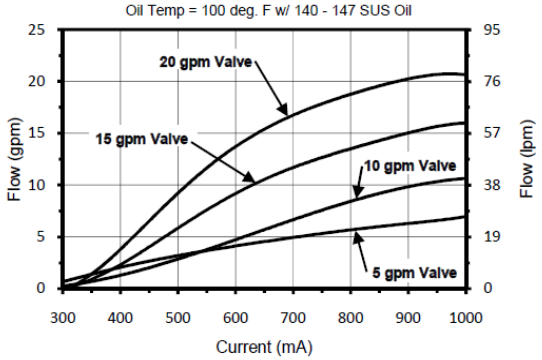

Pressure Drop vs. Flow for EFC Series

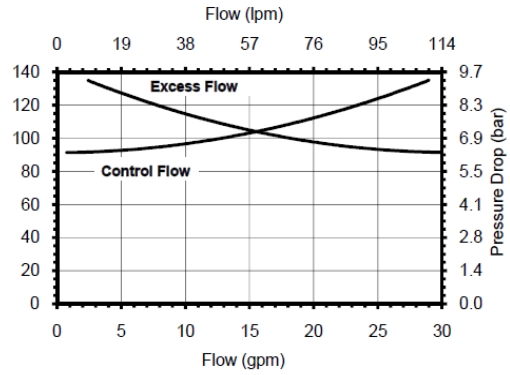

Pressure vs. Flow for EFC with Relief

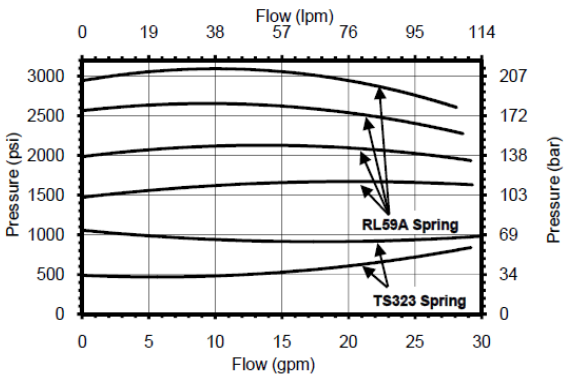

Page B-13

Figure A.4 Continued

BRAND HYDRAULICS

Electric Flow Control

2 & 3 PORT SCHEMATIC DRAWING:

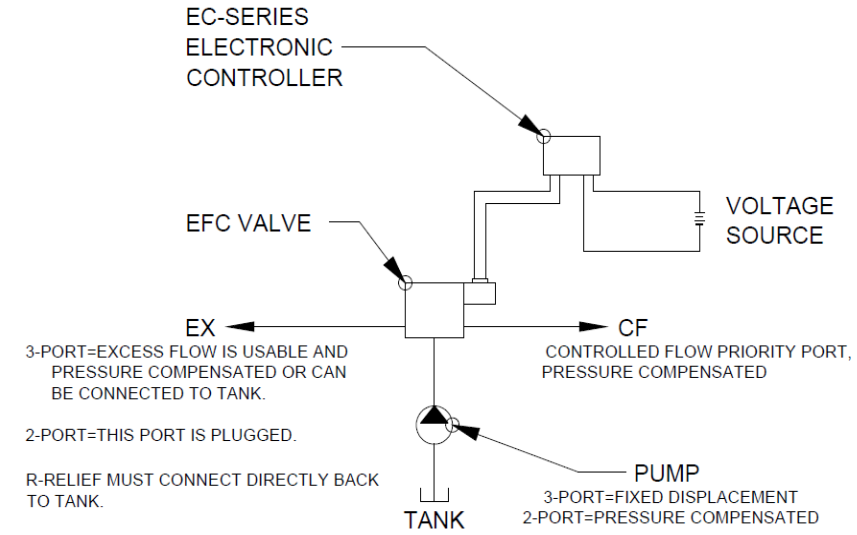

DIMENSIONAL DATA (EFC WITH RELIEF SHOWN):

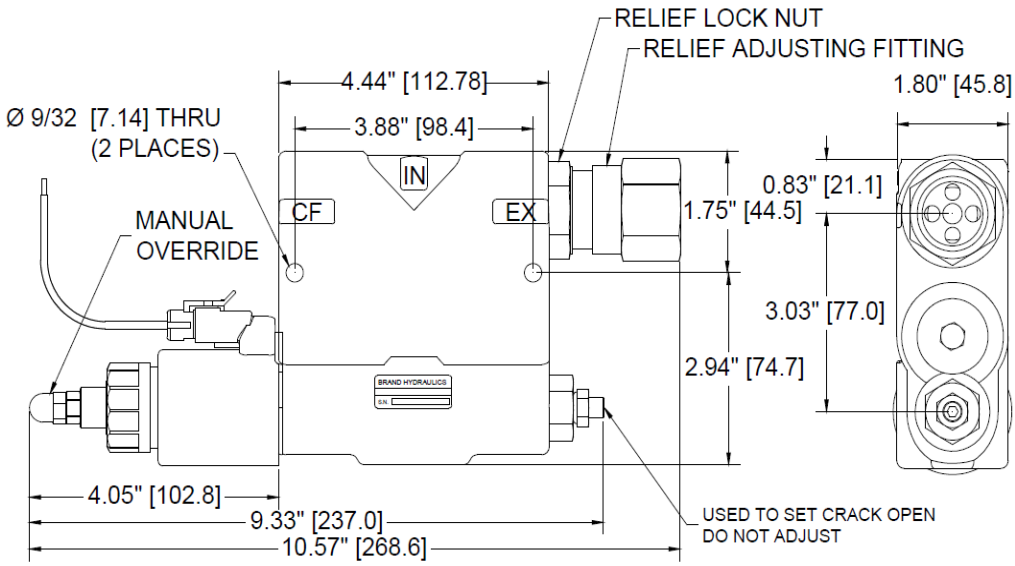

Page B-14

Figure A.4 Continued

FT-110 Series – TurboFlow®
Economical Flow-Rate Sensors

- Low Cost Plus High Accuracy ±3% of Reading
- Measures Low Liquid Flow Rates of .1 to 8 GPM
- Lightweight Plastic Design Enables Mounting in any Position

Gems Hall Effect turbine flow rate sensor is ideal for OEM applications involving low flow liquid monitoring. The low cost coupled with 1/2% repeatability makes it an ideal candidate for replacing dispensing timer systems. Unlike existing timing systems, turbine technology is not influenced by changes in system pressure caused by aging filters. The sensor's standard power and output specifications make it easy to retrofit to existing controllers.

Specifications

Wetted Materials	
Body	Nylon 12
Turbine	Nylon 12 Composite
Bearings	PTFE/15% Graphite
Operating Pressure	200 PSIG
Burst Pressure	2500 PSIG
Operating Temperature	-4°F to 212°F (-20°C to 100°C)
Viscosity	32 to 81 SSU (.8 to 16 Centistokes)
Filter	<50 Microns
Input Power	5 to 24 VDC @ 8mA
Output (Hz)	NPN Sinking Open Collector @ 20mA Maximum Leakage Current 10µA (Pull-Up Resistor Required)
Accuracy	±3% of Reading
Repeatability	0.5% of Full Scale
Electrical Connection	Spade Terminals .110"/.248" x .031" (2.8/6.3 x .8 mm) or 3 ft. cable
Inlet/Outlet Ports	3/8" NPT Male (3/8" G Male also available)

Dimensions

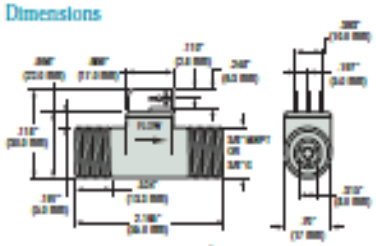

Wiring

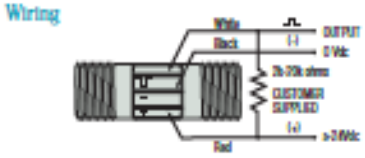

Cable Wire Code: Red = 5 to 24 VDC
Black = Ground
Brown = Signal Output

How To Order – Standard Models

Specify Part Number based on flow range.

Flow Range		Pulses per		Frequency Output	3/8" NPT Part Number	
GPM	Liters/m	Gallon	Liter		Spade	Cable
.13-1.3	.5-5.0	26200	6900	58-575 Hz	1r9831 ⚡	1r2831-C
.13-2.0	.5-7.5	17400	4600	38-575 Hz	1r9833 ⚡	1r2833-C
.26-2.7	1-10	12500	3300	55-550 Hz	1r9832 ⚡	1r2832-C
.26-4.0	1-15	8300	2200	37-550 Hz	1r9834 ⚡	1r2834-C
.26-6.6	1-25	3800	1000	16.7-416 Hz	1r993a ⚡	1r293a-C
.53-9.2	2-35	2640	750	25-437 Hz	23426a ⚡	23426a-C

⚡ – Stock Items.

Pressure Drop—Typical

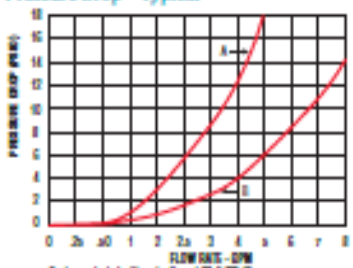

Tests conducted with water flow at 68°F (20°C).

A) Part #173831, 173832, 173833
B) Part #173834, 173835

FT-110 Accessories

Consult factory for special customized OEM versions.

Description	Part Number
Mating connector w/3 foot, 3 conductor, PVC pigtail cable	1r29e1 ⚡
Mating connector w/10 foot, 3 conductor, PVC pigtail cable	1r29e2 ⚡

Figure A.5 Data sheet for flow sensor [44]

GEARTOOTH SPEED SENSOR

GS1005 – GS1007

Description

The GS1005-1007 series gear tooth sensors are Hall Effect devices designed for use in applications where ferrous edge detection or near zero speed sensing (without power up recognition) is needed. Current sinking output requires the use of a pull up resistor.

Features and Benefits

- Immune to rotational alignment
- ESD resistant to 4kV (contact discharge)
- Mating connector: Delphi 12162280
- Discrete wire version: 20awg, tin plated polyolefin insulation.

Applications

- Exercise equipment
- Food processing equipment
- Speedometer

GS1005-GS1007 Specifications

Part Number	Operating Voltage Range (VDC)	Supply Current (mA max)	Output	Output Saturation Voltage (mV max)	Output Current (mA max)	Operating Temperature Range (°C)	Storage Temperature Range (°C)	Thread	Housing Length	Leads
GS100501	5 - 24	6	3-wire sink	400	20	-40 to 125	-40 to 125	M12-1	65mm	12mm circular
GS100502	5 - 24	6	3-wire sink	400	20	-40 to 125	-40 to 125	M12-1	65mm	20 awg x 1 m BBB
GS100701	5 - 24	6	3-wire sink	400	20	-40 to 125	-40 to 125	15/32 - 32	1"	20 awg x 1 m BBB

Notes: These sensors require the use of an external pull-up resistor, the value of which is dependent on the supply voltage
Pull-up resistor should be connected between output (Green) and Vcc (Red).

Note: These sensors require the use of an external pull-up resistor, the value is dependent upon the supply voltage. Pull-up resistor should be connected between output (Black) and Vcc (Brown). See chart on next page for recommendations.

Dimensions mm

GS100701

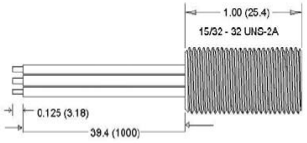

GS100502

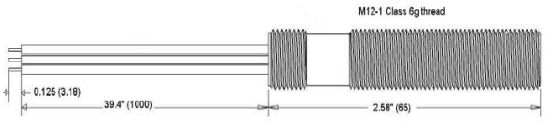

GS100501

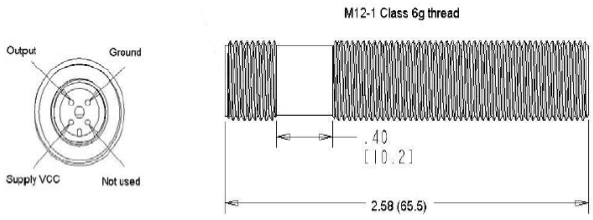

CHERRY®

Figure A.6 Data sheet for speed sensor [45]

GEARTOOTH SPEED SENSOR

GS1005 – GS1007

Mechanical Specifications

Airgrap	Application dependent
Maximum Installation Torque	50 in-lbs (for a ¼ - 20 Hex Cap screw)

Electrical Specifications

Operating Voltage Range	5 - 24 VDC
Supply Voltage	24 - 30 VDC
Supply Current	6 mA max
Output Saturation Voltage	400 mV max
Output Current	20 mA max
Operating Temperature	-40° to +125°C (GS100502 & GS100701) -40° to +105°C (GS100501)
Storage Temperature Range	-40° to +125°C (GS100502 & GS100701) -40° to +105°C (GS100501)
Output Rise time	5µS
Output Fall time	5µS
Electrostatic Discharge Immunity	+ 3kV indirect contact, + 4kV direct contact
Electric Field Radiated Immunity	At 10V/m (using 30% amplitude modulation @ 1kHz) from 26Mz to 1000 MHz
Electrical Fast Transient Test	+ 2kV on DC power supply
Immunity to Magnetic Fields	SAE J1113-22 (600 microT AC field; 5Hz to 2kHz; .2mT & 1mT DC field)
Conducted Immunity Test	Injected with 10Vrms from 150kHz to 80 MHz
Dielectric Withstand Voltage	MIL-STD-202F, Method 301 1000V applied for a minimum of one minute.
Insulation Resistance	MIL-STD-202F, Method 302, Test Condition B 500V applied for one minute.

Water Immersion	MIL-STD 202F, Method 104, Test Condition A
Salt Spray	MIL-STD-202F, Method 101, Test Condition B
Sinusoidal Vibration	MIL-STD-202F Method 204, Test Condition C from 55-2000 Hz
Random Vibration	MIL-STD-20F Method 214, Test Condition IC
Mechanical Shock	18 shocks at 50g's 11ms per Mil Std 202F

Recommended external pull-up resistor:

Volts DC	5	9	12	15	24
Ohms	1k	1.8k	2.4k	3k	3k

Open Collector Sinking Block Diagram

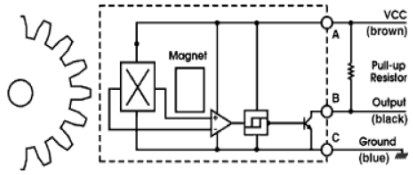

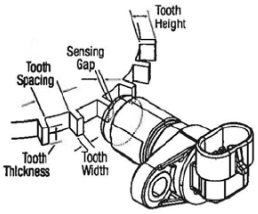

For best results, we recommend targets made from low carbon cold rolled steel. Other factors that influence sensor performance include geartooth height and width, space between teeth, shape of the teeth and thickness of the target. As a general guideline, consider a target with the following minimum parameters:

Tooth Height	Tooth Width	Distance Between Teeth	Target Thickness
.200"	.100"	.400"	.250"

Contact

Call, fax or visit our website
For more information.

ZF Electronics Corporation
11200 88th Avenue
Pleasant Prairie, WI 53158

Phone: 262.942.6500
Web: www.cherrycorp.com

E-Mail: cep_sales@zf.com
Fax: 262.942.6566

Specifications subject to change without notice.

CHERRY®

Figure A.6 Continued

measurement SPECIALTIES

MSP 300 Pressure Transducer

- OEM and End User
- One Piece Pressure Port Construction
- No O-Rings
- No Silicon Oil
- No Welds

DESCRIPTION

The MSP 300 series pressure transducers from the Microfused™ line of MEAS, set a new price performance standard for low cost, high volume, commercial and industrial applications. This series is suitable for measurement of liquid or gas pressure, even for difficult media such as contaminated water, steam, and mildly corrosive fluids.

The transducer pressure cavity is machined from a solid piece of 17-4 PH stainless steel. The standard version includes a 1/4 NPT pipe thread allowing a leak-proof, all metal sealed system. There are no O-rings, welds or organics exposed to the pressure media. The durability is excellent.

MEAS' proprietary Microfused™ technology, derived from demanding aerospace applications, employs micromachined silicon piezoresistive strain gages fused with high temperature glass to a stainless steel diaphragm. This approach achieves media compatibility simply and elegantly while providing an exceptionally stable sensor without the PN junctions of conventional micromachined sensors.

This product is geared to the OEM customer who uses medium to high volumes. The standard version is suitable for many applications, but the dedicated design team at our Transducer Engineering Center stands ready to provide a semi-custom design where the volume and application warrants.

FEATURES

- One Piece Stainless Steel Construction
- Ranges up to 10k psi or 700 Bar
- mV or Amplified Outputs
- Excellent Accuracy
- Wide Operating Temperature Range

APPLICATIONS

- Pumps and Compressors
- Hydraulic/Pneumatic Systems
- Automotive Test Systems
- Energy and Water Management
- Agriculture – Sprayers and Dusters
- Refrigeration – Freon and Ammonia Based
- General Pressure Measurements

STANDARD RANGES

Range	psig	Range	Barg
0 to 100	•	0 to 7	•
0 to 250	•	0 to 17	•
0 to 500	•	0 to 35	•
0 to 1000	•	0 to 70	•
0 to 2500	•	0 to 175	•
0 to 5000	•	0 to 350	•
0 to 10k	•	0 to 700	•

Figure A.7 Data sheet for pressure sensor [46]